Peptide-Mediated Anticancer Drug Delivery

by

Parisa Sadatmousavi

A thesis
presented to the University of Waterloo
in fulfillment of the
thesis requirement for the degree of
Master of Applied Science
in
Chemical Engineering

Waterloo, Ontario, Canada, 2009

©Parisa Sadatmousavi 2009

AUTHOR'S DECLARATION

I hereby declare that I am the sole author of this thesis. This is a true copy of the thesis, including any required final revisions, as accepted by my examiners.

I understand that my thesis may be made electronically available to the public.

Abstract

An ideal drug delivery system should contain an appropriate therapeutic agent and biocompatible carrier. In this study, we investigated the ability of the all-complementary self-assembling peptide AC8 in stabilizing the anticancer compound and determined the *in-vitro* therapeutic efficacy of the peptide-mediated anticancer drug delivery. The all-complementary peptide AC8 was designed based on the amino acid pairing principle (AAP), which contains hydrogen bonding, electrostatic, and hydrophobic interaction amino acid pairs. AAP interactions make the peptide capable of self-assembling into β-sheet structure in solution in a concentration dependent manner. Peptide solution concentration is a key parameter in controlling the nanoscale assembling of the peptide. The critical assembly concentration (CAC) of the peptide was found ~ 0.01 mg/ml by several techniques.

The all-complementary peptide AC8 was found to be able to stabilize neutral state of hydrophobic anticancer compound ellipticine in aqueous solution. The formation of peptide-ellipticine complex was monitored by fluorescence spectroscopy at different mass ratios of peptide-to-ellipticine. The anticancer activity of the complexes with neutral state of ellipticine was found to show great anticancer activity against two cancer cells lines, A-549 and MCF-7. This peptide-mediated anticancer delivery system showed the induction of apoptosis on cancer cells *in vitro* by flow Cytometry.

Acknowledgements

I would like to express my great gratitude to my supervisor, professor Pu Chen, who has provided me unlimited support, great guidance and valuable advisory during my M.A.Sc study at the University of Waterloo. His valuable guidance helped me to overcome any difficulty and discover new aspects in my research. He was one of the most encouraging people in my research to assist me to become a creative and independent researcher. In addition, his critical guidance was important to improve the ideas. I am also grateful to the readers of my thesis, Dr. Frank Gu and Dr. Shirley Tang for their valuable suggestions.

I am glad to work with amazing research group in nano-bio interfacial group in University of Waterloo. All the group members were always ready to help in any part of the project. I am so grateful to receive the fantastic training from Dr. Shane Fung and Dr.Hong Yang during my project. I learned the most valuable experimental skills from them especially in vitro experiments and AFM imaging. Their advice was really helpful for improving the research in all experimental and data analysis aspects. I would like to thank Mousa Jafari for his kindly offer in some in vitro experiments.

I am so grateful to meet and collaborate with amazing technician in University of Waterloo. I would like to thank Mishi, the Flow Cytometry technician in Biology Department for her help to gather important FACS data. I would appreciate nice collaboration with Dr. Liz Meiring for FT-IR measurements and her graduate student Gracie Wang. Also, thanks Dale Weber and Nina Heinig for their valuable trainings for TEM and SEM at Biology and Chemistry Department.

During my M.A.Sc thesis, I have received great help from undergraduate research assistants working in our group: Alvina Chou, Edgar Cao, Ali Sabet, Daniel Bacinello, Vanessa Ng and Ted Mamo. Their efforts are acknowledged.

It is my pleasure to appreciate all my financial supports and scholarships that I have awarded during my masters program such as Ontario Graduate Scholarship (OGS), Ontario Graduate Scholarship in Science and Technology (OGSST), Waterloo Institute of Nanotechnology Fellowship (WIN), and Murray Moo-Young Biotechnology (Biochemical Engineering) Scholarship. Thanks Dr. Hector Budman and Dr. Thomas Duever for their kind support and providing me with their valuable reference letters for scholarship applications.

Most importantly, I would like to thank my true love, Jordan, for his unlimited love, constant patience and great deal of understanding. Also, thank my parents for their endless supports. Even though they were far from me during these years, but they always encouraged me when I encounter any difficulties. Special thank to my most amazing sister, Peivand, for living with me and providing me the nicest home environment. Thanks my lovely sister Parastou, for listening to me having great discussion about my research and her enormous encouragements for pursuing to biotechnology research. Without them none of my achievements would be possible. This thesis is dedicated to all of them.

Dedication

To my true love, Jordan Hamilton

Table of Contents

List of Figures

List of Tables

Chapter 1
Introduction

1.1 Overview

Cancer is the second most fatal disease after heart attack in the world. The National Canadian Statistics has reported 166,400 new cases of cancer found in Canada and 73,800 deaths in 2008.[1] Cancer is a type of genetic disease but in most cases is not inheritable. Cancers are usually traced by genetic alternation resulting from mutation of genes in a normal cell to malfunction in cell cycle. [31]This failure in cell cycle function leads to uncontrollable cell growth and metastasis. Cancerous cells originate from the normal cells in body, so they are not seen by the immune system. This immune invisibility of the cancer cells and uncontrollably proliferation make cancers as the most deadly diseases.[2-5]

The importance of cancer in human society has inspired researchers in diverse fields such as pharmaceutical, medical, and engineering to develop new and practical cancer treatment methods. By far, three major cancer treatment options are: surgery, radiotherapy, and chemotherapy.[6] Surgery and radiotherapy are local treatments and just applicable in early diagnosis, i.e., before the tumor metastasizes. Chemotherapy, on the other hand, becomes a treatment of choice after metastasis. It is also applied as the adjuvant treatment after surgery or radiotherapy. Chemotherapy can prolong life and palliate symptoms but it can also cause a number of deliberating side effects. The new cancer treatments have been developed by studying the cellular and molecular biology of the cancer. Immunotherapy, gene therapy, inhibitors for cancer-promoting proteins, antiangiogenesis therapy, hormone and growth factor antagonists and RNAi therapy are emerging to the cancer therapy strategies, recently.

Although, these strategies already have shown significant development in pre-clinical trials, but there are still challenges toward clinical applications. [2-5,7-8]

There are two main barriers in conventional cancer chemotherapy. One is the severe side effect of the cytotoxic chemicals in normal tissues; the other one is the drug resistance in human body. Most chemotherapeutic agents have harmful side effects on healthy tissues resulting from the lack of specificity in reaching tumor tissue. The defense mechanism of the cancer cells against drugs is categorized as cellular drug resistance. The most noticeable one is the multidrug resistance (MDR) phenotype, which involves active efflux of a broad range of cytotoxic drug molecules out of the cytoplasm by membrane-bound transporters.[9] These obstacles may be overcome with active or passive targeting delivery devices, e.g., nanocarriers. Nanocarriers are small enough to intravasate the blood membrane and extravasate out of tumor microvasculature and accumulate in the tumor, known as enhanced permeability and retention effect (EPR).[8] The targeting molecules can also attach the nanocarriers to recognize and bind specifically to cancer cells. These developments in drug delivery systems increase the therapeutic efficacy and undesired side effects.[7-8, 10]

Many delivery devices have been emerged in cancer therapy to improve drug solubility, targeting, safety, transport, biodistribution and pharmacokinetics.[10] These carriers include polymeric vesicles[11-15], liposomes [16-19], lipoproteins[20], nanoparticles[7-8,11,21-23], microemulsions, dendrimers[22], carbon nanotubes, etc. The main objective of these delivery vehicles for chemotherapy is to provide an enclosed, protective, biocompatible interior that can solubilize anticancer drug and circulate into blood stream.[24]

Besides polymers, liposomes and some inorganic materials, self-assembling peptides have attracted an intensive research focus in drug delivery due to their desirable chemical/physical properties and biological activities.[8, 21, 25-26] First, peptides can be easily designed to form stable structures, such as tubes, fibers, nanovesicles and globules, which can deliver drug into blood stream.[27-31] Second, peptides can be engineered to incorporate natural binding materials, such as targeting motifs, oligonucleutides, siRNA, shRNA and hydrophobic compounds.[8, 32-33] Third, they can also provided with some moieties for cell penetration and targeting.[33]All these spectacular aspects make self-assembling peptides a great potential as delivery constructs for cancer therapy or any nanomedicine.

In this research, a novel designed all-complementary, self-assembling peptide, called AC8 is introduced based on the new design principle called amino acid pairing peptide (AAPP). This peptide is a short self-assembling model facilitating by all three different amino acid pairing strategies: hydrogen bond pair, ionic pair, and hydrophobic pair. The schematic of the peptide molecular structure of AC8 is shown in Figure 1.1. AC8 has eight amino acids in sequence with one exemplary hydrogen bonding pair (QN), one ionic-complementary pair (EK) and two hydrophobic residue pairs (FF). Hydrophobic amino acids were incorporated to create a hydrophobic interior for encapsulation and stabilization of hydrophobic compounds. The hydrogen bonding amino acid pairs stabilized the peptide assemblies; the charged residues enhanced the solubility of the peptide, and the hydrophobic residues also enhanced the peptide-peptide association.

Ellipticine (EPT), a hydrophobic anticancer agent is selected as a drug in this study. The reasons of selecting this drug are anticancer activity, fluorescence properties and its

hydrophobicity. Ellipticine (EPT), a cytotoxic plant alkaloid, is known as a polycyclic molecule that intercalates between DNA base pairs, inhibits topoisomerase II, and induces G2/M phase cell cycle arrest.[34] It has been reported that the fluorescence spectrum of molecularly solubilized ellipticine, depending on the environment, exhibits a peak ~ 430 nm or ~ 520 nm representing its neutral and protonated form, respectively.[35] The fluorescence spectrum of solid ellipticine crystals was shown a similar peak as the colloidal suspensions at ~ 470 nm. Figure 1.2 shows those molecular structures of ellipticine and its different states.[35]

In the first part of this research, I demonstrate the concentration dependent assembly of the peptide by several techniques such as surface tension, static and dynamic light scattering measurements. In the second part, I explore the potential application of the designed peptide in drug delivery. For this objective, the capability of the AC8 in stabilizing hydrophobic anticancer agent, ellipticine, in aqueous solution was studied. The co-assembly of peptide-ellipticine complexes was characterized by fluorescence spectroscopy and dynamic light scattering. The third part of this research is considered for anticancer activity of the peptide-ellipticine complexes *in-vitro*. For this purpose, the complexes were tested on two cancer cell lines: human breast cancer cell MCF-7 and human lung cancer cell A-549. The cytotoxicity of the complexes and their dilutions was investigated by MTT assay. In the fourth part of this study, apoptotic effect of the peptide-ellipticine complex was evaluated on the cancer cells *in-vitro* by flow Cytometry.

Figure 1.1. A schematic of the chemical structure of the chemical structure of AC8 peptide (FEFQFNFK). The pairs of (FF) are hydrophobic residues. (QN) and (EK) are the hydrogen bonding and ionic-complementary residues, respectively.

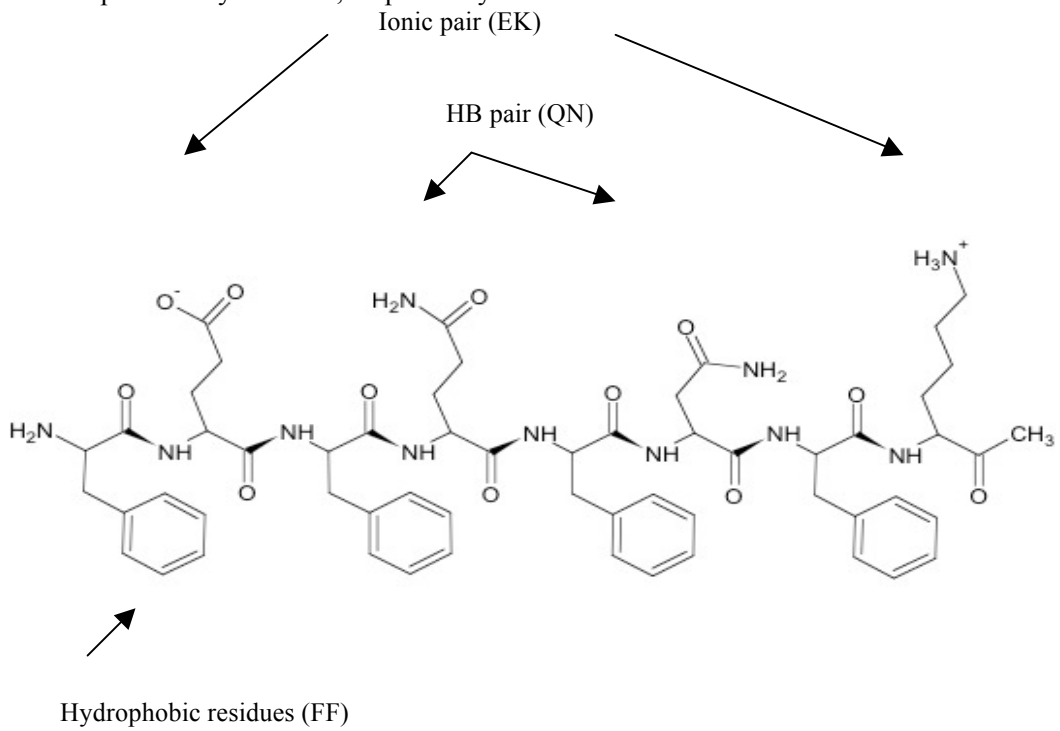

Figure 1.2. The molecular structure of Ellipticine. 5,11-Dimethyl-6*H*-pyrido[4,3-*b*]carbazole. Different states of Ellipticine and their emission wavelength at excitation of 294 nm. Ellipticine transforms within Crystalline, neutral and protonated form depending on the environment.

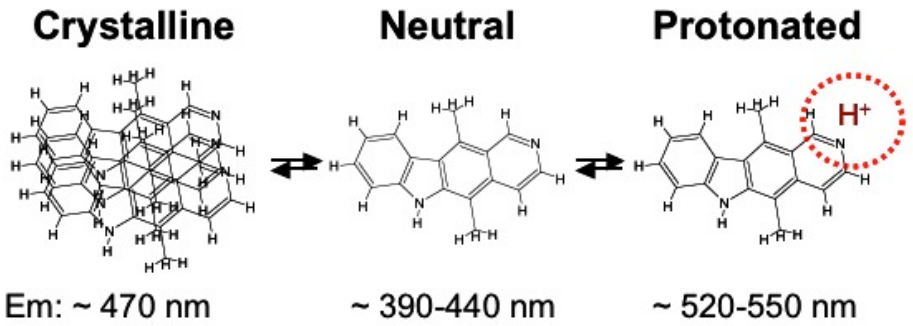

1.2 Research Objectives

The goal of this research is to develop all-complementary self-assembling peptide-mediated delivery of hydrophobic anticancer drugs. To achieve this goal, the anticancer agent ellipticine is selected to examine the basic of the complexation with designed all-complementary peptide. The specific objectives of this research study are listed as below:

1) Study the concentration effect of on assembly of the peptide
2) Characterize the photophysical properties of ellipticine in peptide solution environment
3) Evaluate the therapeutic effect of the peptide-ellipticine complexes *in vitro* with two cancer cell lines: human lung cancer cell A-549 and breast cancer cell MCF-7
4) Investigate the apoptotic effect of the peptide-ellipticine complexes *in vitro* on the same cancer cell lines as above.

1.3 Outline of the Thesis

This thesis consists of five chapters as followings:

Chapter 1 gives the overview of the thesis, including introduction to cancer and cancer therapy and specifically for peptide-mediated hydrophobic drug delivery systems. The main objectives of the research are also listed in this chapter.

Chapter 2 reviews the available literature about principle of cancer and different cancer therapy methods, new drug delivery systems and application of self-assembling peptide as the nanocarrier for anticancer drug delivery.

Chapter 3 gives the experimental methods and required materials in detail applied for this research.

Chapter 4 reports the results and discussion from each objective including concentration effect on assembly of the peptide, complexation of peptide-ellipticine and results of *in vitro* studies.

Chapter 5 presents the conclusions of studies in the thesis and the recommendation for future work.

Appendices give the theory of some techniques applied in this research including dynamic light scattering, MTT assay, and Flow Cytometry.

Chapter 2

Literature Review

2.1 Cancer and Cancer Therapy

2.1.1 Introduction

Cancer is one of the most devastating diseases in the world. The Canadian Cancer Statistics reported 166,400 new cases of cancer found in Canada and 73,800 deaths in 2008 alone.[1] This news inspired researchers in pharmaceutical and engineering fields to develop new and practical cancer treatment methods. Cancer is a genetic disease because it can be traced by genetic alteration, but in most cases it is not inheritable. Genetic changes in DNA level usually lead to cancer and cancer cells proliferate uncontrollably. This genetic alteration can be involved in three possible mechanisms: (i) the impairment of a DNA repair pathway (ii) the transformation of a normal gene to oncogene (iii) the malfunction of a tumor suppressor gene. These genetic changes happen because of environmental agents. Carcinogenic chemicals, such as cigarette and tobacco can almost be mutagenic. Similarly, ultraviolet radiation is another factor, which leads to cancer. There are different strategies to combat cancer or prevent it, which depend on its stage. Generally speaking, cancer is a malignant tumor. Tumors can be identified by their shape, size and growth speed. Benign tumors are localized and they can be removed by surgery. In contrast, malignant tumors tend to metastasize and enter vascular circulation and attack other tissues. In this case, removal of the tumor by surgery is no longer applicable. There are new strategies to overcome cancers recently under research. Immunotherapy, gene therapy, inhibiting the activity of cancer-

promoting proteins and angiogenesis are the cancer therapy methods that can be combined with chemotherapy in case of metastasis.[2]

2.1.2 Basic Properties of Cancer

The most important property of cancer cells, whether in body or on a culture dish, is loss of growth control. When normal cells grow in a culture dish under the condition of cell proliferation, they grow and divide to the point where they cover the bottom of the culture dish to make a monolayer of cells. In contrast, when cancer cells grow in culture dish, they continue to proliferate uncontrollably and make clumps on the top of layer of the cells at the bottom. Cancer cells are not usually as responsive as normal cells to the signals that cause their normal counterparts to cease growth and division. This lack of response to the inhibitory growth signals in malignant cells makes them cancerous.[2]

The rate and timing of cell division in a normal body for all cells are precisely regulated. All the cells follow a specific cycle and timing, which is called “cell cycle clock”. The cell cycle clock is composed of four main stages. G1, or gap one stage, includes increasing the size of the cells and preparing for DNA replication. Once cell decides whether to continue or not, the clock moves to the S phase. In the S phase, or synthesis stage, the cell copies its DNA. After DNA replication, the G2 phase, or gap 2, occurs. In this stage a cell is getting prepared for division. The phase in which the cell divides is called the M-phase, or Mitosis. Segregation of the chromosomes occurs in the M-phase and a cell divides into two daughter cells. The new daughter cells immediately enter the G1 and, depending on the signal they receive, their cell cycle clock moves forward. Therefore, in normal tissues, cell proliferation

and division is completely under control by internal clocks. However, the cell cycle clock in malignant cells is disrupted. Two types of genes play an important role in regulating the cell cycle. Oncogenes and tumor suppressor genes are the two major genes, which interrupt the cell cycle and lead to cancer. The detail about the function of these genes is discussed in the Genetic of Cancer section.[4]

2.1.3 The Causes of Cancer

Percival Pott, a British surgeon, established the correlation between environmental factors and the development of cancer first in 1775. He recognized a form of cancer of the nasal cavity and the skin of the scrotum in chimney sweeps because of the exposure to soot. Within the past several decades, hundreds of chemicals such as, tobacco, alcohol, Radon, asbestoses, etc have shown to cause cancer, so called carcinogenic chemicals. Besides the chemicals ionizing radiation, ultraviolet radiation and some viruses can be carcinogenic. All of these agents have common properties, which they alter the genome and cause DNA mutation.

A variety of DNA and RNA-containing viruses can infect mammalian cells and transform them into cancer cells. They are called oncogenic viruses. In the most cases, these viruses increase the risk of cancer rather than being sole determinant. These viruses are associated with small fraction of human cancers.

Epidemiologists carry out the determination of the causes of different types of cancer. The cause of some cancers is obvious: smoking causes lung cancer and exposure to ultraviolet radiation causes skin cancer. However, the causes of a large number of cancers are not completely known. Today's world is a complex environment, so humans are exposed to

many potential carcinogens. Several types of nucleotide changes induced by chemical carcinogens such as smoking, Aflatoxin B1, UV, etc. More than 50 percent of human cancers are found with deletion or mutation of the TP53 gene.

2.1.4 The Classification of the Cancer

As discussed before, cancer cells have infinite cell division and invade territories normally reserved for other cells. If the proliferation of the cells becomes out of control, it will give rise to a tumor or neoplasm. As long as neoplastic cells localize together in a single mass, the tumor is called benign or Adenoma. Benign tumors are not considered cancer and they can be removed surgically. The tumors are considered cancer only when they are malignant. Malignancy happens when primary tumor cells have this potential to attack surrounding tissues. In this case, primary tumors enter the bloodstream or lymphatic vessels through intravasation and exit the capillaries of vessel through extravasation to enter other tissues and create secondary tumors. This mechanism is called metastasis. These actions make cancers peculiarly dangerous. Figure 2.1 shows the benign and malignant tumors.

Cancers can be classified based on the tissue and the cell type they arise from. Carcinomas are the cancers from epithelial cells such as digestive, respiratory, breast, reproductive and urinary organs. Sarcomas are the cancers arising from connective tissues, muscles and vasculatures. There are other types of cancer, which do not fit in above category. Leukemias derived from hemopoietic cells and nerve cancers arise from cells of the nervous system. Figure 2.2 shows the cancer incidence and mortality in the United States for different types of cancers. [3]

Figure 2.1. Adenoma (benign) Vs. Malignant tumors[3]

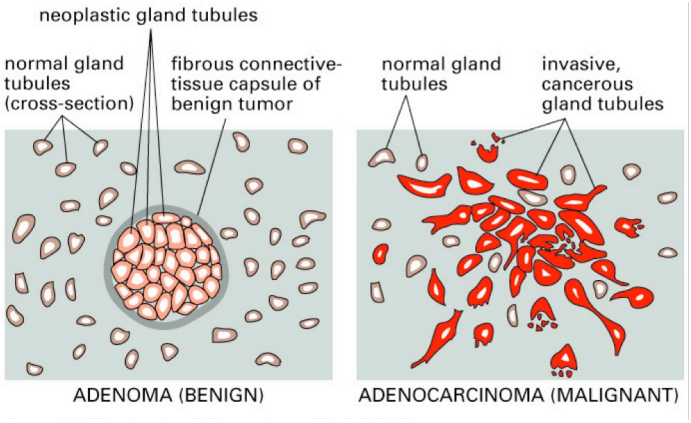

Figure 2.2. The statistics of cancer incidence and mortality in the United States[3]

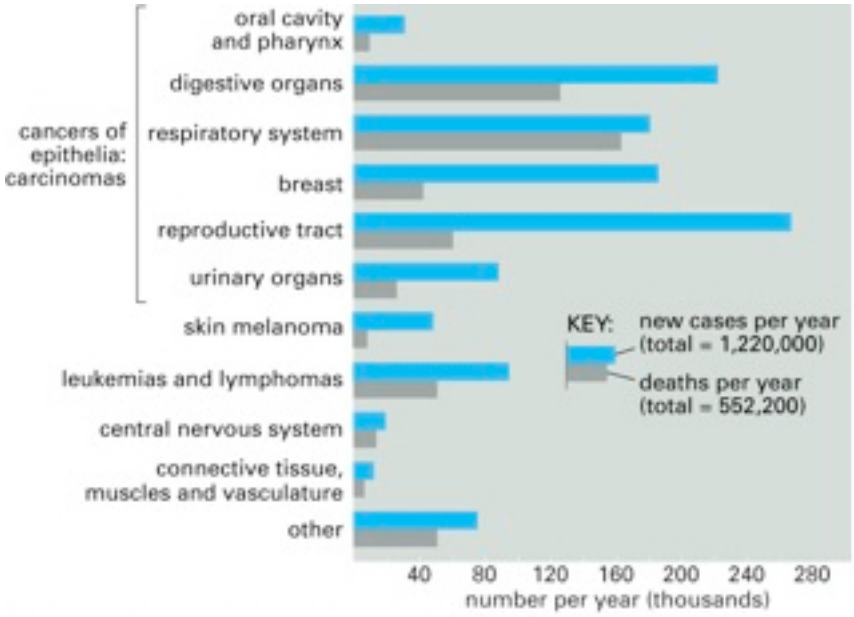

2.1.5 The Genetics of Cancer

Cancer after heart attack is the greatest causes of death in Western countries, afflicting approximately one in every three individuals. Cancer is a common disease, but at the cellular

research level, it is a remarkably new event. As discussed above, cancer is a genetic alteration but in most cases is not inherited disease. Any imbalance between genes causes cancer. Alteration of the genes usually leads to disruption in cell cycle regulation and cell division becomes uncontrollable.

Proto-oncogenes and tumor suppressor genes are two main types of genes, which play a major role in regulating the cell cycle. Proto-oncogenes are the genes, which encourage cell division. Mutation of proto-oncogenes creates oncogenes. These genes encode proteins, which accelerate cell growth and promote malignancy. Example of these proteins would be *BCL 2, HER* 2 and *K-Ras*. They act like accelerators stimulating the cell to grow and divide. In contrast, tumor suppressor genes inhibit cell division. Proteins produced by these genes act like brakes to slow down cell division. *APC, TP53, RB*, and *BRCA1* are examples of tumor suppressor genes. For instance, the *TP53* gene is located at chromosome region 17p13 and is one of the most mutated genes in human cancers. Its normal function is regulation of the cell cycle involving the G1 and the G2 checkpoints in response to DNA damage. Generally speaking, a gain-of-function of oncogenes and a loss-of-function of tumor suppressor genes drive cells toward cancer. Figure 2.3 depictes the function of oncogenes and tumor suppressor genes and their function. It shows that overactivity mutation, or gain-of-function in normal cells, creates oncogenes, both of which stimulate cell proliferation. Underactivity mutation, or loss-of-function in normal cell inactivates tumor suppressor genes, which again stimulates cell proliferation. In both cases, cells proliferate abnormally and create cancer. [2-3]

Figure 2.3. Gain-of-function of oncogene and loss-of-function of tumor suppressor gene leading to cell proliferation. [3]

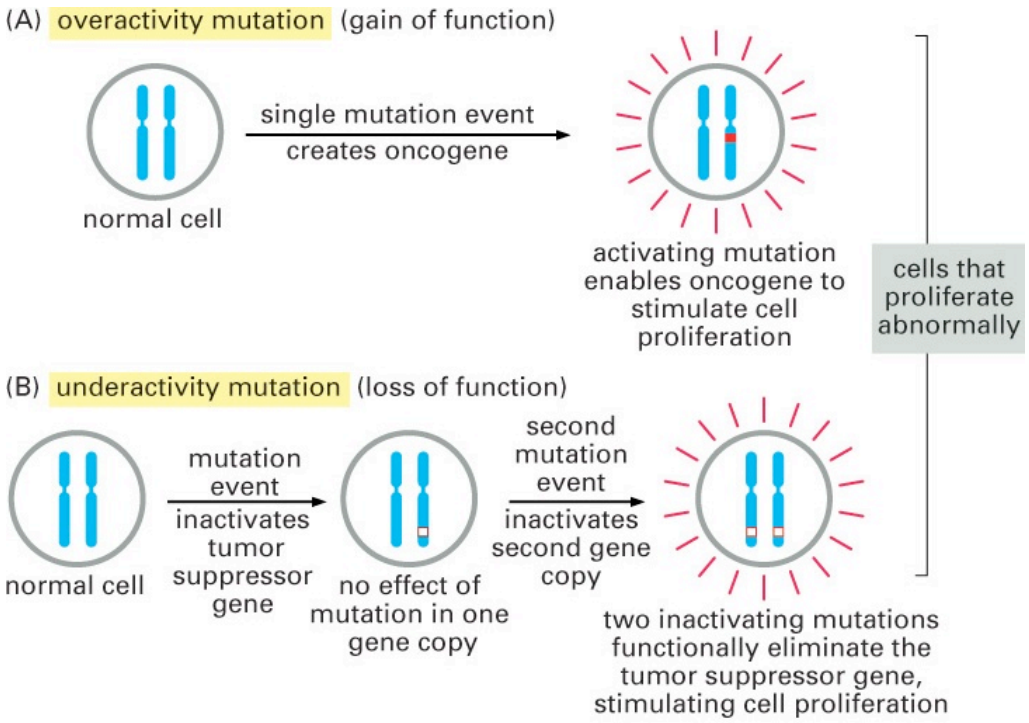

2.1.6 New Strategies for Combating Cancer

There are some conventional approaches for combating cancers such as surgery, radiation and chemotherapy, but, unfortunately, none of these methods can rid a patient of all cancer cells. Surgery and radiation therapy are only effective for early diagnosis, i.e. before the tumor metastasizes. On the other hand, chemotherapy becomes the treatment of choice after malignancy. In most cases chemotherapy can prolong life and palliate symptoms. However, it is painfully evident that chemotherapy is not only a complete cure but also it causes a number of debilitating side effects. Recently, a large number of anticancer strategies, either in laboratories or clinics, are being developed. Before testing a particular drug on humans, that drug has to be shown effective in laboratory animals. In fact, most recently published

new therapies in clinical trials, which were effective at animal level have proven disappointing in humans. Any drug, before it is applied to human body, should be approved by Food and Drug Administration (FDA). There are many pharmaceutical and safety issues for each individual drug which should be considered in clinical trials. As discussed below, there are some notable successes in clinical trials, which are related to genetics of cancer. They provide reason to believe our insight to genetics of cancer would be the basic of therapeutic strategies.

These new strategies to combat cancer are considerably related to genetics and they can be divided into four main groups: (1) immunotherapy, which depends on immune system and antibodies to attack tumor cells, (2) gene therapy, which introduces a particular gene to kill cancer cells or recover normal characteristics, (3) inhibition of the activity of proteins which promote cancer growth, and (4) anti-angiogenesis or inhibition of the growth of blood vessels, which nourish the tumor. The following section describes each strategy particularly.

2.1.7 Immunotherapy

In 1891, William Coley at New York Cancer Hospital discovered human immune system could be stimulated by administration of killed bacterial infusion. He developed the injection of bacterial extract, streptococcus pyogenes, directly into the tumor. Additionally, he postulated that these bacteria would stimulate a patient's immune system to attack and destroy malignancy. His works had great success against soft tissue sarcomas. Coley has confirmed that our body has the capability to destroy a tumor even if it is well established.

Basically, they have divided immunotherapy into two sections: passive and active immunotherapy.

Passive immunotherapy is the strategy to employ antibodies against the proteins that play a key role in the activities of tumors as therapeutic agents. As discussed above, there are specific proteins, which are overactive in some particular cancer cells. Thus, introduction of the monoclonal antibodies, which can bind to particular target antigens, was first developed in the 1970s. The problem with the antibodies was the immune system. Antibodies are recognized as foreign materials and cleared from the bloodstream, so they cannot function. To solve this issue the idea of a "Humanized Antibody" appeared. These antibodies are completely human amino acid sequences. There are some approved antibodies for curing cancers. For example, herceptin is a humanized antibody used against cell surface receptor Her2. The Her2 gene is a receptor connected to more than 30 percent of breast cancers. Herceptin binds Her2 and inhibits the activation of the receptor by the growth factor. Herceptin shows promising results for breast cancer either alone or in combination with chemotherapy. In addition, rituxan is another monoclonal antibody approved as anticancer agent in 1997 for treatment of non-Hodgkin's B-Cell lymphoma. CD20 is an over expressed protein in malignant B cells in approximately 95 percent of this disease. Rituxan binds with CD20 and inhibits its activation and it stimulates the proliferation of B cells. Recently, there are some new strategies to combine antibodies with chemotherapy and radioactive atoms to kill targeted cells.

Active immunotherapy is a creative approach in immunology, which tries to employ person's immune system to fight malignancy. The human immune system shows response

against foreign materials entering the body, so when a tumor, which is a part of the body, starts to grow it cannot be recognized by the immune system. Therefore, active immunotherapy occurs when the immune system distinguishes cancer cells. To end to this goal, cancer researchers tend to produce immunopreventive treatments in which people would be vaccinated with antigens that would prevent them from developing life-threatening cancers. [2]

2.1.8 Gene Therapy

Gene therapy was first established for some inherited diseases such as cystic fibrosis and muscular dystrophy. These diseases need to be cured by correction of the genes, so the normal gene is introduced to targeted tissues. Therefore, scientists have applied gene therapy as a strategy for combating cancers. They assume that gene modification, including deletion, addition or alternation of the particular involved gene in cancer, could be an appropriate method to combat cancer.

As discussed in the genetics of cancer section, two types of genes, tumor suppressor and oncogenes, play a key role in malignancy of the tumor. *TP53* is one of the important gene, which is lost in most cancer cells. In normal cells, when DNA damage occurs, induction of *TP53* arrests the cell cycle which leads to either repair the DNA damage and continuation of the cell division, or, if damage is too extensive, cells will undergo apoptosis. However, in cancer cell, which there is a lack of gene *TP53* no cell cycle arrest exists, so cell growth continues with damaged chromosomes and mutation keep continuing until tumor forms. Figure 2.4 shows the activation of p53 gene.

Researchers presumed induction of the TP53 gene to cancer cells, which lack of this important gene could be a way to stop growing tumors. P53-adenovirus mediated has shown some promising results to stop malignancy in both culture and laboratory animals. Adnexin is a drug approved by the FDA, which contains P53 loaded in the adenovirus. It was first injected directly into the tumor in a patient with neck cancer. It showed significant survival and no evidence of toxicity.

Figure 2.4. TP53 activity in normal cells Vs. Cancer cells [3]

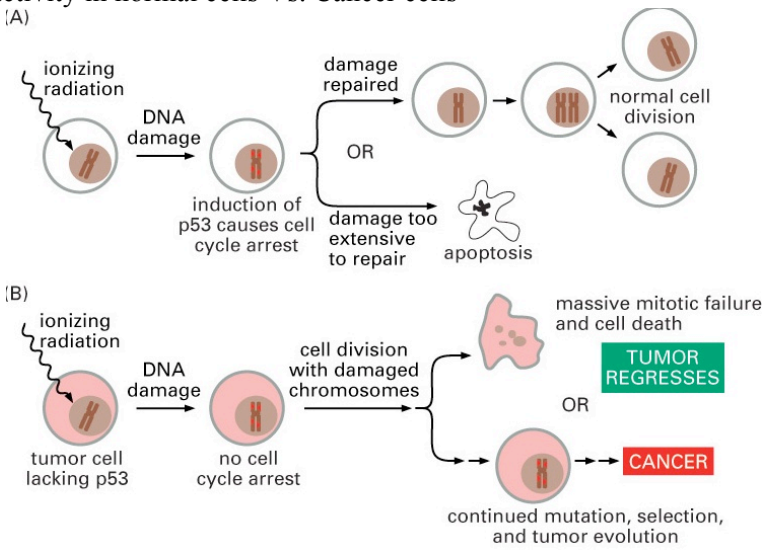

2.1.9 Inhibiting the Activity of Cancer-Promoting Proteins

Cancer cells behave abnormally because they contain some specific proteins, which enhance their tumor activity. If the activity of these proteins is blocked, it is possible to control the over growth of cancer cells. There are some known proteins for particular diseases. For example, BCR-ABL is the protein responsible for chronic myelogenous leukemia (CML). Translocation of ABL proto-oncogene to be contact with another gene BCR causes CML. The compound called Gleevec is identified to inhibit the activity of the ABL kinase. Gleevec binds the inactive form of protein kinase and prevents its phosphorylation by another kinase,

which is required for ABL activation. Figure 2.5 shows how both activate BCR-ABL and blocked BCR-ABL by Gleevec mechanism. Gleevec was approved for human use in 2001. It was very successful for patients with advanced CML when initially treated by Gleevec, but after several month resistance to the drug appears. In addition, this drug has no major adverse effect.

Figure 2.5. Gleevec mechanism for blocking BCR-ABL in leukemia [3]

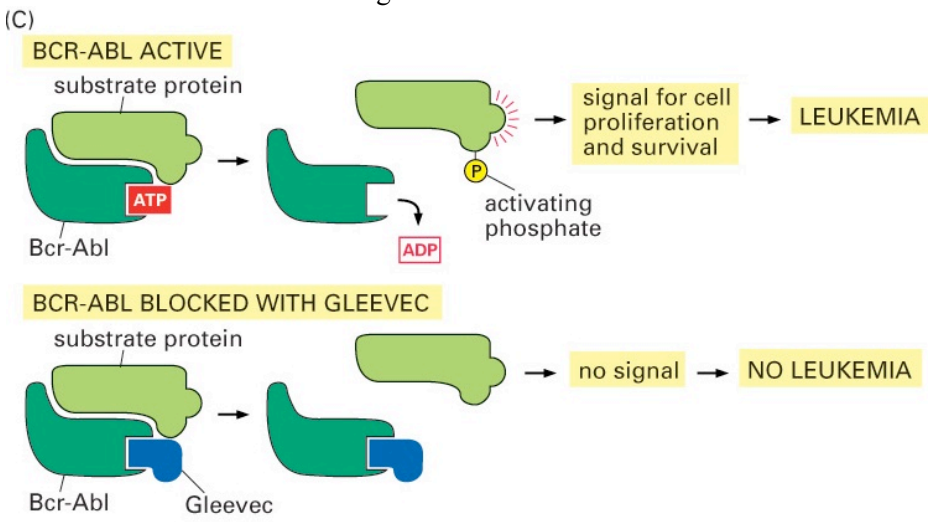

2.1.10 Inhibiting the Formation of New Blood Vessels (Angiogenesis)

Uncontrollable growth of tumor cells stimulates the formation of blood vessels around the tumor area to nourish the cells. The process of increasing the number of blood vessels called *angiogenesis*. In 1972, Jodah Folkman at Harvard University suggested that blocking the blood vessels around solid tumors could destroy tumors. This idea has brightened the anticancer strategies. A protein called VEGF or vascular endothelial growth factor plays an important role in angiogenesis. It stimulates forming blood vessels. A number of angiogenesis inhibitors are established including antibodies and synthetic compounds. Approximately 80 angiogenesis inhibitors are examined on 100,000 patients. Avastin is the

most promising agent, which is a monoclonal antibody against VEGF. It binds VEGF, so it inhibits its function to produce more blood vessels and provide nutrition for tumor cells.

2.2 New Drug Delivery Systems

2.2.1 Introduction

Drug administration used to be in conventional styles such as pills, eye drops, ointments and intravenous solutions. However, in the last few decades a number of novel drug delivery systems have been developed. Theses approaches include pharmaceutical agents encapsulated in carrier systems to injected into bloodstream and deliver to targeted tissue. This research is developed in several aspects: (i) many drug either old pharmaceutics or new-engineered agents can be administrated by delivery system to enhance the safety, efficiency and also permit new therapies. (ii) The new and more complex drugs such as proteins or genes are becoming available and they may need advance delivery systems. (iii) Drug release pattern issue is also introduced to the pharmaceuticals, which improves the therapeutic responses. (iv) potentially, the dosage of drug needed for therapeutic is decreased significantly by drug delivery. (v) facilitation of drug delivery system with the intelligent substance like antibodies is another important development of this novel research. The above advantages must compete with following concerns in the development of drug delivery system: (i) toxicity of the carriers and drug, or other safety issues encountered with unwanted rapid drug release, (ii) discomfort of the drug administration by means of insertion, (iii) high expense due to drug encapsulation in manufacturing process.[11, 36]

2.2.2 Hydrophobic Anticancer Drug Delivery

In past few years, drug delivery has significant improvement in cancer therapy. About 40% of new anticancer drugs discovered recently are hydrophobic compounds. Poor solubility of these candidates limits their application in drug delivery systems, so they necessitate novel carriers for drug delivery formulation. Extremely hydrophobic drugs such as Ellipticine, Nifedipine and Felodipine are the motivations for drug delivery technologies to design the systems, which solves the solubility issue and modifies the therapeutic effects.[22]

Many delivery systems have been designed for hydrophobic drugs as carriers. They are generally categorized into five classes: polymeric conjugates, liposome, emulsions, micelles and nanoparticles. Many pharmaceutical properties of free drug can be improved by drug delivery system (DDS) such as pharmacokinetics (PK), and biodistribution (BD).[10] Drug delivery systems have some major effects to combat non-ideal properties of drugs and their therapeutic implications. Table 1 summarized the advances in each class of hydrophobic drug delivery systems. The following sections are reviewing different drug delivery systems and their application.

Table 2.1. Non-ideal properties of drugs and their therapeutic implications [10]

Problem	Implication	Effect of DDS
Poor solubility	A convenient pharmaceutical format is difficult to achieve, as hydrophobic drugs may precipitate in aqueous media. Toxicities as associated with the use of excipients such as Cremphore (The stabilizer for Paclitaxel in Taxol)	DDS such as lipid micelles or liposomes provide both hydrophilic and hydrophobic environments, enhancing drug solubility
Tissue damage on extravasation	Inadvertent extravasation of cytotoxic drugs leads to tissue damage, e.g., tissue necrosis with free doxorubicin	Regulated drug release from the DDS can reduce or eliminate tissue damage on accidental extravasation
Rapid breakdown of the drug in vivo	Loss of activity of the drug follows administration, e.g., loss of activity of camptothecins at physiological pH.	DDS protects the drug from premature degradation and functions as a sustained release system. Lower doses of drug are required.
Unfavorable pharmacokinetics	Drug is cleared too rapidly, by the kidney, for example requiring high doses or continuous infusion.	DDS can substantially alter the PK of the drug and reduce clearance. Rapid renal clearance of small molecules is avoided.
Poor biodistribution	Drug that have widespread distribution in the body can effect normal tissues resulting in dose-limiting side effect, such as the cardiac toxicity of doxorubicin	The particulate nature of DDS lowers the volume of distribution and helps to reduce side effects in sensitive, non-target tissues.
Lack of selectivity for target tissues	Distribution of the drug to normal tissues leads to side effects that restricts the amount of drug that can be administrated. Low concentration of drugs in target tissues will result in suboptimal therapeutic effect.	DDS can increase drug concentrations in diseased tissues such as tumors by the EPR effect. Ligand-mediated targeting of the DDS can further improve drug specificity.

2.2.3 Polymer-based drug delivery systems

Polymeric conjugated systems are widely used for anticancer drug delivery systems. The hydrophobic drugs covalently bind to hydrophilic or amphiphilic polymers to enhance solubility in aqueous solution. There are basically, three general mechanisms of drug delivery by polymers: (1) diffusion of the drug substance from he system, (2) degradation or cleavage of the drug from the system by a chemical or enzymatic reaction, (3) activation of solvent through osmosis or swelling of the system, (4) conjugation of drug into polymer, and cleavage of the polymer inside the body.[11]

Figure 2.6. Four mechanisms of polymeric-based drug delivery[11]

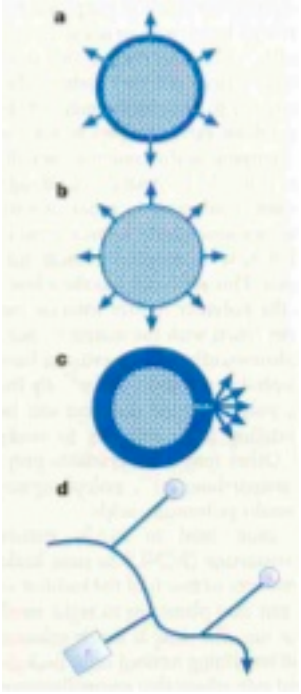

The concept of chemically binding drugs to polymers confers new properties such as, decreasing in immunogenicity or tissue targeting. For instance, polyethylene glycol (PEG) binds to adenosine deaminase (ADA) as a new treatment of lymphoblastic leukemia shows promising decrease in immunogenicity.[11, 13]

Polymer-based drug delivery has been developed extensively in both active and passive targeting delivery. The approach of passive targeting includes polymer-drug linkage circulating in bloodstream then enters to cells by endocytosis. The circulation of polymer-drug conjugates is longer than drug alone, which is another advantage of polymer-based systems. The polymers employed to conjugate anticancer drugs are classified into synthesis and natural materials. The synthetic polymers are non-immunogenic but in most cases are not biodegradable. Some of the examples of synthetic polymers are as follow: N-(2hydroxypropyle) methacrylamide (HPMA copolymer), poly(styrene-co-maleic anhyride) (SMA), poly(divinylether-co-maleic anhydtide) (DIVEMA) and poly(ethylene glycol) (PEG). Natural polymers are biodegradable materials, which used for the conjugation to drugs. Poly(L-glutamic acid) (PG), some proteins, dextran and chistotan are the examples of natural polymers. Doxorubicin, Paclitaxel and Camptothecin, anticancer drugs, conjugated with HPMA, PG and PEG successfully for different cancer therapy. For example, HPMA conjugates to doxorubicin, anticancer drug, through peptidyl linker that is cleaved by thiol-dependent proteases in lysosomes. In this case, the maximum tolerated dose (MTD) is 5-10 times higher than the free drug in animals and human.[11, 14]

Some of the polymer-drug conjugates are in clinical trial for different cancer therapy purposes as listed in Table 2.[12]

Table 2.2 Polymer-drug conjugates in clinical trials[12]

Conjugates	Indication	Status	Company
HPMA-doxorubicin (PK1: FCE28068)	Lung and Breast Cancers	Phase II as of 2002	Pfizer, Cancer Research Campaign UK
HPMA-doxorubicin-galactosamine (PK2; FCE28069)	Hepatocellular carcinoma	Phase I/II	Pfizer, Cancer Research Campaign UK
HPMA-camptothecin	Solid tumors	Phase I; discontinued	Pfizer, Cancer Research Campaign UK
HPMA-paclitaxel	Solid tumors	Phase I; discontinued	Pfizer, Cancer Research Campaign UK
HPMA-platinate	Ovarian, melanoma and colorectal cancers	Phase I	Access pharmaceutical
PEG-Camptothecin	Solid tumors	Phase I; discontinued	Enzon
PEG-SN38	Solid tumors	Phase I; initiated as of October 2007	Enzon
Polymeric micelles	Pancreatic cancer	Phase II	Nippon Kayaku, Japan
Cyclodextrin-based polymer-CPT	Solid tumors	Phase I	Insert Therapeutics
Carboxylmethyldexteran-exateean	Solid tumors	Phase I	Diiachi Pharmaceuticals, Japan
PG-TXL	Lung, ovarian, colorectal, breast and esophageal cancer	Phase III	Cell Therapeutics
PG- Camptothecin	Colorectal, lung and ovarian cancers	Phase I	Cell Therapeutics

Besides the passive targeting of polymer-based systems, active targeting can be achieved by complexation of polymer-drug system with a targeting molecules such as antibodies or carbohydrates. These targeting molecules can recognize cell surface receptors in specific tissue. HPMA-Taxol copolymer drug conjugate binds galactose to target the cell surface asialoglycoproteins receptors in liver cells.[14] Another approach of active targeting is polymeric drug utilizing with poly[N^2-(2-hydroxyethyl)-L-glutamine)] immunoconjugates of adriamycin and human IgG antibody against tumor-associated antigen.[15] Conjugated system has shown great promise in advance chemotherapy. However, the synthesis of multicomponent conjugates requires series of chemical reactions and purifications, which makes complications and high expense of manufacturing process.

2.2.4 Liposome-based delivery systems

Liposomes, small lipid vesicles, have shown great promise of drug delivery among many drug carrier systems. Liposomes are bilayered phospholipids membranes, which are made from natural lipids such as phosphatidylcholine (PC), phosphatidylglycerol and cholesterol. Lipids have different range of size based on their preparation method (sonication or filteration). There three major types of liposomes: multi-lamellar vesicles (MLV. > 0.1 μm), small unilamellar vesicles (SUV, < 0.1μm) and large unilamellar vesicles (LUV, >0.1 μm).

Liposomes could encapsulate drugs rather than binding polymer chains. This drug encapsulation by liposomes provides high capacity of drug loading. In addition, they are biodegradable and essentially non-toxic vehicles. However, there are some issues should be solved to apply liposomes more effectively such as shelf life, targeting ability and stability in

reticuloendothelial system (RES).[17] RES rapidly clears most of the conventional liposomes systems. Thus, modification of liposomal surfaces such as PEG modification is required for long-circulating and avoiding RES.

A significant advance liposomal delivery is the development long-circulating liposome (LCL) system associated with PEG, poly(ethyleneglycol) or other polymers including poly(acrylamide) and poly(N-vinyl pyrrolidine). PEG-conjugated liposmes enhance the circulation longevity of the liposome to avoid mononuclear phagocyte system (MPS) uptake.[16] The size of liposome is an important factor to affect the longevity and targeting efficiency. To achieve this end, the optimal size of liposome is required for long blood circulation and higher tumor accumulation ranges from 50 to 200 nm.[18]

The other significant factor in development of liposome-based drug delivery is incorporation of targeting moieties. The delivery system contains liposome and tumor vasculature targeted ligands is recently developed to deliver Combretastatin A4 as a novel antivascular agent. PEG_{2000} is sterically stabilized on the surface of long circulating liposome (LCL). Cyclic RGD (Arg-Gly-Asp) peptides with affinity for growth factors expressed on tumor vascular endothelial cells were coupled to PEG on the liposome surface.[16] Figure 2.7 depicts the schematic of the targeted liposome delivery system. Figure 2.8 represents the coupling reaction to form the final targeted liposome.

Other advance in liposomal drug delivery in clinical trial is pegylated liposome carrier for doxorubicin (Doxil) in metastatic breast carcinoma (MBC). There was a magnificence

development to in pharmacokinetics and decrease toxicity of Doxil with this delivery system.[19]

Figure 2.7. Schematic representation of the targeted liposome delivery system. Cyclic RGD peptides coupled to the distal end of maleimide-PEG-DSPE in the liposome bilayer of PEG-grafted LCL.[16]

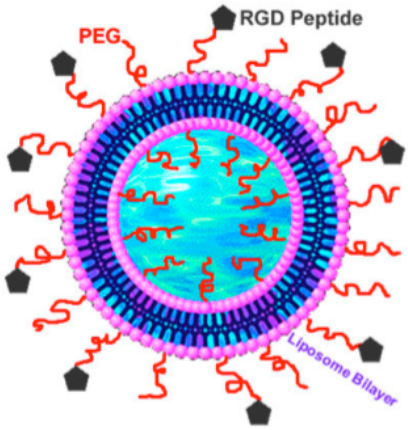

Figure 2.8. Schematic representation of the coupling reaction between maleimide functional group at the distal end of PEG chain on the LCL and thiol group in the cyclic RGD peptide.[16]

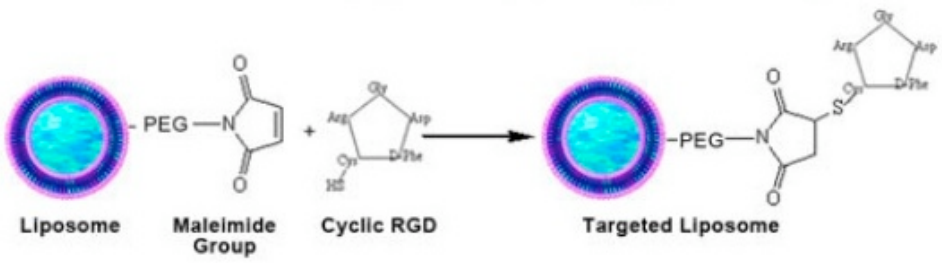

2.2.5 Lipoprotein targeted drug delivery

Low-density lipoprotein (LDL) is the major ligand for the low-density lipoprotein receptors (LDLR) and it is also the major transporter of cholesterol in the plasma. The modified LDL was synthesized to determine its utility as a drug delivery vehicle targeted to tumors by Berekely Lab. The synthetic nano-LDL nanoparticles were constructed by combining a

synthetic peptide containing a lipid binding motif and the LDL receptor(LDLR) binding domain of apolipoprotein B-100 with a lipid emulsion consisting of phosphatidyl choline, triolein, and cholesteryl oleate. This technology is already applied on Glioblastoma multiforme (GBM) tumors, which is considered as a highly aggressive malignant tumor for approximately 85% of primary brain tumors in adults. Tumor cells generally require high cholesterol for their cell division, so they over express LDLR on the surface. nLDL-based drug delivery system selectively binds to LDLRs and inhibits cell growth in GBM cells.[20]

2.2.6 Nanoparticles

The magnificent development of nanotechnology incorporates cancer chemotherapy and diagnosis over the pas decades. Novel nanoparticles have been designed and applied for drug delivery for different therapeutic purpose. Nanoparticles are defined as submicrons (<1μm) colloidal particles, but not necessarily biodegradable polymers.[7]Based on preparation method, nanocarrieres are classified as nanocapsules, nanospheres and nanoparticles. Nanospheres are the matrix systems in which the drug is dispersed through out the particles. Nanocapsules are considered as reservoir systems in which the drug is entrapped in a cavity surrounded by a polymeric membrane. Figure 2.9 shows the schematic of nanosphreres and nanocapsules.[7]

Figure 2.9. Nanoparticles are nanosphere (matrix systems) (top) or nanocapsule (reservoir system) (bottom). [7]

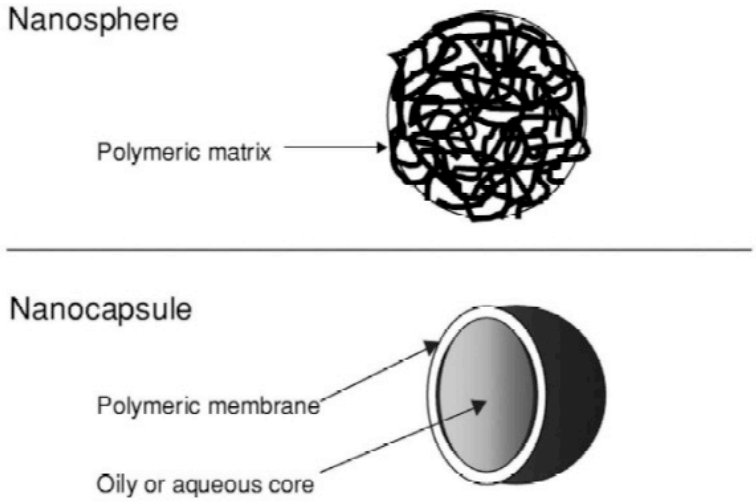

According to the above definition, micelles and liposome are considered as nanoparticles. There are other nanoparticle systems for drug delivery such as gold nanoparticles, chitosan nanoparticles, carbon nanotubes (CNT), dendrimers, hydrogels and magnetic nanoparticles. For example, hydrogels are the polymeric nanoparticles designed for drug delivery systems. Drug can be encapsulated in the hydrogel, which is stable enough to circulate in bloodstream. The molecular weight, size and hydrophobicity of hydrogels are tailored to evade mononuclear phagocyte system (MPS). Chitosan-based drug delivery is another example of nanoparticle applying for drug delivery. Chitosan is polysaccharide, similar structure as cellulose. Different drugs can be loaded into chitosan for various therapeutic purposes. Drug release kinetic from chitosan particles is derived in three major mechanisms: release from the surface, release from erosion, and diffuse from swollen matrix. Chitosan nanoparticles have shown promising results for doxorubicin encapsulation and gene delivery.[21]

Dendrimers are another examples of nanoparticles for drug delivery. They are polymeric nanoarchitectures, which enhance solubility of the drugs. They have well-defined size regarding to the generation and controlled surface functionalities. They can carry diverse molecules via hydrophobic interaction, ionic interaction and hydrogen bonding.[22]

The major aim of using nanoparticles for cancer chemotherapy is to achieve intelligent delivery system in terms of active and passive targeting.[11] As it discussed in previous sections, monoclonal antibodies (mAb), nucleic acid ligands (aptamers) and peptides like TAT, folic acids (folates) and nanobodies are targeting molecules for passive targeting.[8, 23, 33]

Peptides have gained a lot of attention as the promising alternative to antibodies because of their small size, low immunogenicity, biodegradability and high stability. Examples of peptides applied in this area are cyclic RGD peptide, cell-surface hormone receptors (LHRH receptor) and tumor vasculature antigens, which binds vascular endothelial growth factor (VEFG) in tumor cells.[8]The development of protocols to design or select a potent peptide sequence as targeting ligand opens new window for peptide-mediated cancer chemotherapy.

2.3 Self-Assembling Ionic-Complementary Peptides

2.3.1 Introduction

In the past decades, building advanced materials in diverse application has been tremendously developing. Self-assembly is ubiquitous in nature at both macroscopic and microscopic view. New technology through molecular self-assembly is one of the important approaches in designing materials. “Self-assembly defines as spontaneous association of numerous individual entities into a coherent organization and well-defined structures to maximize the benefit of the individual without external instruction. Molecular self-assembly

is spontaneous organization of molecules under thermodynamic equilibrium conditions into structurally well-defined and rather stable arrangements through a number of noncovalent interactions."[37]The key engineering to build up self-assembly systems is artfully design molecular bindings that are able to undergo spontaneous assembly.

Recently, short peptide sequences have attracted material scientists to construct functional nano/microstructures for different application in nanoscience.[37-38] These peptides are designed to be self-assembled through the weak interactions including hydrogen bonds, ionic bonds, and hydrophobic interaction. A new class of peptide was discovered in yeast, which shows potential self-assembling for many biomedical applications. They originally derived from EAK16-II of a Z-DNA binding protein in yeast. These derivatives share common properties including amphiphilic molecular structure and self-assemble in β-sheet-rich fibers. In addition, they have shown relatively good biocompatibility and biodegradability, so they can be used in scaffold in tissue engineering as well as carriers for therapeutic agents.[37, 39]Table 2.3 shows the few numbers of self-assembling peptides have been designed and developed.

Table 2.3. Self-assembling peptide studies.[39]

Name	Sequence (N→C)	Ionic modulus	Structure
RADA16-I	+ – + – + – + – n-RADARADARADARADA-c	I	Beta
RGDA16-I	+ – + – + – + – n-RADARGDARADRGDA-c	I	r.c.
RADA8-I	+– + – n-RADARADA-c	I	r.c.
RAD16-II	++ – – + + – – n-RARADADARARADADA-c	II	Beta
RAD8-II	+ + – – n-RARADADA-c	II	r.c.
EAKA16-II	– + – + – + – + n-AEAKAEAKAEAKAEAK-c	I	Beta
EAKA8-I	– + – + n- AEAKAEAK-c	I	r.c.
RAEA16-I	+ – + – + – + – n-RAEARAEARAEARAEA-c	I	Beta
RAEA8-I	+ – + – n-RAEARAEA-c	I	r.c.
KADA16-I	+ – + – + – + – n-KADAKADAKADAKADA-c	I	Beta
KADA8-I	+ – + – n-KADAKADA-c	I	r.c.
EAH16-II	– – + + – – + + n- AEAEAHAHAEAEAHAH-c	II	Beta
EAH8-II	– – + + n-AEAEAHAH-c	II	r.c.
EFK16-II	– – + + – – + + n-FEFEFKFKFEFEFKFK-c	II	Beta
EFK12-I	– + – + – + n-FEFKFEFKFEFK-c	I	Beta
EFK8-II	– + – + n-FEFKFEFK-c	II	Beta

The following sections are discussing the detailed information of physical and biochemical properties of self-assembly ionic-complementary peptides.

2.3.2 Molecular Structure and Physical/Biochemical Properties

Molecular Structure

Over the past two decades, a new class of peptides, self-assembly ionic-complementary peptides, has been systematically studied.[40-41] Self-assembling peptides have been emerged as the promising nanomaterials in bio-nanotechnology research. Peptide is a chain of amino acids from 2 to 40 amino acids in length. Self-assembling ionic-complementary peptides are characterized by either alternating arrangement of charged residues or hydrophobic/hydrophilic amino acid residues.[42]

The self-assembly process of ionic-complementary peptides depends on charge distribution along the peptide backbone. There are three types of charge distribution that are widely studied for self-assembling peptides. They are type I (−+ or +−), type II (−−++ or ++−−) and type IV (−−−−++++ or++++−−−−). These charge distribution is the determining factor in self-assembling conformation, which results nanostructure stabilization of ionic-complementary peptides. Jun et al. have widely studied the effect of charge distribution and molecular structure of model peptide EAK16s on theslef-assembly process. Figure 2.10 shows the AFM images of three types EAK16 in terms of charge distribution. These pictures show EAK16-I and II self-assembled in febrile nanostructures, but EAK-IV shows globular form.[42-43]

Figure 2.10. AFM images of EAK16-I (a), -II (b) and –IV (c) at a concentration of 0.1 mg/ml. EAK16-I and II form fibrillar nanostructures, whereas EAK16-IV forms globular ones. The scan size of the images is 2*2 μm and the z-scale of 5nm.[43]

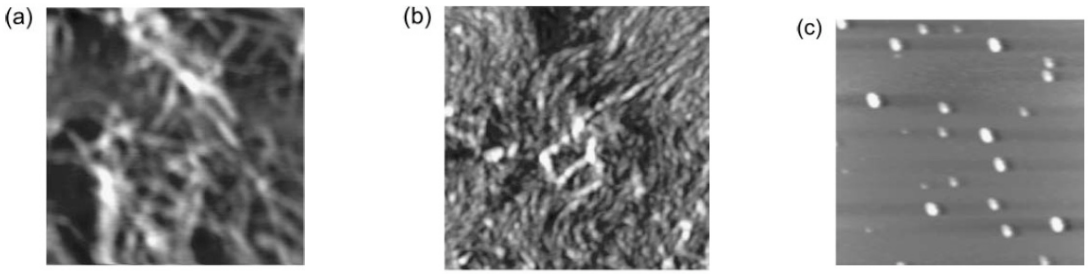

Another feature of self-assembling ionic-complementary peptides is a special arrangement of hydrophilic and hydrophobic amino acid residues alternating in sequence. This arrangement leads to "side-to-side" amphiphilic structure, which is different from "head-to-tail" in surfactants. β-Sheet secondary structure of peptides is the result of hydrophobic interactions unlike micelle formation of surfactants.

EAK16 is a famous self-assembling ionic-complementary peptide, which has been studied since 1993.[40] It is originally found in a region of alternating hydrophobic and hydrophilic residues in zuotin, a yeast protein that was initially identified for its ability to bind to left-handed Z-DNA. The EAK 16 peptide consists of three amino acids Alanine, Glutamine and Lysine. Figure 2 shows the molecular structure of three derivatives of EAK16, such as EAK16-I, EAK16-II and EAK16-IV. It has been found by circular dichroism and FTIR that these peptides or the peptide in this family can self-assemble into β-sheet fibrils.[41] The fibril formation is assumed the result from the following interactions: hydrogen bonding from the peptide backbone, electrostatic interaction from ionic-complementary residues, and the hydrophobic interactions from the hydrophobic side. Figure 2.11 shows the three-dimensional molecular structure of EAK16s.

Figure 2.11. **(A)** Chemical structure of ionic-complementary peptide EAK16-II. **(B)** Three-dimensional structure of EAK16s. From top to bottom EAK16-I, EAK16-II, and EAK16-IV[24]

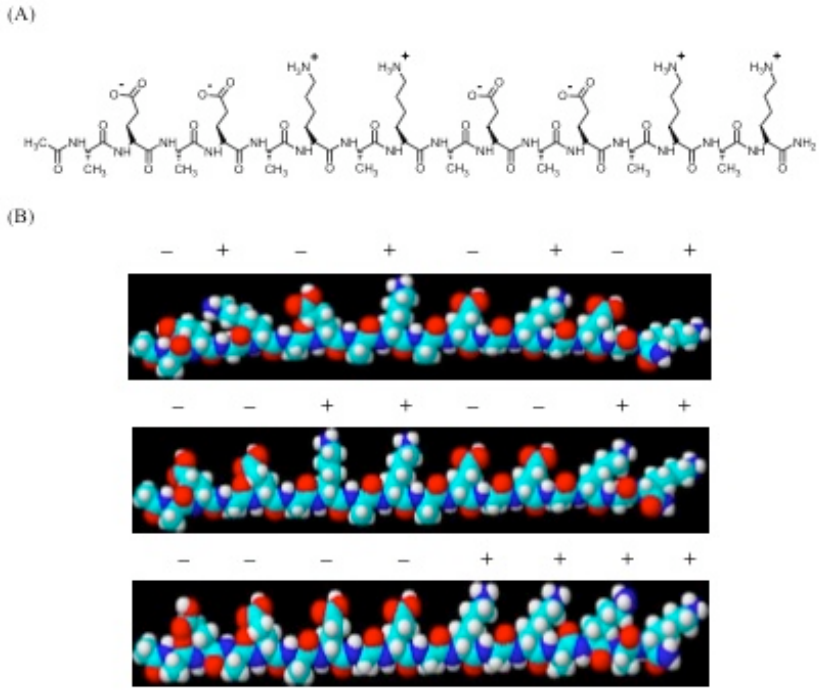

The unique structure of EAK16 is a basis of designing of other self-assembling peptides, like RAD16, to enhance bioavailability and compatibility for cell adhesion and tissue scaffolding. RAD can be derived from EAK by replacing the residues glutamic acid (E) and lysine (K) with arginine (R) and aspartic acid (D), respectively. RAD16-I has been used in bone, cartilage and shown great promises in neural regeneration studies. Zhang et al have achieved the novel advanced approaches in angiogenesis through directly coupling pure RAD16-I with short biologically angiogenesis motifs.[30, 44] Figure 2.12 shows the molecular structure of RAD16-I and the coupling functional motifs accompanied with AFM and SEM images.

Figure 2.12**.** Molecular models of designer peptides and schematic illustrations of self-assembling peptide nanofiber scaffolds. **(a)** Molecular modes of designer peptides RADA16-I, PRG, and KLT. **(b)** Schematic illustrations of self-assembling peptide nanofibers formation after mixing RADA16-I with PRG peptides, representing a b-sheet double-tape structure. Hydrophobic alanine side groups are present on one side of self-assembling motif RADA16-I b-sheet and the other side is populated with alternating positive and negative charges due to the arginine and aspartic acid residues, respectively. The functional motifs extrude from nanofiber backbones. **(c)** Typical SEM morphology of the functionalized peptides nanofiber scaffold. **(d)** Typical AFM image of self-assembling functionalized peptides solutions. **(e)** Typical CD spectrum of RADA16-I with high beta-sheet content and the mixtures with functionalized peptides, the two additional spectra (red and teal) show considerably less beta-sheet contents.[44]

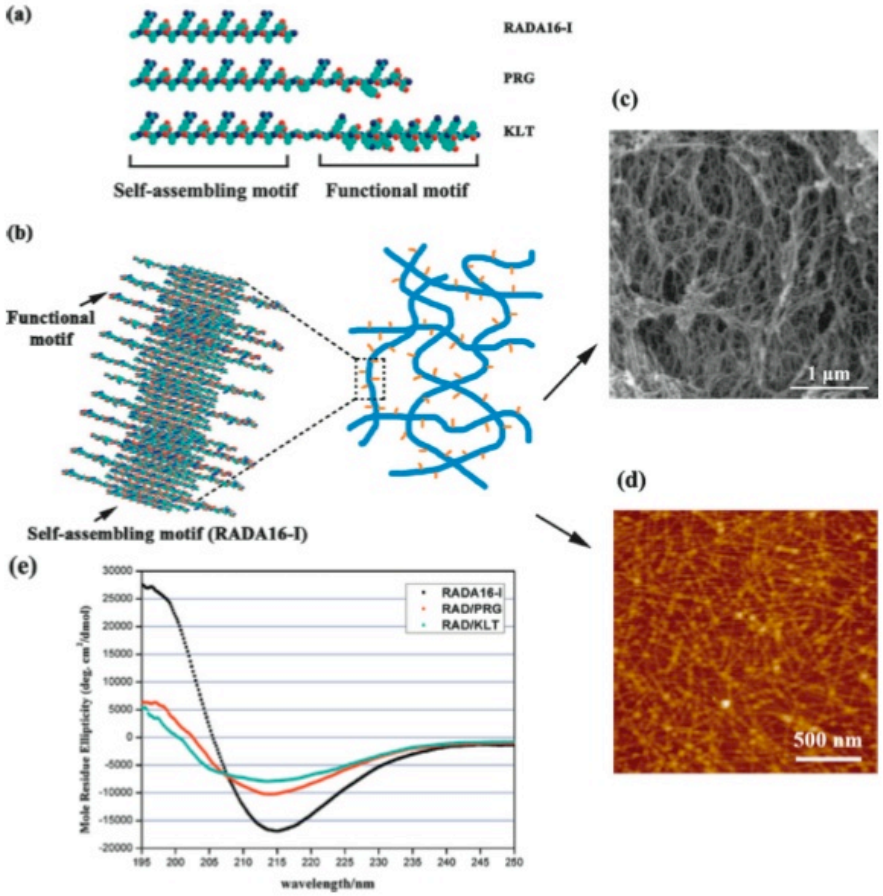

The functional motif PRG with two units of RGD binding sequences increases the tendency of attachment and promotes endothelial cell survival. The functional motif of KLT acts as VEGF agonist. Therefore, the designer functionalized self-assembling peptides PRG

and KLT have potentially great value for promoting angiogenesis *in vitro* and perhaps *in vivo* as well.[44]

Three important features of ionic-complementary peptides are charge distribution, chain length, amino acids replacement. First, their charge distribution in peptide chain can alter molecular self-assembly and secondary structure. Second, specific peptide chain length is required to achieve ionic complementarity. The minimum number of amino acids required to build type I peptide is four, while for type II and IV peptides eight and sixteen amino acids are required, respectively. Third, the ionic complementary peptide can be improved by replacing amino acids in peptide chain to enhance functionality. For example, RAD and EFK are the derivatives of EAK just be replacing amino acids as discussed above.

Secondary Structure

An important characteristic of self-assembling ionic-complementary peptide is ability to form an unusually stable β-sheet structure in aqueous solution. The β-sheet structure is stable at various physicochemical conditions (extreme pH, wide range of temperature, and various dilution) and even in the presence of denaturizing agents. EAK16-II and RAD16-I are the examples of ionic-complementary peptides, which exhibit strong β-sheet structure in various conditions.[44] Zhang et al. have studied β-sheet stability of EAK16-II in detail.[45]

The β-sheet character of EAK16-II shows a maximum absorbance at 218 and a minimum at 195 nm in the circular dischorism CD spectra in the range of concentration of 0.612 μM to 20 μM. In addition, CD spectra exhibit that β-sheet remains stable in high temperature as 90°C and at extreme pH (1.5 or 11). Unlike normal proteins that denature in

the presence of high concentration of denaturation agents, such as guanidine-HCl and urea, is above 4 M, EAK16-II maintains its β-sheet stability even in 7 M guanidine-HCl or 8 M urea. It also has shown high stability in 1% sodium dodecylsulphate (SDS) solution.[45]

CD spectra of RAD16-I have shown high β-sheet content in both peptide alone and mixture with the functionalized peptides such as PRG and KLT. A typical spectrum for β-sheet structures with a whole minimum mole residue ellipticity at 215 nm and a maximum as 195 nm was observed from RAD16-I and its mixture. The functionalized peptides mixture exhibited similar structural properties as RAD16-I but in lower intensity of mole residue at 215 nm. Figure 2.12(e) shows the above explanations.[44]

The analysis of the molecular structure and interactions show the formation of stable β-sheet is very important and necessary for peptide self-assembly and nanofibers formation. Hydrogen bonding between individual peptide backbones and charged residues in peptide sequence are the main causes of formation of β-sheet, which are evident in protein folding and aggregation. Similarly, the hydrophobic interactions from the nonpolar residues also play a role in stabilizing the β-sheet structure.

2.3.3 Peptide Self-Assembly and Control of Structure Formation

The understanding of the general self-assembly mechanism is important to control the nano/microstructure for formulation of peptide-drug complexes. There are many internal and external controlling factors that influence the self-assembly mechanism. These factors are: (i) amino acid sequence, (ii) molecular size, (iii) peptide concentration, (iv) solution pH, (v) temperature, (vi) presence of denaturation agents, (vii) ionic strength, (viii) solvent.[40-41,46]

The effect of peptide concentration, amino acid sequence, pH and presence of mechanical force on peptide structure are more relevant to this thesis which have been discussed in below.

Effect of Amino Acid Sequence

There is a considerable interest in the relationship between amino acid sequence and self-assembly mechanism. The type, number and arrangement of amino acids in the peptide chain play important role in interactions and secondary structures. For example EFK8-I has β-sheet structure, however by replacing F with A with the same charge distribution in sequence, resulting peptide EAK8-I exhibits random coils instead. The reason of that is not clear, but the possibility is the hydrophobicity of phenylalanine helping β-sheet formation.

Hong et al. 2003 has studied the effect of amino acid sequence on formation of self-assembling peptides EAK16-II and EAK16-IV. The peptides chosen consisted of 16 alternating hydrophobic and hydrophilic amino acids, where the hydrophilic residues possess alternating negative and positive charges. Two types of peptides, AEAEAKAKAEAEAKAK (EAK16-II) and AEAEAEAE- AKAKAKAK (EAK16-IV), were investigated in terms of nanostructure formation through self-assembly. The results from AFM imaging and surface tension measurement show that in the same pH EAK16-II forms fibrillar assemblies, meanwhile EAK16-IV self-assembles to globular forms. Figure 2.13 shows the AFM images of these two peptides in the same pH.[47] The difference in charge distribution as discussed above can alter peptide self-assembly into different nanostructures. The assembly of β-turns

may result in the formation of globular aggregates. On the other hand, EAK16-II prefers a stretched β-stand to form linear fibrils.

Figure 2.13**.** AFM images of EAK16-II**(A)** and EAK16-IV**(B)** EAK16-II shows fibril assemblies, whereas EAK16-IV shows globular assemblies. The scale bars are 200 nm.[47]

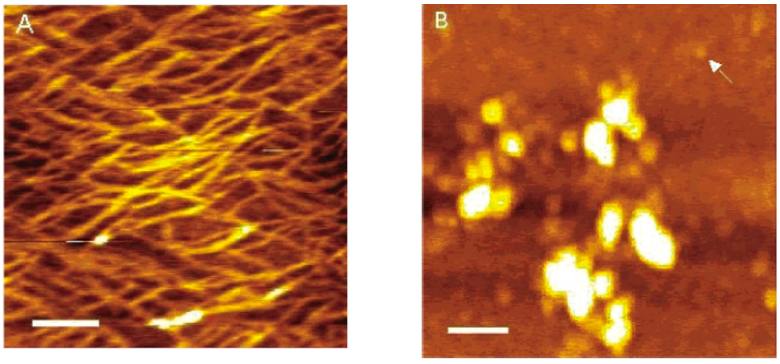

Effect of Peptide Concentration

The important parameter to trigger the peptide self-assembly and control nanostructure formation is the peptide concentration. The concentration dependence of peptide self-assembly is expected to be similar to surfactants. Applying the concept of micellar systems, critical micelle concentration CMC, one may anticipate peptides would be dispersed in solution below the critical assembly concentration CAC and begin to aggregate or assembly at or above the CAC. This CAC has been reported for many proteins and amphiphilic peptides.[46]

Recently, a CAC value of the self-assembling ionic-complementary peptide EAK16-II has been found as 0.1 mg/ml (60 μM) via surface tension measurements, light scattering and AFM imaging. AFM studies of the EAK16-II shows that nanofiber networks are formed

when the peptide concentrations are above CAC, while filaments and globules are observed at concentrations below CAC. Surface tension measurements reveal that EAK16-II has a CAC around 0.1 mg/ml. This value is comparable with CAC of human serum albumin (HAS) around 0.05 mg/ml. The light scattering also shows that EAK16-II aggregates over the time at concentrations below the estimated CAC of 0.1 mg/ml.[31]

Effect of Solution pH

The solution pH is an important factor, which affects protein and peptide structures. A pH change influences the ionic state of the charged residues as well as the net charge of peptides/proteins. Admittedly, pH will affect the self-assembling ionic-complementary peptide and protein folding or aggregation. Self-assembly of EAK16s was determined at various pH values by Hong et al. 2003.[47]The results show that the assemblies of self-assembling ionic-complementary peptides depend on the solution pH according to the charge distribution. Regardless of pH values EAK16-II forms fibrils. However, EAK16-IV shows changes in nanostructure in different pH values. EAK16-IV forms globular forms in pH between 6.5 and 7.5, but fibrils structures form in pH below 6.5 or above 7.5.[47] These results illustrate that the charge distribution in peptide sequences plays an important role in self-assembling of peptide nanostructures. Type IV charge distribution has strong intramolecular electrostatic attractions at neutral pH which leads to globular nanostructures. However, at extreme pHs, 4 or 11, intramolecular electrostatic interactions weaken which leads to smaller tendency for β-turn structures. Thus, nanofibers form predominantly.

2.3.4 Self-Assembling Peptide-Mediated Hydrophobic Drug Delivery

To date, biomaterials are widely used in numerous medical applications. Chemical engineering is playing a central role in biomedical research and its development. Polymers, liposome, micelles, peptides and proteins are the novel approaches in drug delivery systems and tissue engineering. Drug delivery is a topical subject, which attracts researchers and engineers to design effective therapeutic delivery systems. An ideal delivery system should be able to control pharmacokinetics and pharmacodynamics. Not only it should have high therapeutic effect, but also should avoid non-specific toxicity and has no immunogenecity. Peptides have great potential to overcome some major issues among the other emerging drug carriers like liposomes or polymers. They have shown promising results to enhance safety, efficiency and cell targeting. The most attractive aspect from peptide-based drug delivery systems is the natural properties of many peptides for cell penetration and targeting.[27,29,30,38,44]

Self-assembling ionic complementary peptides are the promising biomaterials for drug delivery systems. Their attractive properties including alternating hydrophobic and hydrophilic amino acids and stable β-sheet structure make them unique structures for encapsulating both hydrophobic chemotherapeutics and hydrophilic gene therapeutics. In addition, some peptides are capable to target cells or penetrate cell membrane based on their sequences. Accordingly, the discovery and design of novel biomaterials have become increasingly important for advanced tissue engineering and control drug delivery systems.[28,41,44]

Self-assembling peptides have shown a great potential in encapsulating hydrophobic materials and enhance their solubility in aqueous solutions. Micro/nanocrystals of hydrophobic compound, pyrene, and a hydrophobic anticancer agent, ellipticine, are stabilized by self-assembling ionic-complementary peptide EAK16-II in aqueous environment. The formation of the complex of pyrene and EAK16-II is simply mixing pyrene crystals with peptide solution in water under continuous mechanical stirring. Peptides assemblies seem to be more effective to stabilize pyrene than mature fibrils in aged peptide solution.[35] The release mechanism of the pyrene and ellipticine from the complexes were determined by liposomes as the cell membrane mimics.[27] The release rate has been found proportional to the peptide-to-pyrene or ellipticine ratio during the complexation. Figure 2.14 (a), (b) show the release profile of pyrene and ellipticine from EAK16-II into liposomes, respectively. The release rate has been found proportional to the peptide-to-compound ratio during the complexation. All the profiles have a similar trend with a fast increase initially and gradually reaching to plateau. These results indicate a rapid release of ellipticine in first 30s in the concentration of 0.5 mg/ml of EAK16-II, which corresponds the protonated form of ellipticine in the peptide environment. These protonated ellipticine molecules may easily migrate into lipid bilayers. However, other ratios of peptide-to-ellipticine concentrations do not stabilize protonated ellipticine, which show the lower rate of release. All these results show the possibility of such self-assembling peptides in the drug delivery of hydrophobic anticancer agents.[24]

Figure 2.14. Release profile of Pyrene and Ellipticine into liposome.[24,27-28]

a)

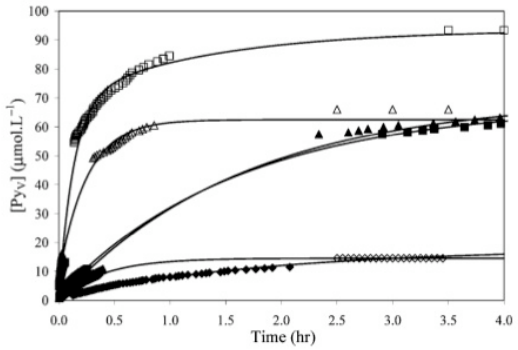

b)

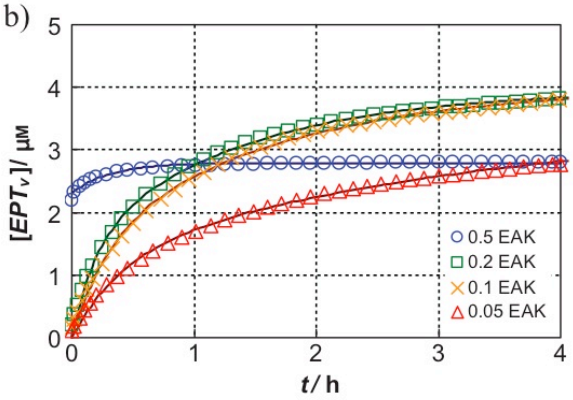

Besides the capability of peptides to encapsulate hydrophobic compounds, there is another novel approach from self-assembling peptide nanofibers scaffolds in tissue engineering. The self-assembling peptide scaffold, RADA16-I has shown great promises in 3-D tissue cell culture and has been used in bone, cartilage, and neural regeneration. They have developed designer functionalized self-assembling peptide nanofiber scaffolds for mouse neural stem cell 3-D cultures as well as for growth, migration, and tubulogenesis of human umbilical vein endothelial cells. In both case RADA16-I peptide was utilized with two functional motifs. Cell adhesion, differentiation and bone marrow homing motifs were attached to RADA16-I peptide and self-assembled into nanofibers. BMHP1 (SKPPGTSS) and BMHP2 (PFSSTKT) belong to the family of peptides (bone marrow homing peptide) rich in K, P, F, S, and T, which have been shown to home into bone marrow. The results show significant enhancement in neural cell survival. On the other hand, KLT (KLTWQELYQLKYKGI) and PRG (PRGDSGYRGDS) were reported to modulate angiogenesis. RGD is a key binding sequence for cell attachment and KLT acts as a vascular

endothelial growth factor (VEGF) agonist. Binding these sequences to self-assembling peptide RADA16-I indicated the higher possibility to increase cell attachment and then promote endothelial cell long-term survival. Figure 2.15(a), (b) shows the molecular schematic of RADA16-I with the motifs for above applications.[29-30]

Figure 2.15. **(a)** Molecular structure of RADA16-I with the BMHP1 and BMHP2 functional motifs. **(b)** The molecular structure of RADA16-I with the PRG and KLT functional motifs. [29-30]

(a) (b)

2.4 The Anticancer Agent Ellipticine

The original strategy of the anticancer agent selection is the mode of action of the drug to eradicate cancer cells. There are many anticancer drugs have been discovered from natural resources. Most of the anticancer agents are very cytotoxic and their mode of action related to cancer biology. These anticancer chemicals are classified into five categories: antimetablites, covalent DNA binding drugs, noncovalent DNA binding drugs, inhibitors of chromatin function, and drugs affecting endocrin function.[6] The cytotoxicity of these drugs is usually very high, but most of them have severe side effects. Therefore, novel delivery systems are necessary to minimize the side effects and enhance the therapeutic efficacy.

Ellipticine was selected as a model of anticancer agent in this study because of the following reasons. First of all, ellipticine is an extremely hydrophobic agent, with a water solubility of 6.2×10^{-7} M.[48] Thus, amphiphilic molecules are required to stabilize them in aqueous solution. Self-assembling ionic-complementary peptides would be appropriate candidates to stabilize hydrophobic agent, ellipticine, in water or culture media. Second, ellipticine showed the fluorescent property in different state. Therefore, its photo physical properties make it easy to be monitored either in physicochemical characterization or *in-vitro* experiments. Third, ellipticine and its derivatives have shown anticancer activity as well.[34-35] The anticancer activity of ellipticine is due to its polycyclic structure, which intercalates between DNA base pairs and induces G_2-M-phase cell cycle arrest. Other molecules studies suggested that ellipticine acts via its binding to nucleic acids and inhibition of topoisomerase II (topo II) and topo II-mediated DNA damage.[49] Figure 1.2 in the previous chapter depicts the molecular structure of ellipticine with three different possible formations.

Chapter 3

Experimental Methods

3.1 Materials

The peptides AC8, EAK16-II, and EFK16-II were purchased from CanPeptide Inc. (Montreal, Canada) and used without further purification. The sequences of the peptides are AcN-FEFQFNFK-CNH_2 (Mw=1106.25 g/mol) AcN-AEAEAKAKAEAEAKAK-CNH_2 (Mw=1657 g/mol) and AcN-FEFEFKFKFEFEFKFK-CNH_2 (Mw=2265.61), respectively. A corresponds to alanine (ala), E to glutamic acid (glu), K to lysine (lys), F to phenylalanine (phe), N to asparagines (asn), and Q to glutamine (gln). The N-terminus and C-terminus of the peptide were protected by acetyl and amino groups, respectivelyThe estimation of average hydrophilicity of these peptides are -0.4 for AC8, 1.3 for EAK16-II and 0.3 for EFK16-II, and the ratio of hydrophilic residues to total number of residues is 50% for all of them. . Figure 3.1 depicts the molecular structure of these three peptides. Crude peptides were used in this study.

The anticancer agent ellipticine (99.8% pure) was purchased from Sigma-Aldrich (Oakville, ON, Canada). Tetrahydrofuran (THF, reagent grade 99%) was from Calendon Labratories Ltd. (Georgetown, ON, Canada). Cell culture reagents including Dulbecco's modified eagle medium (DMEM), fetal bovine serum (FBS) and penicillin /streptomycin was purchased from Invitrogen Canada Inc. (Burlington, ON, Canada). Trypsin-EDTA was purchased from Sigma-Aldrich (Oakville, ON, Canada). MTT assay and APOAF kit for cell

viability and apoptosis detection, respectively, were both obtained from Sigma-Aldrich (Oakville, ON, Canada).

Figure 3.1. Molecular structure of AC8, EAK16-II and EFK16-II[50]

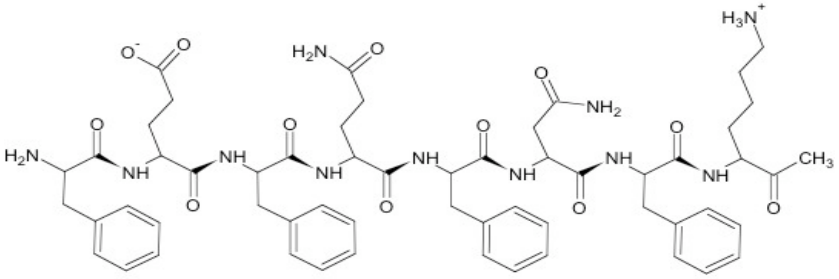

AC8: n-FEFQFNFK-c

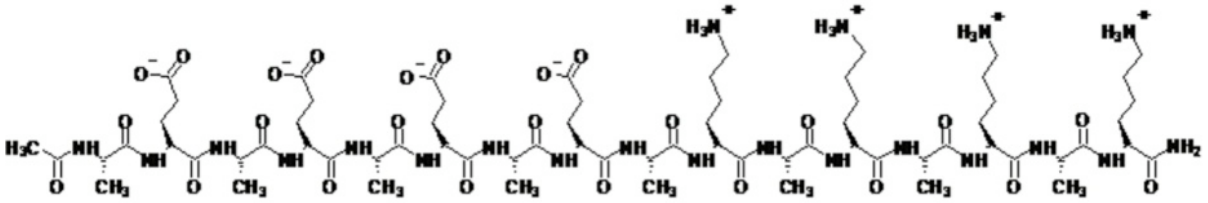

EAK16-IV: n-AEAEAEAEAKAKAKAK-c

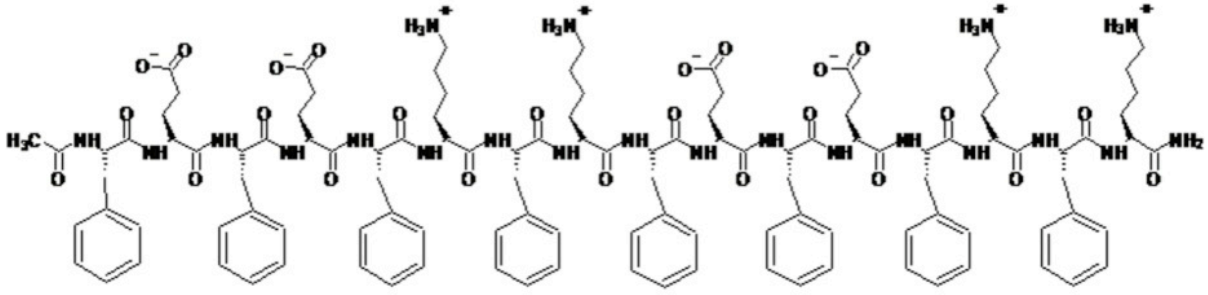

EFK16-II: n-FEFEFKFKFEFEFKFK-c

3.2 Peptide Solution Preparation

Peptide solutions were prepared for different experiments, such as surface tension measurement, static light scattering and complexation with anticancer compound. For surface tension and light scattering measurements, the peptide solutions were prepared by dissolving the peptide in pure water (18.2 MΩ; Millipore, Milli-Q A10 synthesis) at concentrations ranging from 0.001 mg/ml to 0.1 mg/ml. The solution was then sonicated in a bath sonicator (Branson, model 2510) for 10 min. Low AC8 concentrations (<0.005 mg/ml) were obtained by diluting the stock solution (0.005 mg/ml) using a 10-100 μl micropipette. The surface tension measurements were performed one day after the sample was prepared. The time-dependent light scattering (LS) measurements were performed less than 30 min after the solution preparation. All experiments were conducted at room temperature.

3.3 Surface Tension Measurement

The Axismmetric drop shape analysis-profile (ADSA-P) technique was used to study the dynamic surface tension of the peptide solutions over a period of 1 hr. The surface tension varied as a function of time in a dynamic process. The peptide solution was released at a speed of 0.04 ml/s for 5 s using a 1-ml motor-driven syringe to form a pendent drop at the tip of the syringe needle (inner diameter, 0.92 mm). The experimental sample chamber was saturated with pure water vapor to keep consistent humidity. ADSA-P system acquires images at 60s intervals for the first 3600 s (1hr). An optical Microscope magnified the images then CCD camera captured the images before transferring to the computer. All the images were digitized and analyzed to extract the drop profiles. The surface tension was obtained as a fitting parameter when the experimental drop profile was fitted to the

theoretical curve by the Laplace equation of capillarity. The schematic of the ADSA-P setup is shown in figure 3.2.

Figure 3.2. Schematic of ADSA-P experimental setup [51]

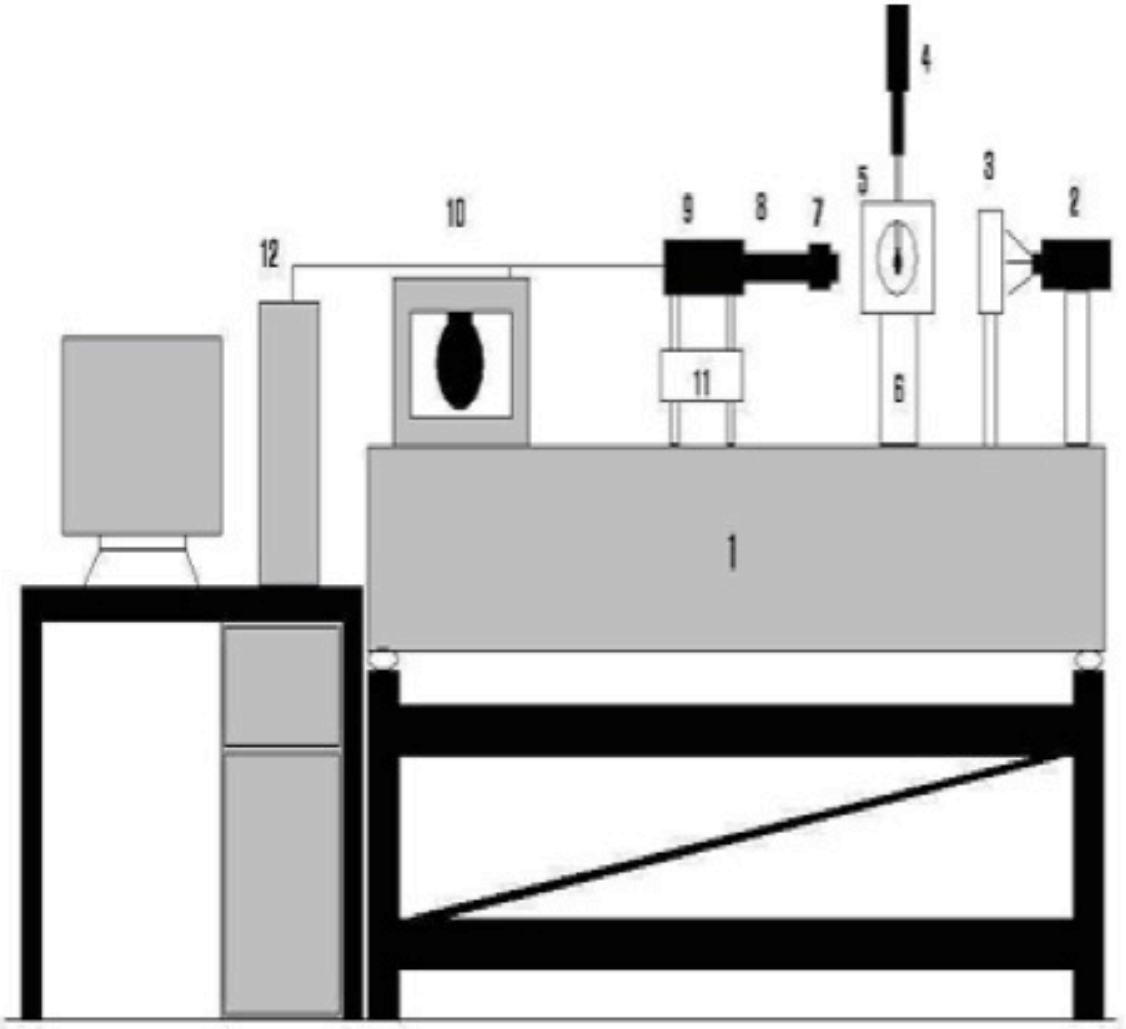

1-Work Station 2- Light Source 3- Diffuser 4- Syringe 5- Environment Chamber 6- Stage 7- Microscope 8- Lens 9- Camera 10- Monitor 11- Stage 12- Computer

3.4 Steady-state Light Scattering (SLS)

In static light scattering a beam of light is focused on the particle and the scattered light is detected with a photodiode detector. The intensity of this light is measured, which is

proportional to the molar mass and the concentration of the particles in solution. The following formula describes the phenomena:

$$I_{LS} \sim M_w.C \qquad (1)$$

I_{LS}: light scattering intensity, M_W: Molar mass weight-average, C: Sample concentration

The light scattering experiments were carried out on a steady state fluorescence system (type LS-100, Photon Technology International (PTI) London, ON, Canada) with a pulsed xenon flash lamp as the light source. The peptide samples were irritated at 314 nm, and the scattered light was monitored from 295 nm to 330 nm.[31] The light scattering peak arose from the interaction of the peptide AC8 aggregates and the incoming light. The excitation and emission slit width of monochromators were set at ½ and 2 turns to yield the spectra resolution of 1 nm and 4 nm, respectively. 80 μl of the peptide solution was transferred into a square cell by a micropipette for each test. The lamp intensity was monitored for each sample, and each scattering-intensity was divided by the lamp intensity to account for potential lamp fluctuations. The experiments were started 30 min after sample preparation. All samples were tested in 1-hr intervals initially, and every three hours in the second day, and then once a day or once two days over a period of two weeks.

The light scattering intensity was expected to increase with the size of the particles present in solutions. Fung et al. confirmed the sensitivity of LS to particle size previously by latex particles.[31] The solution with larger particles gives a larger LS intensity. The LS intensity was obtained with the PTI spectrofluorometer and monitored as a function of concentration. The DLS data (see below) also accompanied the LS data.

3.5 Dynamic light scattering (DLS)

Particle Size Distribution

The hydrodynamic diameter of the peptide assemblies and peptide-drug complexes were obtained on a Zetasizer Nano ZS (Malvern Instruments, Worcestershire, U.K.). The appropriate settings, viscosity, refractive index, and dispersant solvent, were set at for each measurement at 25 °C during the measurement. A small volume of 45 μL of the sample was transferred from the vial to a quartz microcell with a 3 mm light path (Hellma, Canada). The scattered light intensities of the samples were collected at the angle of 173°. This was known as backscatter detection. The relationship between the size of a particle and its scattered light intensity obtained with the multimodal algorithm CONTIN, which was provided in the software package Dispersion Technology Software 5.1 (Malvern Instruments, Worcestershire, U.K.). Three measurements were acquired to generate the intensity-based, volume-based and number-based size distribution plots.

Zeta Potential

The surface charge of AC8 assemblies and EPT-AC8 complexes in solution were determined by zeta potential measurements on a Zetasizer Nano ZS (Malvern Instruments, Worcestershire, UK) at 25°C. A prepared peptide solutions 20 μM AC8 solution was used for each measurement. The pH of the peptide solution was adjusted to the desired value using small amounts of 2 M NaOH or 2 M HCl. Samples were injected into a disposable cell (folded capillary DTS-1060 from Malvern, Worcestershire, UK) with a volume of ~1 ml and analyzed at constant voltage. The zeta potential distribution (in mV) was automatically

calculated from the electrophoretic mobility distribution based on the Smoluchowski formula. For each solution condition, the zeta potentials were repeated with two independent samples; at least three measurements were carried out for each sample. The zeta potentials reported herein correspond to the average of the peak values of the zeta potential distributions from the repeated measurements. The same method was applied for the measurement of the EPT-AC8 complexes and compared with the zeta potential of AC8 samples to determine the effect of complexicity on assemblies. The pH of the complexes was measured before each measurement.

The theory of the function of dynamic light scattering for measuring the size and zeta potential is explained in Appendix A.

3.6 Peptide-Ellipticine Complex Preparation

As discussed above, the peptide samples were prepared by dissolving peptide powder in pure water (18 MΩ; Millipore, Milli-Q system) at concentration of 0.01 to 0.5 mg/ml. The solutions were sonicated for 10 min in a tabletop ultrasonic cleaner (Branson, model 2510, USA).

The stock solution of ellipticine was prepared in THF at a concentration of 0.4 mg/ml by dissolving ellipticine crystals in pure THF. To fix ellipticine's concentration at 0.05 mg/ml, 250 μl of ellipticine-THF was transferred into a vial and then the THF was blown away with filtered air (0.22 μm pore size filter) for about 5 min to make a thin film of ellipticine at the bottom of vial. Afterwards, 1 ml of fresh peptide solution was added into ellipticine film to have the final concentration of ellipticine as 0.05 mg/ml followed by mechanical stirring at

900 rpm for 24 hr. 1ml of pure water was added into ellipticine instead the peptide solutions into another vial to make a control sample. All the vials and solvents were sterilized and the samples were prepared in a biological safety cabinet to avoid possible contamination, for cell culture experiments. The complexes were photographed with digital camera (Sony Cybershot) and characterized with different techniques: dynamic light scattering and fluorescence spectroscopy, to obtain complex dimensions and molecular states of ellipticine in the peptide-ellipticine complex. Figure 3.3 depicts the preparation method of the complex.

Figure 3.3 The schematic of preparation method of ellipticine-peptide complex

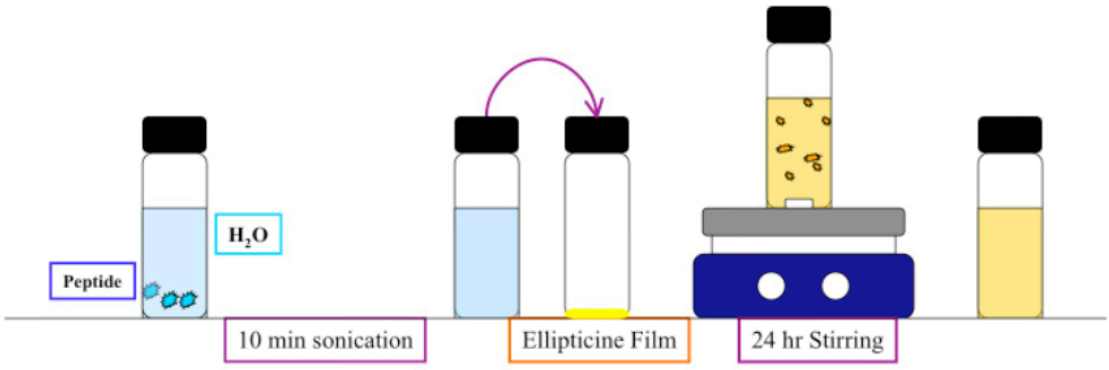

3.7 Fluorescence Spectroscopy

To study the molecular states of ellipticine in the complexes, fluorescence spectroscopy (type LS-100, Photon Technology International (PTI) London, ON, Canada) was applied. 60 µl of peptide-ellipticine solution was transferred to a microcell, 10 mm light path quartz glass (Hellma, Canada), and then tested on the spectrofluorometer. The excitation was set at 294 nm and the emission was set to be collected from 320 to 650 nm. The excitation and emission slit width were set at 1 and 4 nm, respectively. The fluorescence intensities were monitored

for each sample and then normalized with an ellipticine standard sample (2 μM in ethanol, sealed and degassed), to account for potential lamp fluctuations. The fluorescence spectra of ellipticine-peptide complex solutions showed major peaks around 430 nm and 520 nm, which represent neutral and protonated state of ellipticine molecules, respectively.[35]

3.8 Cell lines and culture

Two cancer cell lines, non-small cell lung cancer cell A549 and breast cancer cell MCF-7, were kindly provided by Dr. Mingyao Liu at the University of Toronto for *in-vitro* cellular toxicity experiments on the peptide-drug complexes. These cell lines were cultured in DMEM containing 10% fatal bovina serum (FBS) and 1% penicillin/streptomycin, and kept in an incubator at 37°C and 5% CO_2. When the cells grew to reach about 90% confluence, they were detached from the culture dish with trypsin-EDTA, centrifuged at 500 rpm for 5 min, and then resuspended in fresh cell culture media at a concentration of 5×10^4 cells/mL. The cells were seeded in 96 and 6-well plate (Costar) dishes for viability and apoptosis assays. Figure 3.4 shows the MCF-7 and A-549 cell lines with the 100 μm scale bar.

Figure 3.4 A-549 on left and MCF-7 on right. Scale bar: 100 μm.

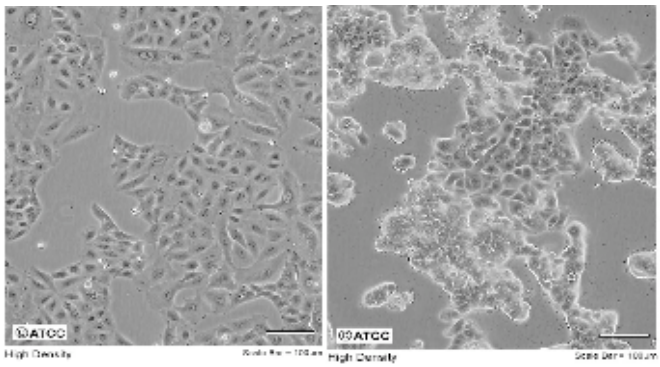

3.9 Cytotoxicity assay (MTT)

The MTT ((3-(4,5-Dimethylthiazol-2-yl)-2,5-diphenyltetrazolium bromide, a tetrazole) assay kit (TOX1 from Sigma-Aldrich, Oakville, ON, Canada) was applied for the cell viability after treatments with the peptide-drug complexes. 200 μL of the cell suspension was seeded on a flat bottom 96-well plate (costar) with a concentration of 5×10^3 and 1×10^4 cell/well for A549 and MCF-7 cell lines, respectively, followed by incubation for 24 hr at 37°C and 5% CO_2. After 24 hr, the culture media was removed from the each well to be replaced by 50 μL of the treatment and 150 μL of fresh culture media. The plates were incubated for 6, 24, and 48 hr prior the MTT assay. 5 mg of solid MTT was dissolved in 3 mL of PBS solution, followed by 10 times dilution with culture medium. All the treatment and medium were taken out from each well, and then 100 μL of the MTT solution was added into each well of the treated cells. The plates were incubated for 4 hr before addition of 100 μL solubilization solution (anhydrous isopropanol with 0.1 N HCl and 10% Triton X-100). After overnight incubation, the absorbance at 570 nm was collected for each well by a microplate reader (BMG FLUOstar OPTIMA, Germany) and subtracted by the absorbance of background signals at 690 nm. The absorption intensities were averaged from 4 replicates and normalized to the untreated cells (negative controls) to generate the cell viability. The theory behind of the MTT assay to determine cell viability is explained in Appendix B.

3.10 Flow Cytometry

The Annexin V-FITC Apoptosis Detection kit (APOAF, Sigma-Oakville, ON, Canada) was used for detection of apoptotic and necrotic cells using flow Cytometry. Both MCF-7 and

A549 cell lines were seeded on 6-well plates (Costar) with a concentration of 1×10^5 cell/ml in a 2 ml medium (2×10^5 cell/well) and then incubated for 24 hr prior to treatment After 24 hr, the culture medium was replaced with 500 μl of treatment (including complexes and control samples) and 1500 μl of a fresh culture medium. The cells were incubated with the treatment for 6, 24, and 48 hr prior to apoptosis analysis. After the treatment period, the medium was collected from the wells in a 15 ml centrifuge tube to collect dead cells floating in the medium. 1 ml Trypsin-EDTA was added to each well and the plates were incubated for 5 min to collect adherent cells. After the incubation, 2 ml medium was added to each well to detach the cells and then transfer into the same centrifuge tube. The tube was centrifuged for 5 min at 800 rpm. The supernatant was discarded from each tube and cell pellets were resuspended in ice-cold 100 μl of 1x binding buffer (100 mM HEPES/NaOH, pH 7.5, 1.4 M NaCl and 25 mM $CaCl_2$). After suspension, cells were transferred to a 1.5 ml eppendorf tube, and 1 μl of Annexin V-FITC solution and 5 μl of PI were added to each tube. The tube was kept in ice and dark for 10 min and then 400 μl 1x binding buffer was added prior to Flow Cytometry analysis. Flow Cytometry (BD Biosciences, BD FACSVantage SE Cell Sorter, USA) detected the apoptosis and necrosis within 30 min. FL1 and FL3 channels were considered for Annexin V-FITC and PI, respectively. The cells labeled with Annexin V-FITC represented the early apoptosis. Flow Cytometry data analysis has been done by software FlowJo 8.7. The theory of the function of Flow Cytometry in terms of apoptosis detection and cell sorting is described in Appendix C.

Chapter 4

Results and Discussion

4.1 Concentration effect on assembly of the peptide

Concentration is a key parameter in controlling the assembly of self-assembling peptides. The concentration dependence of self-assembling peptides is expected to be similar to that of biosurfactants, which have both hydrophobic and hydrophilic parts. The concept of micellar systems can be applied for amphiphilic peptides; it is anticipated that the peptides would be disolved in a solution below a critical assembly concentration (CAC), and starts to assemble at or above CAC. This expectation is acceptable since the CAC has been reported for many peptides such as EAK16s.[31, 46] Time is an important factor in the kinetics of assembly. Previously, Fung et al. have determined the CAC of a self-assembling peptide through different techniques, including surface tension measurement, light scattering and AFM imaging.[31] In this study, we have characterized how the concentration affects the assembly of the all-complementary peptide AC8.

4.1.1 Surface tension measurement

The dynamic (or time dependent) surface tension is plotted over the time for a range of concentrations of AC8 from 0.001 to 0.05 mg/ml. Figure 4.1(A) shows the plot for the extremely low concentrations of 0.001 and 0.002 mg/ml, surface tension does not change significantly with time. At high concentrations of AC8 (> 0.01 mg/ml) the surface tension decreases exponentially with time. It drops fast at the first about 200 sec, and slowly reaches

the equilibrium. From the concentration of 0.003 to 0.01 mg/ml the dynamic surface tension profile shows an induction time at the beginning.

The equilibrium surface tension was determined by two methods: “end point” or “ last measurement” meethod and “extrapolation” method. The first method calculated the equilibrium surface tension by averaging a certain number of points at the end of each run (10 points were considered in this study).[52] For the second method, the surface tension is plotted versus $1/t^{0.5}$ in figure 4.1(B). This plot is based on the assumption of a diffusion-controlled mechanis.[53] The equilibrium surface tension is estimated as the intercept of a straight line, which is fitted to the portion of plot ($1/t^{0.5}$ <0.05), with the *y*-axis The equilibrium surface tensions obtained by the extrapolation method were plotted versus of concentration of AC8 in figure 4.1(C). The plot shows that the equilibrium surface tension of very low concentrations of AC8 (0.001-0.003 mg/ml) is close to water surface tension, while the concentration increases, the surface tension drops significantly to the minimum at 49.0±1.4 mJ/m^2. The small dip curve in the graph is due the small impurity of the peptide. It has been reported depending on the surface activity, the impurities may cause either minimum or higher break point in the surface tension versus peptide concentration.[31] The similar trend is obtained from the “end point” method which is shown in the same figure 4.1(C). The critical assembly concentration could be determined either at the concentration before the small dip or the intersection of two linear lines fitted on the data in two distinct part of the graph. The results from both methods presented in figure 4.1(C) and (D) demonstrated the critical assembly concentration of AC8 as around ~ 0.01-0.02 mg/ml.

Induction time in dynamic surface tension measurement is one of the characteristics of the surface-active molecules. The surface tension drops after this time as a result of a sufficient number of molecules adsorbed at the surface to affect the surface tension. This induction time is also related to size and amphiphilicity of the particles.[31] The induction time was plotted with the concentration of AC8 in figure 4.1(E). It shows AC8, a surface-active peptide, has a induction time for the very low concentrations. At the concentration of lower than 0.003 mg/ml, the induction time was too large to be recorded during experimental period. However, as the concentration decreased the induction time dropped significantly. Almost no induction time was observed for AC8 concentrations above 0.01 mg/ml, which may consider as critical assembly concentration.

Figure 4.1. **(A)** Dynamic surface tension of AC8 solutions. The concentrations are ranging from 0.001 to 0.05 mg/ml. **(B)** Surface tension versus $1/t^{0.5}$ for different concentrations of AC8 (0.001-0.05 mg/ml) for $1/t^{0.5} < 0.05$**. (C)** Relationship between equilibrium surface tension and concentration of AC8 peptide in water solution. When the concentration of peptide increases the surface tension drops dramatically to the minimum point, then it increases slightly to reach the plateau based on the results from "extrapolation" method (▲) and "end point" method (◆) The critical assembly concentration is found around 0.01- 0.015 mg/ml. **(D)** Induction time versus concentration of AC8 peptide. The induction time is observed as a period before the surface tension starts to drop in dynamic surface tension measurements. The induction time drops significantly from after concentration of 0.005 mg/ml and after the concentration of 0.01 mg/ml induction time is close to zero. Followed by next pages.

A

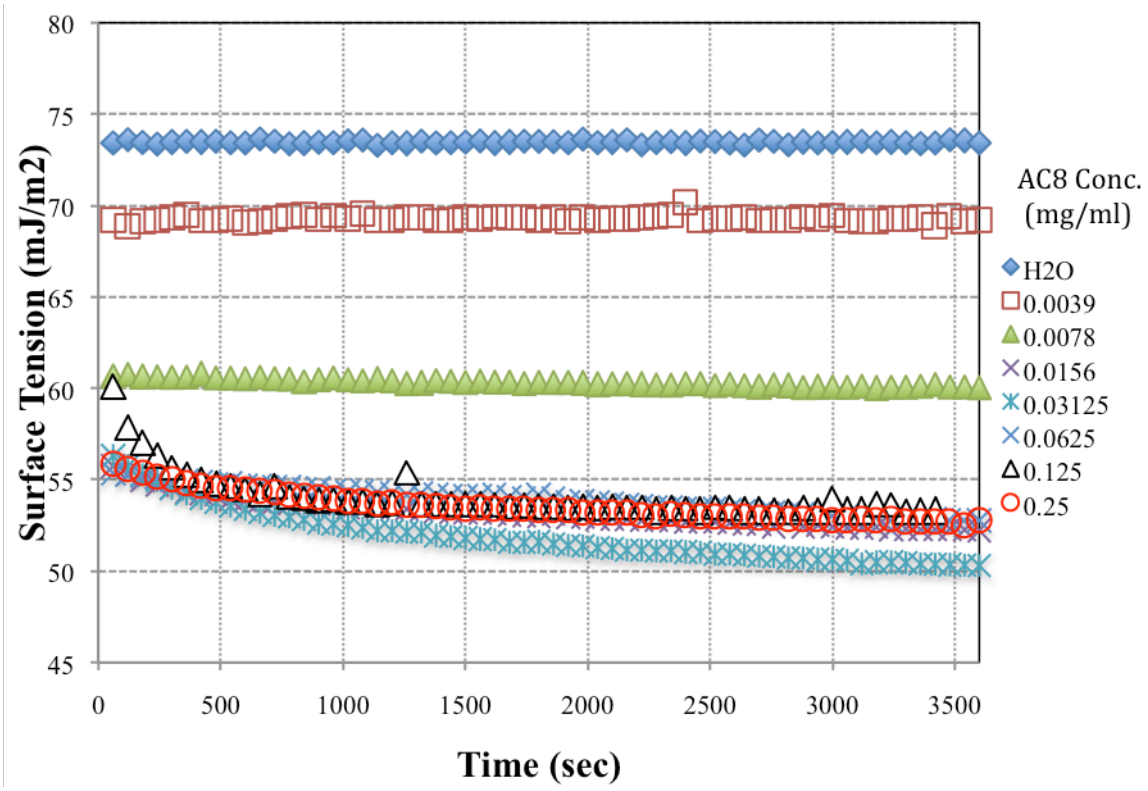
Surface Tension (mJ/m2)
80
75
70
65
60
55
50
45
0
500
1000
1500
2000
2500
3000
3500
Time (sec)
AC8 Conc. (mg/ml)
H2O
0.0039
0.0078
0.0156
0.03125
0.0625
0.125
0.25

B

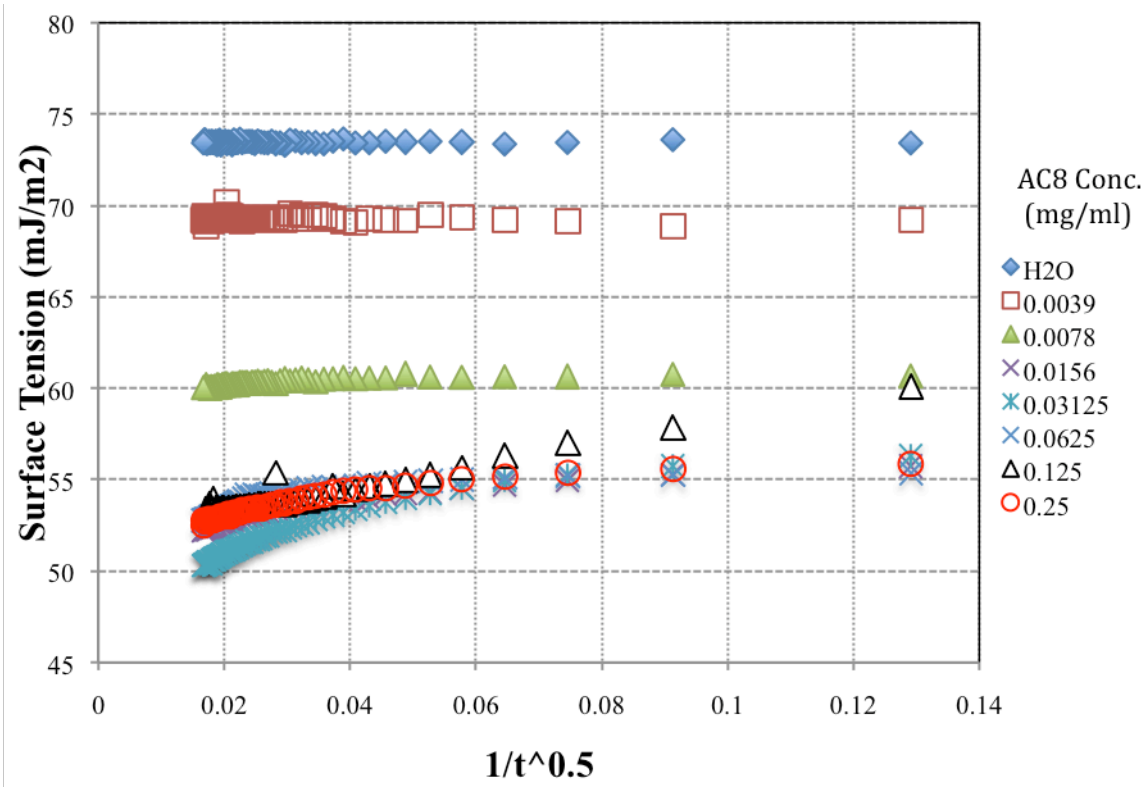
Surface Tension (mJ/m2)
80
75
70
65
60
55
50
45
0
0.02
0.04
0.06
0.08
0.1
0.12
0.14
1/t^0.5
AC8 Conc. (mg/ml)
H2O
0.0039
0.0078
0.0156
0.03125
0.0625
0.125
0.25

C

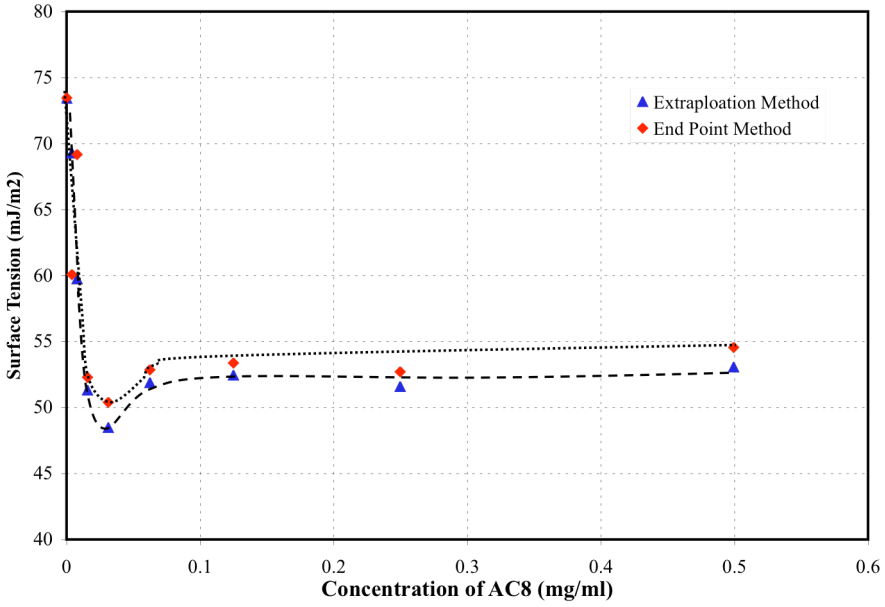
Extraploation Method
End Point Method
Surface Tension (mJ/m2)
Concentration of AC8 (mg/ml)
80
75
70
65
60
55
50
45
40
0
0.1
0.2
0.3
0.4
0.5
0.6

D

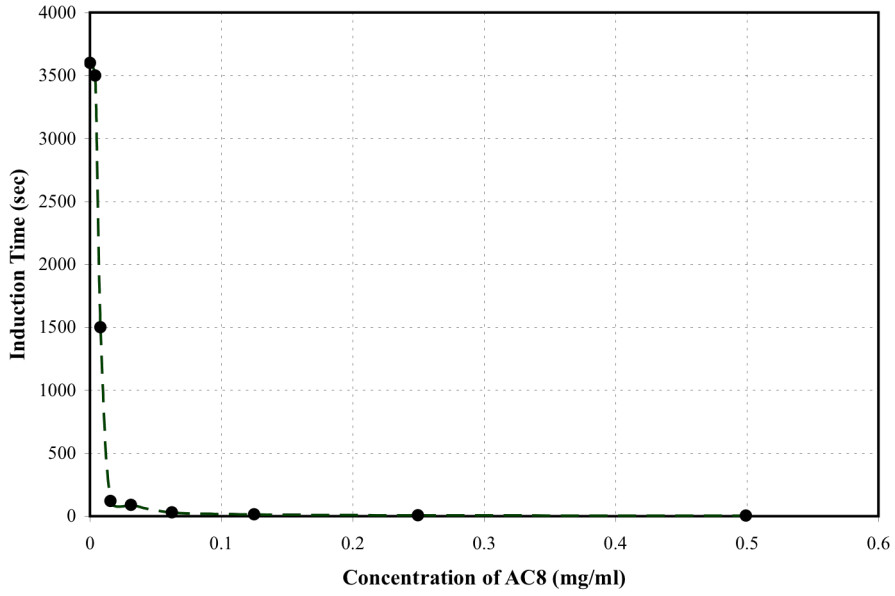
Induction Time (sec)
Concentration of AC8 (mg/ml)
4000
3500
3000
2500
2000
1500
1000
500
0
0
0.1
0.2
0.3
0.4
0.5
0.6

4.1.2 Light Scattering

Light scattering intensity from the solution is proportional to the dimension of the particles present in the solution. The light scattering intensity from the peptide solutions is plotted in figure 4.2. Figure 4.2(A) shows the normalized light intensity as a function of time. The experiments have been performed over a week for a range of concentrations from 0.001 to 0.05 mg/ml. This plot shows the profiles in two groups depending on the concentration. The concentration of around 0.01 mg/ml would be a breakpoint between high and low concentrations, so it would be presumed as critical assembly concentration (CAC). The LS intensity of the peptide with the concentration below CAC seems to remain unchanged over time. On the other hand, a sharp increase occurs for the concentration above CAC at the first 48 hr before they reach to plateau.

In addition, figure 4.2 (B) shows the equilibrium LS intensity as a function of concentration. These data indicates that the equilibrium LS intensity is has no significant difference for the low concentrations, say below 0.01. However, the concentrations above that the equilibrium LS increases by increasing the concentration. This experiment demonstrates AC8 assemblies in bulk solutions with time.

Figure 4.2. **(A)** Light scattering of AC8 peptide solutions with time in different concentrations from 0.001 to 0.05 mg/ml. The data are separated into two groups depending on the concentration of peptide. The light intensity of high concentration group (0.01-0.05 mg/ml) increases sharply at the first 10 hr and then approaches to plateau after 50 hr. However, in the low concentration group (0.001-0.008 mg/ml), the LS intensity does not change significantly over the time. **(B)** The intensity of light scattering plotted versus concentration of AC8. The normalized light intensity of low concentration of AC8 are almost zero, but the intensity of light scattering of AC8 with the concentrations above 0.01 increases by increasing the concentration. Followed by next page.

A

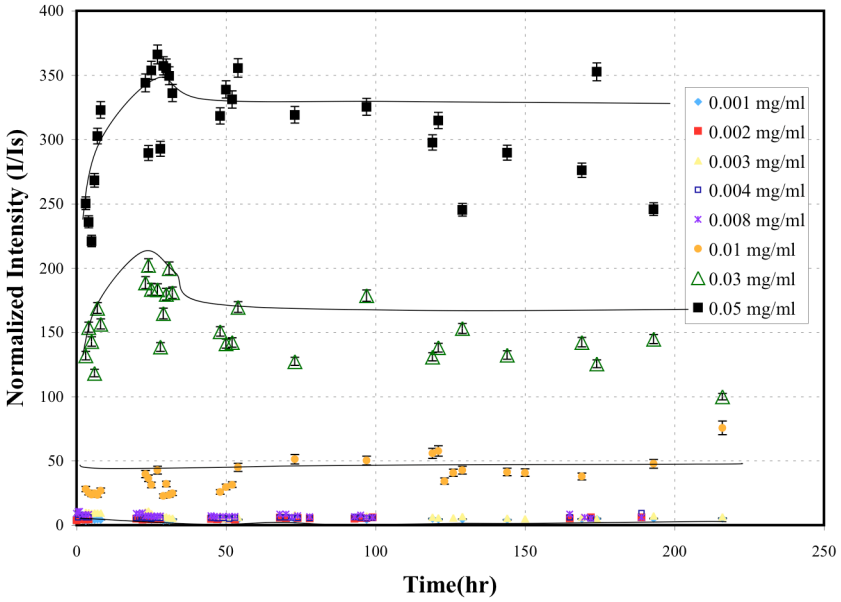
Normalized Intensity (I/Is)
Time(hr)
0.001 mg/ml
0.002 mg/ml
0.003 mg/ml
0.004 mg/ml
0.008 mg/ml
0.01 mg/ml
0.03 mg/ml
0.05 mg/ml

B

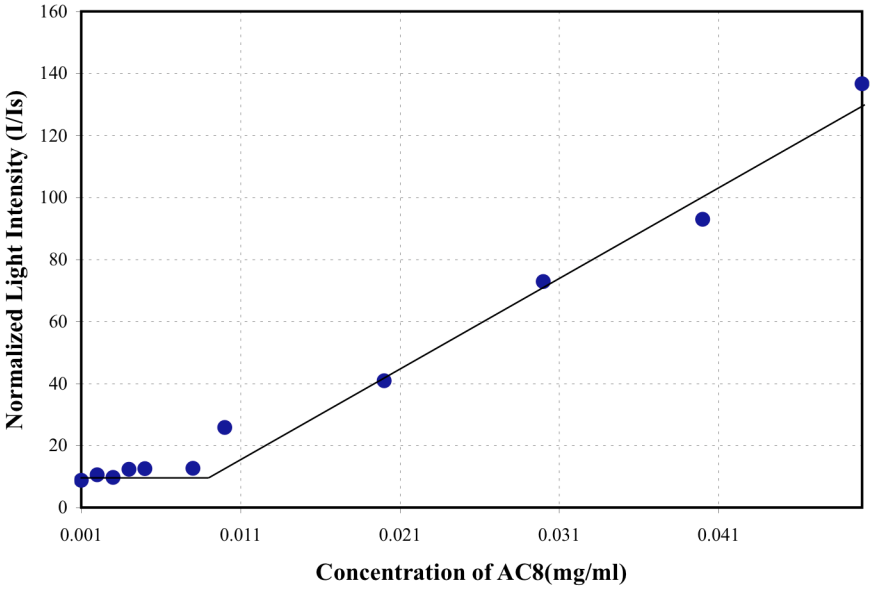
Normalized Light Intensity (I/Is)
Concentration of AC8(mg/ml)

4.1.3 Particle Size Distribution

Dynamic light scattering method is the professional technique to determine hydrodynamic diameter of particles in solution. The hydrodynamic size of AC8 peptide was found relatively larger for low concentrations below CAC, while above CAC the size decreased significantly in sense of assembly of the particles. The range of concentrations of AC8 was prepared for this experiment at 0.003 to 0.5 mg/ml. The Figure 4.3 shows the hydrodynamic size of particles versus concentration of AC8 after 24 hr and 48 hr sample preparation.

Figure 4.3. Hydrodynamic diameter (nm) for varying concentrations of AC8 peptide (numeric-based size distribution)

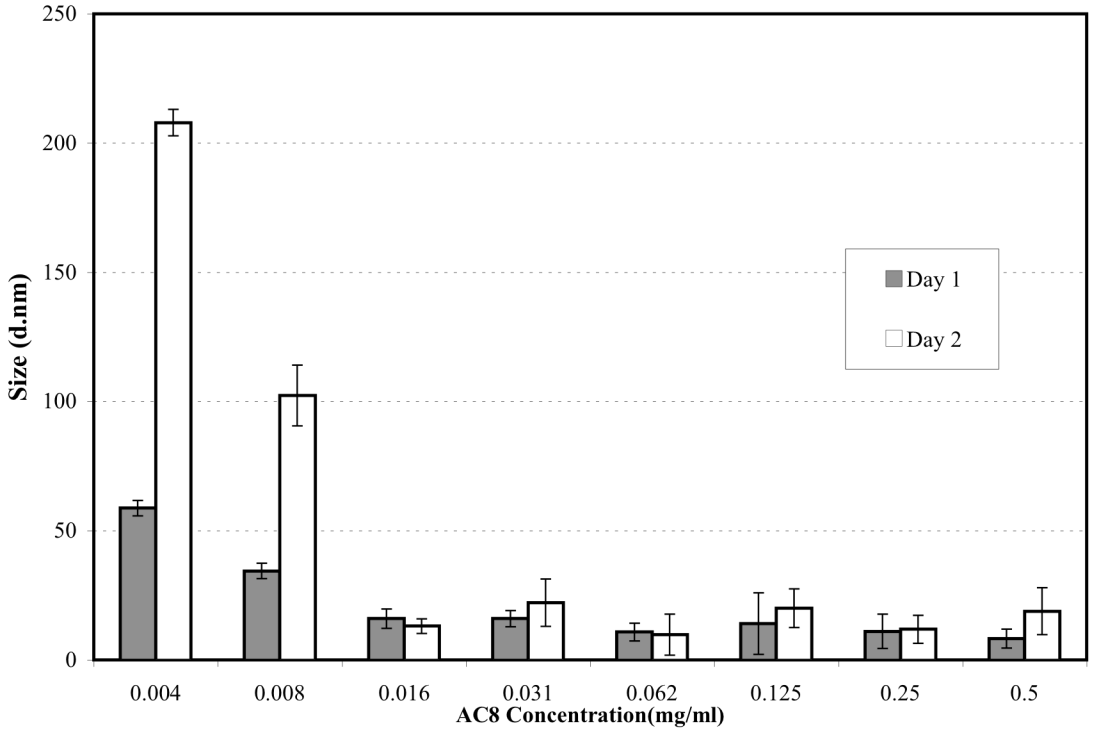

4.1.4 Zeta Potential

Zeta potential measurement was performed to determine the surface charge of AC8 assemblies in solution. The net surface charge of particles helps to investigate the tendency

of the particle to aggregate and absorb onto surface. The magnitude of the zeta potential indicates the potential stability of the colloidal system. Theoretically, if all the particles in suspension have a large negative or positive zeta potential then they will tend to repel each other and to tendency to flocculate (i.e., no aggregation). However, if they have lower zeta potential, there is no force to prevent them from flocculating. The most important factor that affects zeta potential is pH. Basically the zeta potential value on its own without a quoted pH is a meaningless number. Zeta potential alters in solution by adding alkali or acid. Adding alkali to solution the particles will tend to be more negative charge and then by adding acid in suspension the particles change to neutral from negative and any further addition of acid can cause a build up of positive charge. Therefore, a zeta potential versus pH curve will be positive at low pH and negative at high pH. The point where the plot passes the zero zeta potential is called the isoelectric point. It shows normally where the colloidal system is less stable.[54-55]

Figure 4.4 shows the zeta potential versus pH of the 0.02 mg/ml AC8 solution. The isoelectric point derived from this curve is about 7.04. It is comparable from the calculated value for theoretical values as 7.45. The theoretical value is determined by regressed theory. This method is based on the pK_a and pK_b for major acidic and basic groups. In the case of acid-rich proteins this equation will be applied:

$$pI = pK_a - \log R \qquad for \quad R \geq 1 \tag{1}$$

while in the symmetrical case of base-rich proteins:

$$pI = pK_b - \log R \qquad for \quad R \leq 1 \tag{2}$$

in the case of amino acid sequence with an almost balance acid/base composition the pI will be the average of (1) and (2):

$$pI = \left(pK_a + pK_b\right)/2 \qquad (3)$$

R is the molar ratio of acidic group over basic group. In AC8 case, because of glutamic acid and lysine R is equal to 1. Regressed acidic and basic dissociation constants were determined to be pK_a=4.9 and pK_b=10.0. These calculation shows pI as 7.45 for AC8 wich is comparable with experimental value as 7.04. Note that the isoelectric and pH was measured here for the mixture of monomers and aggregates not the monomers alone.[57]

Figure 4.4. Zeta potential of AC8 as a function of pH. The standard deviation of zeta potential are less than 3 mV.

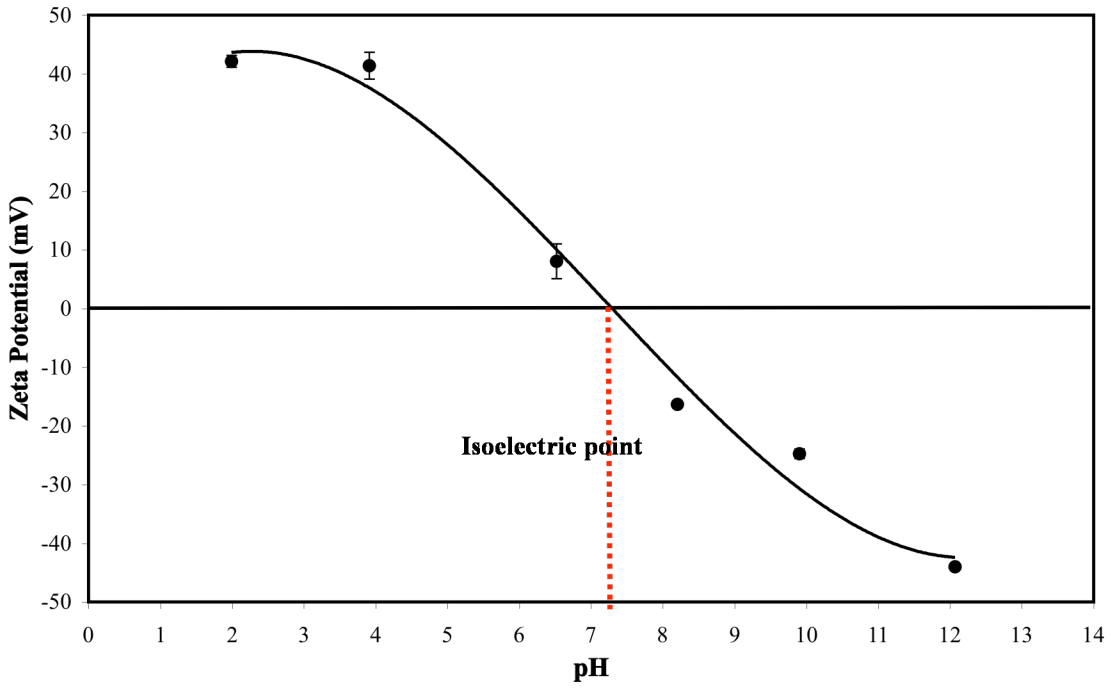

4.2 Peptide-drug complex formulation

Ellipticine was selected as a model of anticancer agent in this study because of the following reasons. First of all, ellipticine is an extremely hydrophobic agent, with a water solubility of 6.2×10^{-7} M.[48] Thus, amphiphilic molecules are required to stabilize them in aqueous solution. Self-assembling peptides would be appropriate candidates to stabilize the hydrophobic agent, in water or culture media. Second, ellipticine is fluorescent compound that emits the light in different wavelength at certain excitation wavelength. Therefore, its fluorescence properties make it conventional to be monitored either in physicochemical characterization or *in-vitro* experiments. Third, ellipticine and its derivatives have shown anticancer activity as well.[34-35] The anticancer activity of ellipticine is due to its polycyclic structure, which intercalates between DNA base pairs and induces G_2-M-phase cell cycle arrest. Other molecules studies suggested that ellipticine acts via its binding to nucleic acids and inhibition of topoisomerase II (topo II) and topo II-mediated DNA damage.[49] Figure 2.1 depicts the molecular structure of ellipticine with three different possible formations. An appropriate peptide-drug complex in terms of particle size, solubility and activity is the first step toward developing a delivery system for ellipticine and further for other hydrophobic anticancer agents.

Therefore, complexation of anticancer agent, ellipticine, with self-assembling peptide has been studied in this work. Since, peptide can self-assemble over the time, there is a competition between peptide-peptide association and peptide-ellipticine complexation. To better understand of the complexation of self-assembling peptide and ellipticine, several

physicochemical characterization experiments, such as fluorescence spectroscopy and dynamic light scattering, were performed in this study.

As discussed above, fluorescence property of ellipticine in aqueous solution helps characterization of complex in different environment. Basically, fluorescence spectra of ellipticine in colloidal suspension show different peaks depend on the dispersants and concentrations. The fluorescence of the ellipticine suspension in neutral form is around 430 nm and the protonated form of ellipticine exhibits the major peak at 520 nm. The crystalline form of ellipticine in some environment shows a maximum peak at ~470 nm, which is due to the colloidal suspension systems.[35] Fluorescence spectroscopy with PTI has been applied in this study to determine ellipticine form in all-complementary peptide AC8.

Dynamic light scattering have also applied for particle characterization of peptide-drug nanoparticles.

4.2.1 Fluorescence Spectroscopy

4.2.1.1 Sequence effect on peptide-ellipticine complexation

In this study, three different peptides including AC8, EAK16-II and EFK16-II were used for ellipticine stabilization to determine the sequence effect on ellipticine formation. Since, ellipticine is fluorescent, it shows distinct maximum peak in fluorescent spectra depending its interactions. The complexes with ellipticine and peptides were prepared at fixed concentrations of 0.1 mg/ml and 0.5 mg/ml for ellipticine and peptides, respectively. The previous study in by S. Fung have shown the optimum ratio for peptide-to-ellipticine as 5:1.[24,28] Figure 4.5(A) and (B) shows the fluorescent spectra for AC8, EAK16-II and EFK16-

II and the control sample of ellipticine in pure water since peptides are prepared in pure water. The complexes with AC8 and EFK16-II exhibits a peak at ~430 nm which indicates the presence of neutral form of ellipticine. Besides the peak at 430 nm, there is evidence of a peak at ~ 470-490 nm, indicating the presence of small portion of ellipticine in crystalline form for EPT-AC8 and a peak at 520 nm for EPT-EFK16-II. On the other hand, the spectra of ellipticine in EPT-EAK16-II shows the dominant peak at ~ 520 nm, which is the evidence of protonated form of ellipticine. The control sample of ellipticine in water without a peptide had a similar fluorescence spectrum as EPT-EAK16-II with the peak around 520 nm, but in with much less intensity. The reason of the similarity of the spectra of EPT-H2O and EPT-EAK16-II but not the other two complexes is due to the higher hydrophilicity of the EAK16-II compare to AC8 and EFK16-II. Ellipticine forms more in protonated state in more hydrophilic environment, while in more hydrophobic environment stays neutral. The ellipticine and peptide interaction is directly related to molecular structure of the peptide solution. Figure 4.5(C) shows the photograph of the three complexes after 24 hr stirring on magnetic stir plate. The appearance of the complexes indicates the more protonated complex is more yellowish and the more neutral complex is more colorless.

Figure 4.5. Fluorescence spectra of the peptide-ellipticine complexes. (**A**)The blue and red arrows indicate the fluorescence from neutral (~ 430 nm) and protonated (~520 nm) ellipticine, respectively. The green arrows indicates the low fluorescence intensities from 450-470 nm representing the crystalline form of ellipticine. (▲) EAK16-II, (■) EFK16-II , (♦) AC8 and (✕) Water in corporation with Ellipticine. (**B**) The fluorescence spectra of EPT in water. (**C**) The photograph of the three complexes.

A

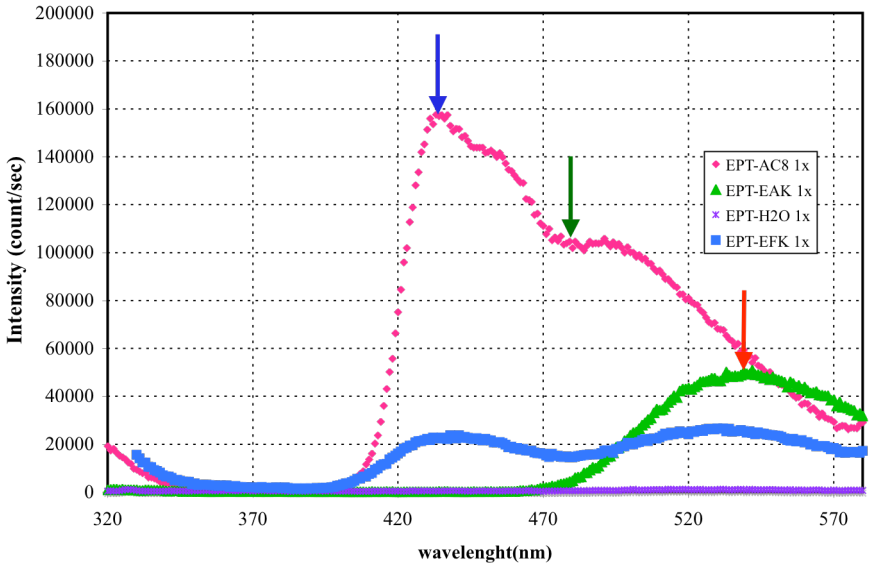
200000
180000
160000
140000
120000
100000
80000
60000
40000
20000
0
Intensity (count/sec)
320
370
420
470
520
570
wavelenght(nm)
EPT-AC8 1x
EPT-EAK 1x
EPT-H2O 1x
EPT-EFK 1x

B

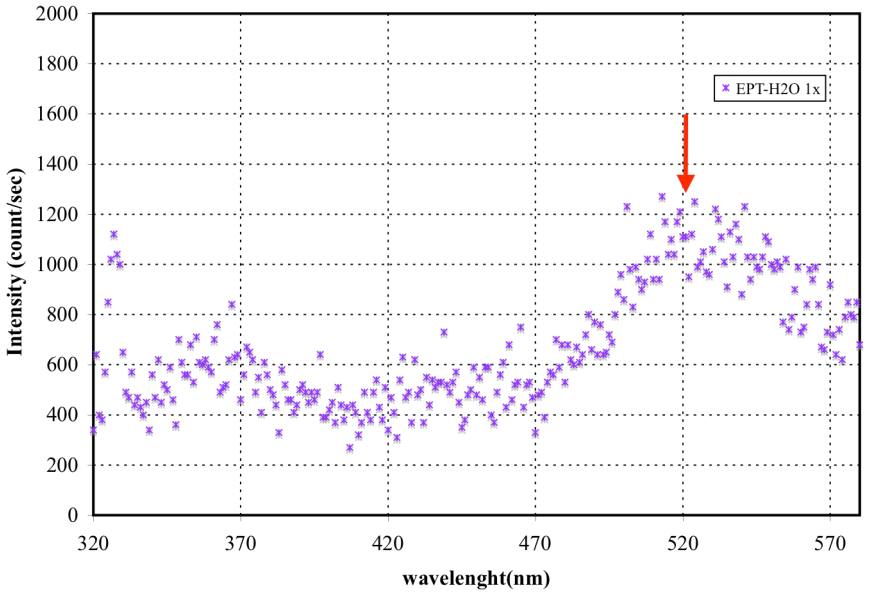
2000
1800
1600
1400
1200
1000
800
600
400
200
0
Intensity (count/sec)
320
370
420
470
520
570
wavelenght(nm)
EPT-H2O 1x

C

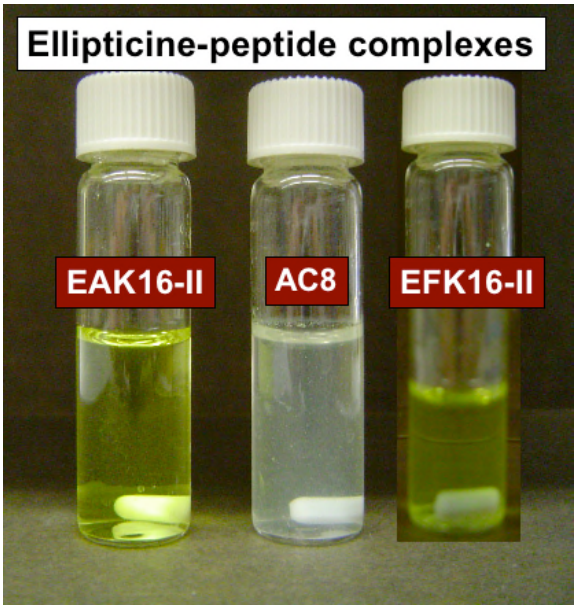

4.2.1.2 Concentration Effect on peptide-ellipticine complexation

The second part of this study is peptide concentration effect on ellipticine stabilization. In this study we focused on all-complementary AC8 peptide to stabilize ellipticine in neutral form. Ellipticine was stabilized in different concentrations of all-complementary peptide AC8 in a range of 0.01-0.3 mg/ml to find out the optimized formulation. The Ellipticine concentration was fixed at 0.05 mg/ml in solution. The fluorescence spectrum of peptide-EPT complexes were monitored at different concentrations of AC8 with the fixed concentration of ellipticine at 0.05 mg/ml over 120 hr. Figure 4.6 shows the peptide concentration effect on the formation of peptide-ellipticine complexes through fluorescence spectra. Ellipticine formed in two distinct states, neutral and crystalline form, even at low AC8 concentrations. The results show that the dominant contemporary state of ellipticine in AC8 solution is neutral form. Such a neutral ellipticine must be stabilized in a hydrophobic

environment provided by peptide assemblies. This is anticipated because of the four-phenylalanine residues in AC8 structure provide more hydrophobic environment than the other peptides as discussed above about hydrophilicity of the self-assembling peptides.

Figure 4.6. **(A)** Fluorescence spectra of the complexes of ellipticine at fixed concentration of 0.05 mg/ml and various concentration of AC8 peptide from 0.01 to 0.3 mg/ml.

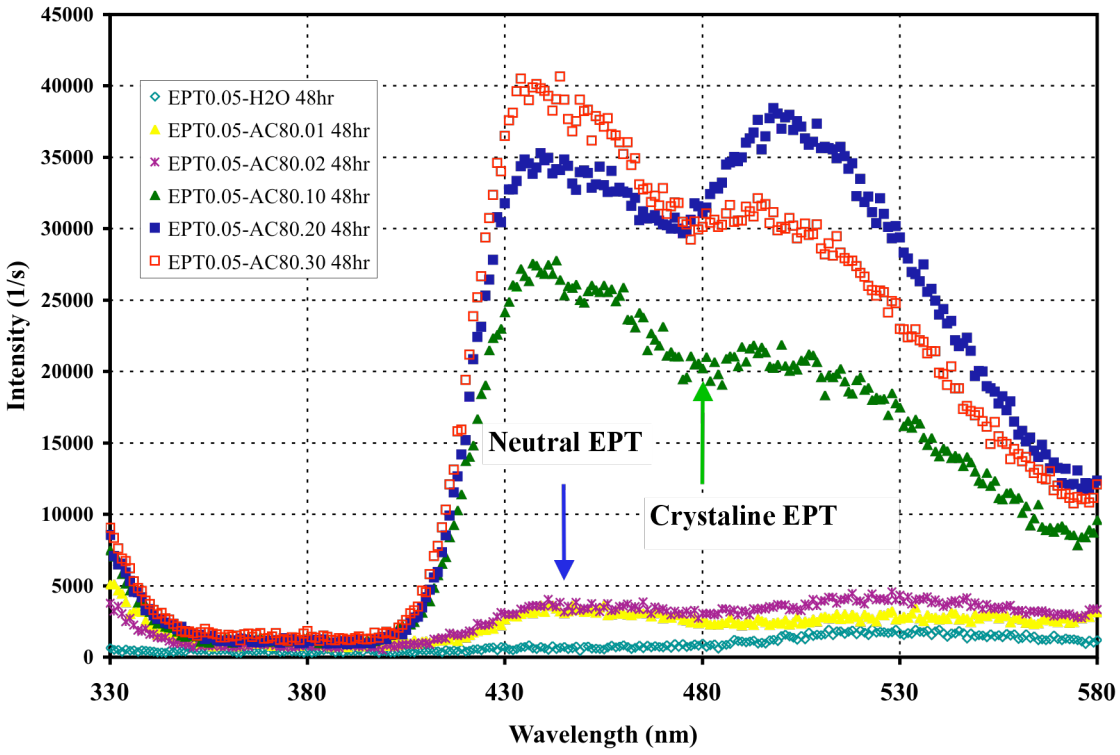

Since the peptide assemblies happened at concentrations above the CAC, the AC8 concentrations were selected from CAC and above CAC to encapsulate the ellipticine. The peptide assemblies are assembled into b-sheet structures at the CAC and above concentrations. Therefore, we assume that the complexation with any hydrophobic compounds, such as ellipticine, is happened when the peptide is assembled to encapsulate EPT. From the low concentration of AC8 as 0.01 mg/ml to 0.3 mg/ml the dominant stable neutral form of ellipticine was observed. Figure 4.7 shows the stability of neutral form of

ellipticine over the time for the all peptide-ellipticine complexes. In this figure, the normalized intensity of each complex at the wavelength of ~ 430 nm (average of 21 data points around 430 nm, (420-440 nm)) are shown over the time. As discussed above the lower AC8 concentrations with ellipticine shown the relatively lower intensities but more stable neutral ellipticine over the time. However, the complexes with the higher concentrations have a significant increase in fluorescent intensity compare to low concentrations. This is an evidence of formation larger particles in the complex and relatively low stability over the time. This is also confirmed by figure 4.6, which shows the increasing the intensity over the time and reaching to plateau after about three days. At the same time, the particle size and the zeta potential of the complexes was determined with dynamic light scattering, which agreed the difference between low and high concentrations of AC8 to make the stable complex. The results are shown in next section. Figure 4.8 is a photograph of the peptide-ellipticine complexes at different peptide concentrations. It shows the formation of colloidal suspensions of ellipticine-peptide solutions after ~24 hr stirring. The control sample, without AC8, remained clear compared to the complex solutions. Here, the ellipticine concentration is 0.1 mg/ml and the AC8 concentration varies from 0.01 to 0.3 mg/ml. From the low concentration to high concentration of AC8 in samples, the appearance of the sample varies from clear to turbid. The turbidity of the complexes of high concentrations, more than 0.1 mg/ml, is obvious and the stability is relatively low comparing the others. The stability of the complexes was determined by leaving the samples for several hours without stirring. The high peptide concentrations complexes have shown phase separation faster than the low concentration ones.

Figure 4.7. The stability of the neutral state of ellipticine in different concentration of AC8 peptide over the time.

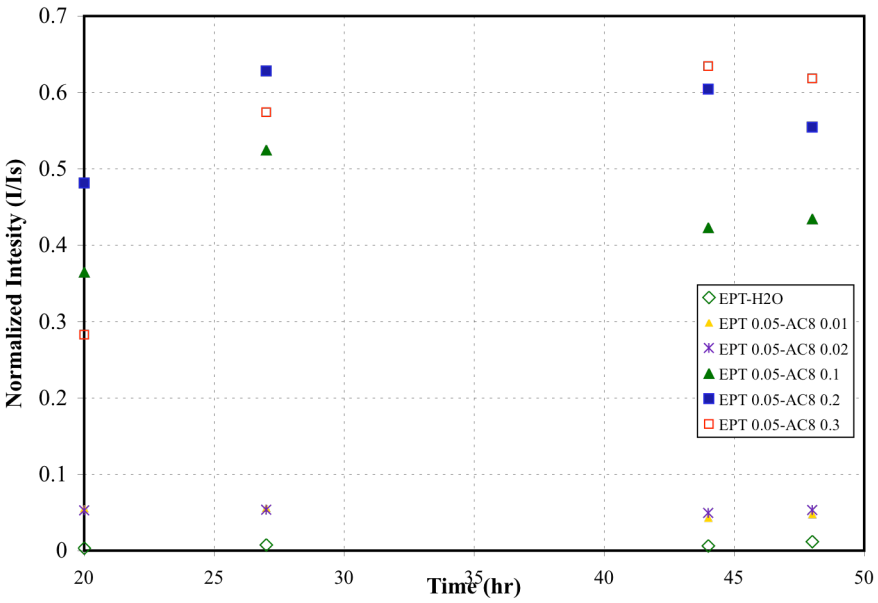

Figure 4.8. The photographs of Ellipticine- AC8 complexes after 24 hr stirring. Ellipticine concentration was fixed at 0.05 mg/ml ad the peptide concentration varies from 0.01 to 0.3 mg/ml from left to right. The turbidity of the samples increases by increasing the concentration of AC8 peptide.

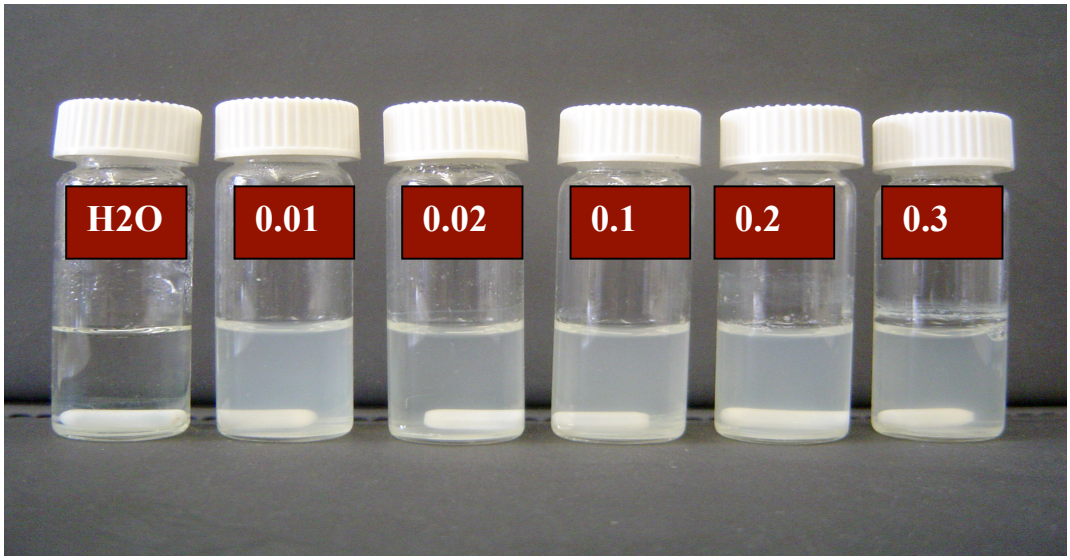

4.2.2 Dynamic Light Scattering (DLS)

4.2.2.1 Particle Size Distribution

Dynamic light scattering was applied to determine the size of the particles in complexes. The hydrodynamic size of the peptide-ellipticine complexes was found to increase with increasing AC8 concentration from DLS measurement after 24 hr stirring. However, by keep stirring the samples for another 24 hr the size of the particles in the complexes increased for all the complexes but the complex with 0.1 mg/ml AC8 concentration. This particular concentration of was considered as critical assembly concentration of peptide-ellipticine complex. It was also shown by fluorescence spectroscopy in previous section, after this concentration the behavior of complex changed in terms of fluorescence.

Figure 4.9. The number-based size distribution (%) (hydrodynamic diameter in nm) for EPT-AC8(0.05:0.1) mg/ml . (A) 24 hr, (B) 48 hr

A

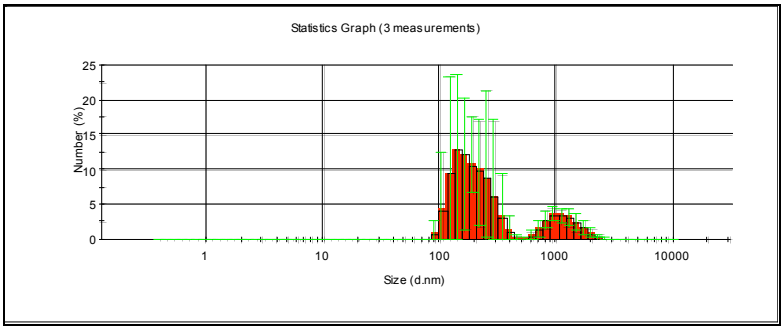

B

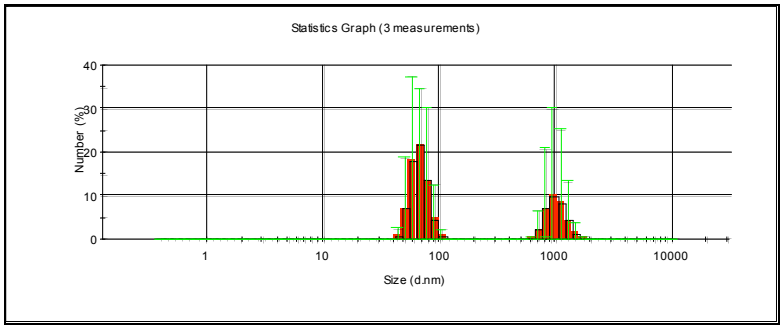

Figure 4.10 shows the comparison results from the size of all other complexes with different peptide concentration but the same ellipticine concentration. The results indicate that the complexes with lower concentration of AC8 have lower particle size than the high concentration ones. and over the time the size got larger because of the complexation and assemblies of peptide and ellipticine. The exception here in these demonstrations is the complex with AC8 at 0.1 mg/ml. The longer stirring time make smaller particles for this complex. We assume the critical assembly concentration for the AC8-ellipticine complexes around the ratio of (2:1) for peptide-to-ellipticine based on the DLS and fluorescence results.

Figure 4.10. Hydrodynamic diameter in nm for varying concentration of AC8 peptide and fixed ellipticine concentration. Standard deviation is about 5%.

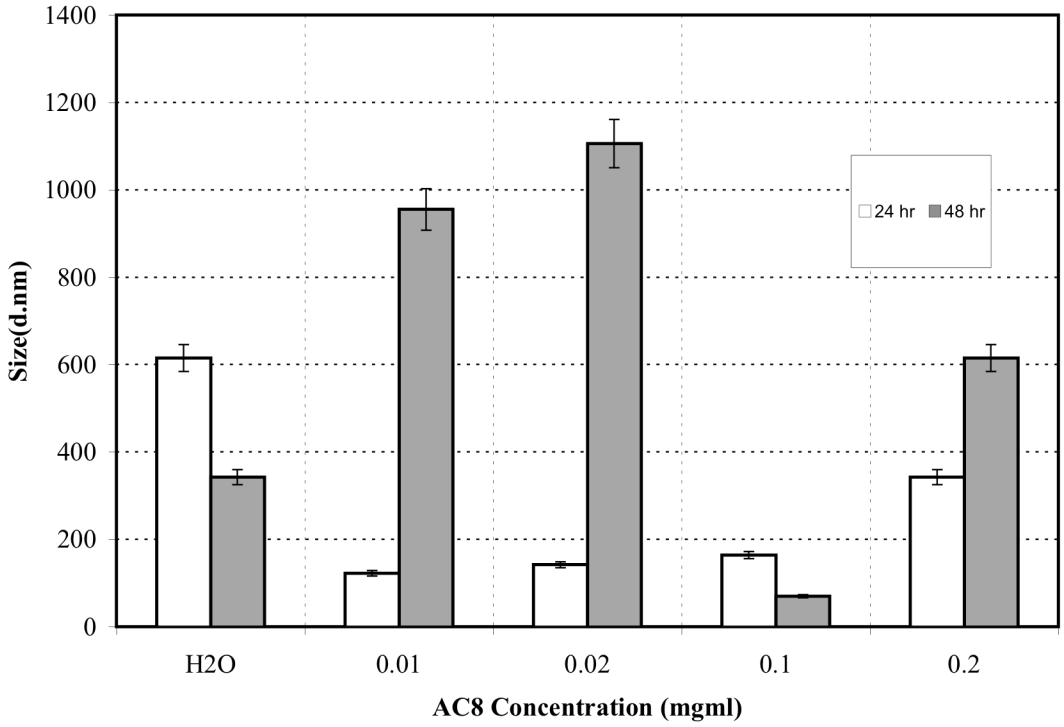

4.2.2.2 Zeta Potential

Zeta potential was measured for the above complexes to determine the stability of the samples in terms of net charges and mobility. As discussed above, the solutions with the zeta potential above ±30 are considered as quite stable, but below this limits particles tend to fluctuate a lot and no aggregation will occur. For these complexes the zeta potential measurements have shown the relatively stable samples over the time by stirring. The stability is more obvious for the complexes with medium concentration of peptide. The pH of the complexes was measured over the time. Complexes have shown relatively stable pH ~7 after 2 days preparation. Table 4.1 indicates the pH values for peptide-ellipticine complexes.

Figure 4.11. Zeta potential of AC8-Ellipticine complexes for varying concentration of AC8 and fixed concentration of ellipticine

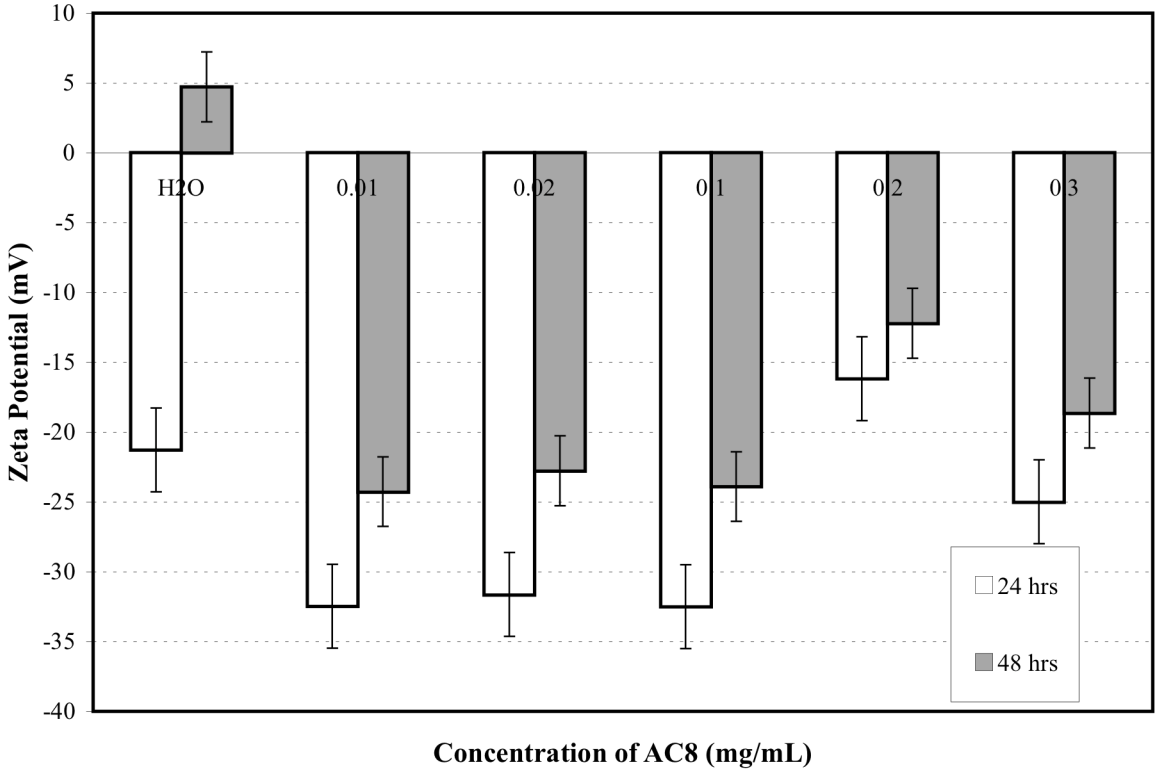

Table 4.1 pH Values of the complexes for the 24 and 48 hr. [AC8] in mg/ml, [EPT]:0.05 mg/ml

[AC8] mg/ml	27 hrs - pH	48 hrs - pH
0	7.17	7.31
0.01	7.3	7.39
0.02	7.3	7.32
0.1	7.29	7.27
0.2	7.04	7.06
0.3	7.09	7.03

4.3 Cellular toxicity of the peptide-drug complexes: MTT Assay

As discussed above, AC8 can stabilize ellipticine in neutral form in aqueous solution, depending on peptide and ellipticine concentrations. AC8 can stabilize neutral form of ellipticine in aqueous solution with two ratios of peptide-to-ellipticine: 2:1 and 6:1 (peptide:ellipticine (by mass)) As it showed in previous section, when the ratio of peptide-to-ellipticine is higher than 3:1 (by mass), the stable neutral state of ellipticine forms after about two days with a relatively large particle size. However, when the ratio of peptide-to-ellipticine is lower than 3:1, the stabilized ellipticine is not predominantly in neutral form but crystalline in complex. This indicates that the ratio of peptide-to-ellipticine is important in determining the molecular state of ellipticine in the complexes.

Two human cancer cell lines, MCF-7 and A549, were used in this study to investigate the cytotoxicity of neutral form of ellipticine against cancer cells over time. The results of MTT assay for the cytotoxicty of the serial dilutions of 2:1 and 6:1 ratio of peptide-to-ellipticine for both MCF-7 and A549 cell lines after 48 hr treatment are shown in figure 4.12. The toxicity of the complex on the cell lines was increasing over the time even for the higher dilutions. The complexes are still effective in killing both cancer cells up to 16 times dilution complex compare to the ellipticine control group. Figure 4.13 depicts the comparison between the cytotoxicity results of serial dilutions of the two complexes with fixed concentration of ellipticine and different concentration of peptide, for both MCF-7 and A-549 cell lines. The dashed lines represented complex with low concentration of peptide and the filled lined shows the complex with high concentration of peptide in both cell lines.

Results indicated that the complex with lower ratio of peptide-to-ellipticine, 2:1, in more effective on killing cells than the higher ratio 6:1. This is because of the complex formation. The higher concentration of peptide leads to larger aggregates, which prevent cell penetration. However, the smaller particles in complex, as it showed in the complex with low concentration of peptide, have more efficacies on killing cell over the time. Figure 4.14 shows the comparison between the general results of two complexes on two cell lines. The neutral ellipticine in AC8-EPT complex seems to be slightly more effective at killing MCF-7 cells than A549 cells, around 1-2% difference in viability. This may be due to the fact that MCF-7 cells sensitivity and membrane integrity of A549 cells. Fung et al. have showed the same effects for protonated ellipticine. In the study of protonated ellipticine incorporated with EAK16-II, MCF-7 cells were more sensitive to protonated ellipticine, compared to A549 cells. On the other hand, the complex with lower concentration of peptide shows higher efficacy on both cell lines compare to the high ratio-complex.

Therefore, these results lead to select the appropriate formulation of complexes to kill different cancer cells. Peptide sequence and the ratio of peptide-to-ellipticine are the key factors for this drug delivery system for combating particular cancer cell. Since the ellipticine formed in either neutral or protonated state in various peptide solutions, and each molecular state of ellipticine could be effective on specific cancer cell lines.

MTT assay has been done for control samples as well such as peptide control and ellipticine control. The results from the peptide control samples indicate the non-significant toxicity on both cell lines as well as ellipticine control sample. This present that the toxicity is from the peptide-ellipticine complex, which is desirable for this study. (Data not shown)

Figure 4.12. Viability of A549 cells treated with the complex AC8-EPT (A) (0.3:0.05) (B) (0.1:0.05) mg/ml over the time. Viability of A549 cells treated with the complex AC8-EPT (C) (0.3:0.05) (D) (0.1:0.05) mg/ml.

A

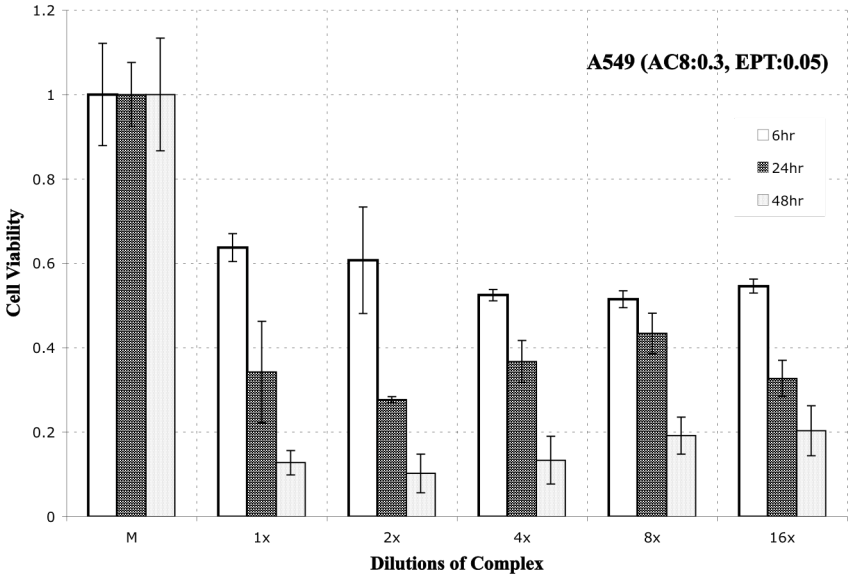

B

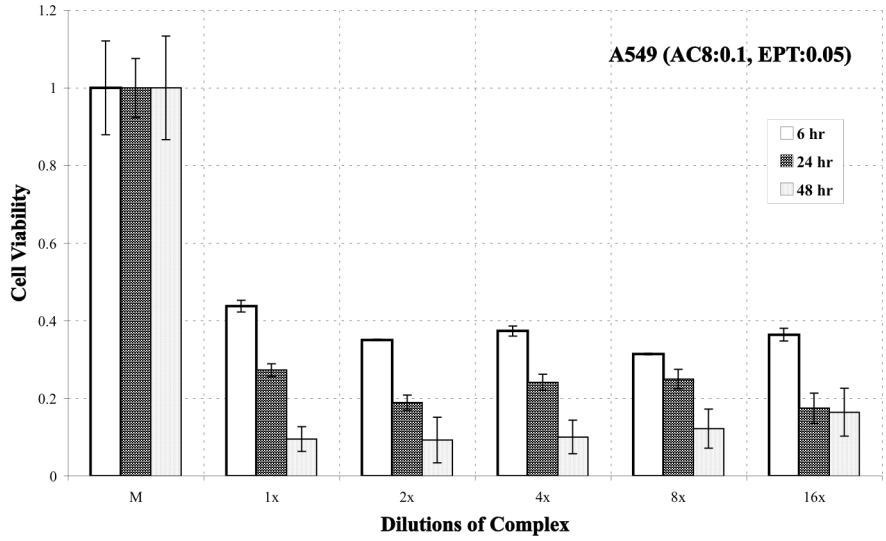

C

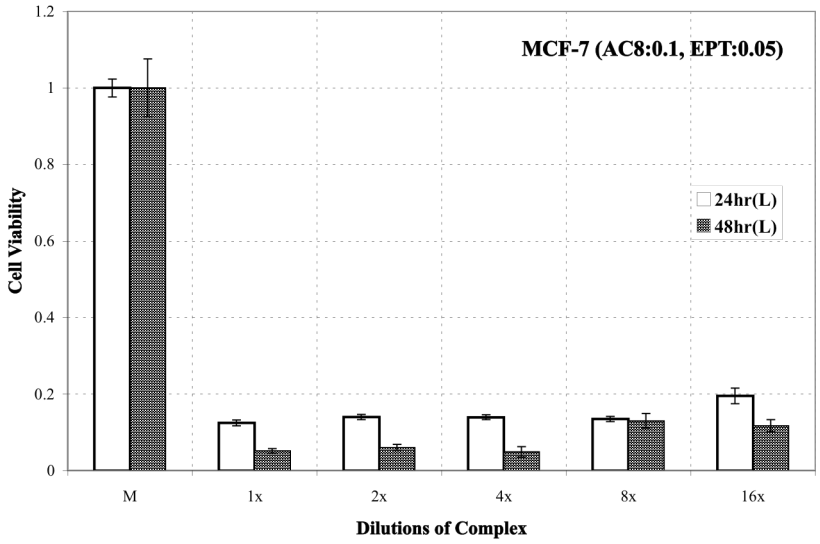
MCF-7 (AC8:0.1, EPT:0.05)
24hr(L)
48hr(L)
Cell Viability
1.2
1
0.8
0.6
0.4
0.2
0
M
1x
2x
4x
8x
16x
Dilutions of Complex

D

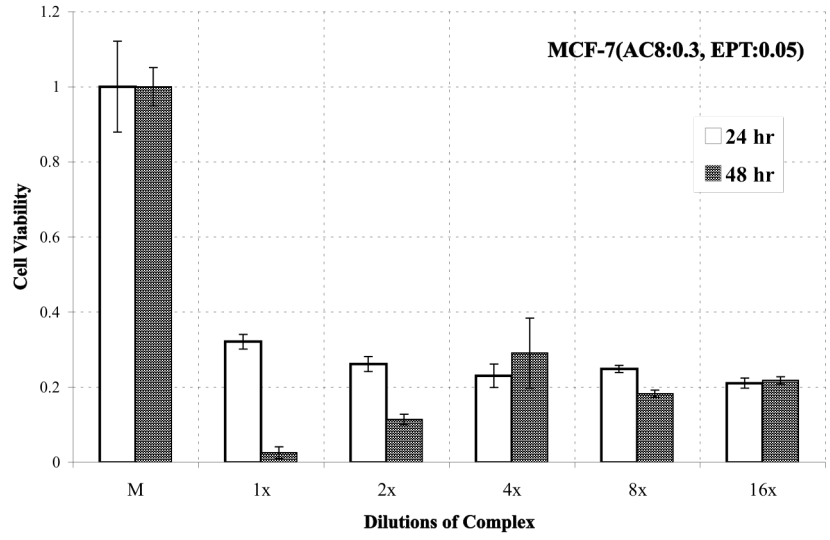
MCF-7(AC8:0.3, EPT:0.05)
24 hr
48 hr
Cell Viability
1.2
1
0.8
0.6
0.4
0.2
0
M
1x
2x
4x
8x
16x
Dilutions of Complex

Figure 4.13. The comparison of the cell viability over the time between two complexes. (- - -) is (L) low concentration of peptide (AC8:0.1, EPT:0.05). (—) is (H) the complex with high concentration of peptide. **(A)** A549 cell lines. **(B)** MCF-7 cell lines.

A

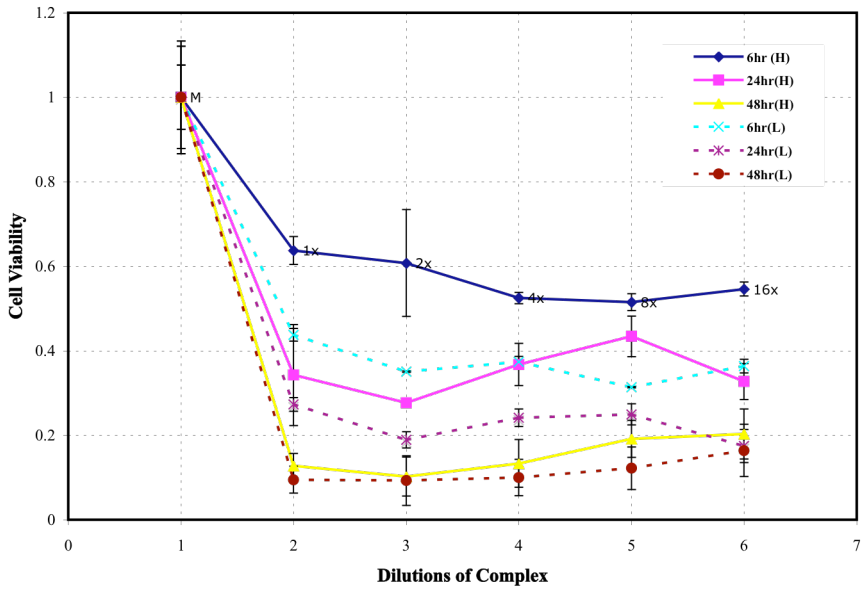

B

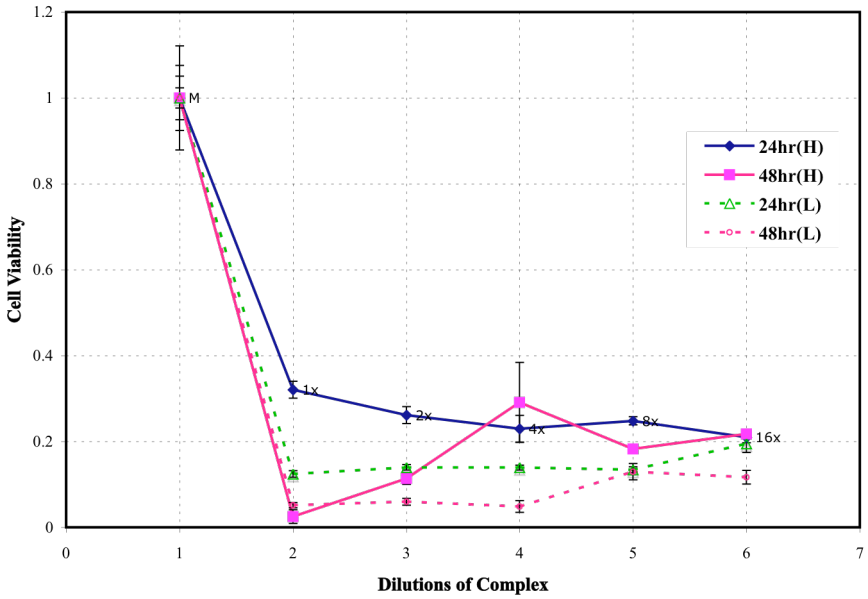

Figure 4.14. Comparison between the complexes on both MCF-7 and A549 cell lines

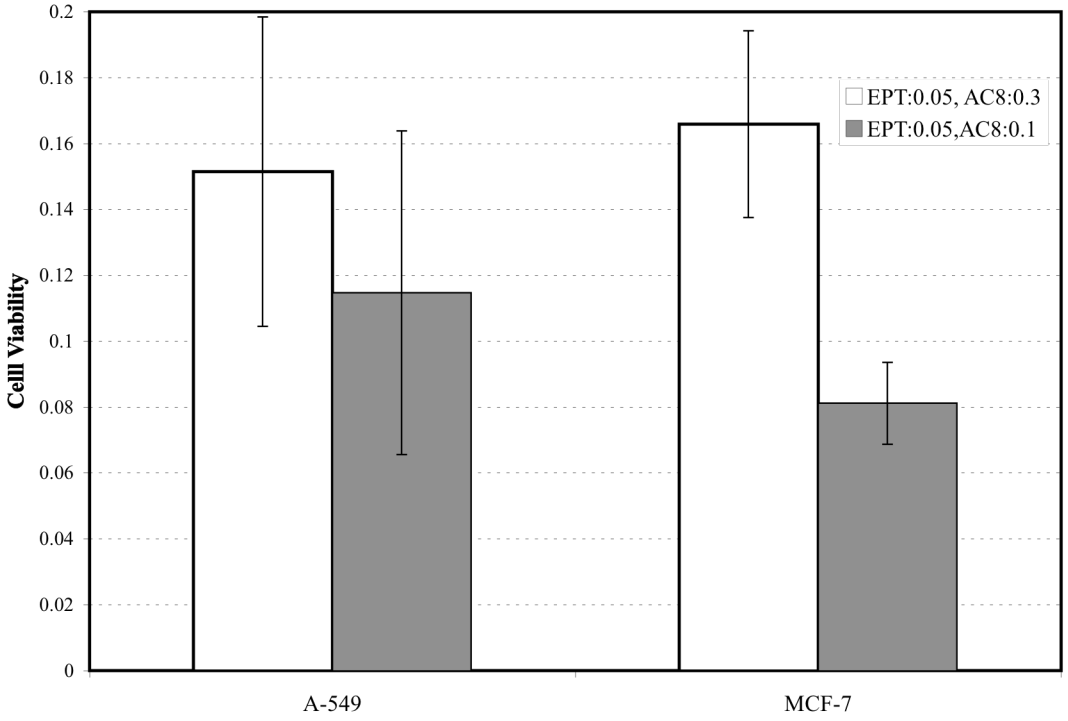

4.4 Apoptosis induced by Ellipticine-AC8 complexes

Two alternative modes of cell death can be distinguished, programmed cell death and accidental cell death, which are called as apoptosis and necrosis, respectively. Apoptosis is referred to as “programmed cell death”, which is an active and physiological mode of cell death. Cells die in a response to a variety of stimuli, but in the case of apoptosis they do so in a controlled and regulated fashion. This makes apoptosis distinct from necrosis in which uncontrolled cell death leads to lysis of cells, inflammatory responses and to serious health problem. Under normal circumstances damaged cell undergo apoptosis, but in the case of cancer, cell mutations may have occurred to prevent cells from apoptosis. Due to the lesser apoptosis in cancer cells, compared to normal cells, most of the tumors or cancer cells are difficult to eliminate, so cancer treatments rely on damaging the cells by radiation and chemicals and mutations in apoptotic pathway. Apoptotic cells show distinctive morphology during the apoptosis process. Condensation of nuclear chromatin because of cell dehydration is the main characterization of apoptosis at early stages. DNA cleavage by activation of endonucleose is another feature of apoptosis, which can be determined by agarose gel electrophoresis. Another characteristic feature of apoptosis are the preservation of the structural integrity and the plasma membrane function, at least at the initial phase of apoptosis. However, the loss of asymmetry of the phospholipids on the outer leaflet occurred in apoptotic cells in early stages. Recently it was shown that the anticoagulant Annexin V binds to negatively charged phospholipids like phosphotidylserine. Apoptotic cells, which still have intact membranes, become Annexin V positive after nuclear condensation had

started. In the case of labeling of Annexin V for Flow Cytometry analyses, vital cells are Annexin V-negative, and apoptotic cells are Annexin V-positive.[58]

Light scattering of the cells by flow Cytometry technique is another method to discriminate different types of cell death such as apoptosis and necrosis. In most cases, apoptosis can be distinguished from necrosis on the basis of the scattering parameters in Flow Cytometry measurements.[59-60] The forward-angle light scattering (FSC) is related to cell diameters, which means the magnitude of forward scattering is proportional to the cell size. Whereas the side-angle light scattering reflects the inner conformation of cellular structures and caused by granularity and complexity of the cell. During the initial stages of apoptosis the cell shrinks, but the membrane of the cell remains intact. However, during necrosis the cell swells as a result of failure of membrane integrity, so FSC increases. As a consequence of the structural changes of the cell, during early phases of apoptosis FSC decreases, while SSC increases or remains unchanged. After several hours, both FSC and SSC decrease. During necrosis, cells swell and FSC increases immediately, while SSC decreases because of lower complexity in necrosis nucleus. Accordingly, the appearance of apoptotic bodies is represented by separate particles with low forward light scatter. This method can be done easily by Flow Cytometry. The advantage of this technique is the combination of measurements simultaneously with analysis of cell markers.[58-61]

To investigate the effect of ellipticine on the apoptosis of cancer cells, MCF-7 and A-549 cells were exposed to the complexes of ellipticine-peptide at the ratio of 3:1 (by mass) and its dilutions. Flow Cytometry analyses were used to discriminate apoptosis and necrosis through cell light scattering and fluorescence labeling. For the light scattering detections,

cells were seated in 24-well plates and treated for three different treatment periods, 6 hr, 24 hr and 48 hr. The signals were collected from the cells treated with the EPT-AC8 complexes and control samples. Figure 4.15 shows the scattering plot of the MCF-7 cells treated with the complexes. SSC is plotted versus FSC to observe the changes in light scattering of the cells over the time. Forward scattering of the cells decreases from short treatment time to longer treatment time. The cells treated with the complexes show shrinkage over the time, which is an indication of apoptosis. Whereas the cells treated with the peptide only control samples do not show any change in scattering plots, which means cell size remained unchanged. For the cells treated with the ellipticine only control sample, swelling of the cells occurred over the time, which is an indication of necrosis. The same results were obtained for the complexes of ellipticine with other peptides, such as EAK16-II and EFK16-II. From the results of light scattering of the cells, the ellipticine-peptide complexes induced apoptosis after 48 hr treatment on the cancer cells with no indication of apoptosis induction from control samples.

Figure 4.15. Cell light scatter of MCF-7 cell lines treated with three different complexes over the time and the ellipticine control. SSC versus FSC for three treatment times, red dots for untreated cells, blue for 6 hr treatment time, green for 24 hr treatment time, and orange represents 48 hr treatment period.

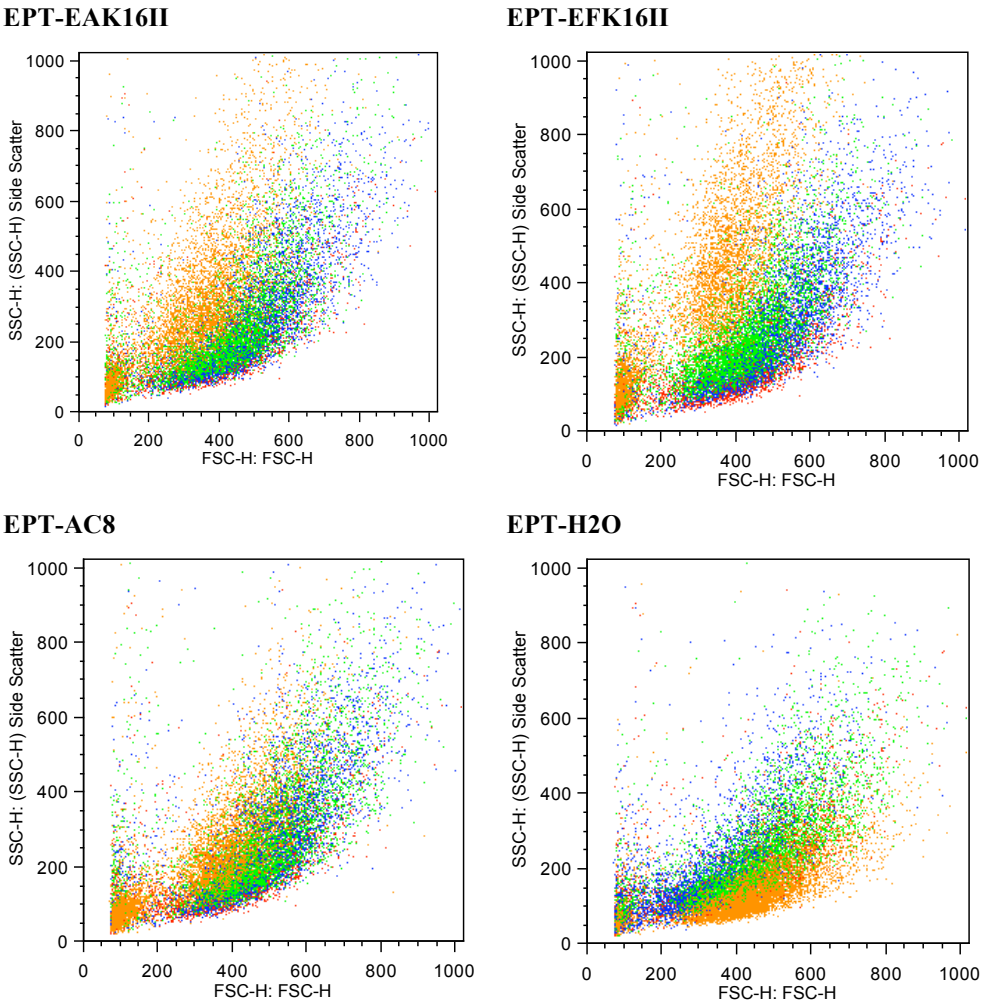

The alternative technique to observe apoptosis would be fluorescence labeling of the cells using Annexin V, which indicates apoptotic cells. MCF-7 and A-549 cell lines were exposed to ellipticine-AC8 peptide complex and control samples for 48 hr. Cells were harvested and stained with Annexin V for Flow Cytometry analyses. Based on the flow Cytometry analyses of Annexin V staining, the degree of programmed cell death resulting

from EPT-AC8 treatment at ~ 45% was marginal compared with EPED3, ellipticine derivative, at 45.5% reported by Tian et al, 2008.[34] They were studied on an ellipticine derivative as an apoptosis inducer.[34] They have shown 45.5% apoptosis on Myeloma cells and compared with positive control apoptosis inducer, which was bortezomib at 51.4%. Our results from ellipticine with the interaction of peptide are considerably comparable with the previous results. Figure 4.16 represents the flow Cytometry results for both cell lines, MCF-7 and A-549. Untreated cells showed a low percentage of the Annexin V- positive at ~ 4%. The treated cells with AC8 as the peptide control showed ~ 6-10% of Annexin V-positive with is not significant compare to ~ 45% Annexin V-positive cells treated with ellipticine-peptide complexes for both cell lines. These data are compatible with cytotoxicity results from MTT assay. All the apoptosis and cytotoxity consequences suggest that the ellipticine-AC8 complex is toxic in sense of inducing apoptosis on the both cancer cell lines.

Figure 4.16. Flow Cytometric analyses of cell viability with ellipticine-AC8 treatment for **(A)** MCF-7, and **(B)** A-549 cell lines. Annexin V used as a apoptosis marker. The viable cells are located in left handed gates and Annexin V-positive cells are located in right handed gates, which show the apoptosis.

(A)

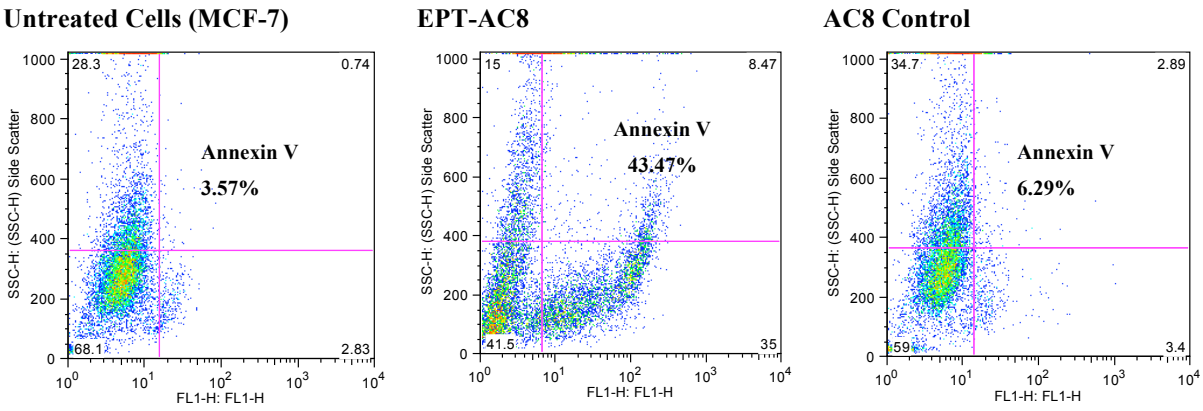

(B)

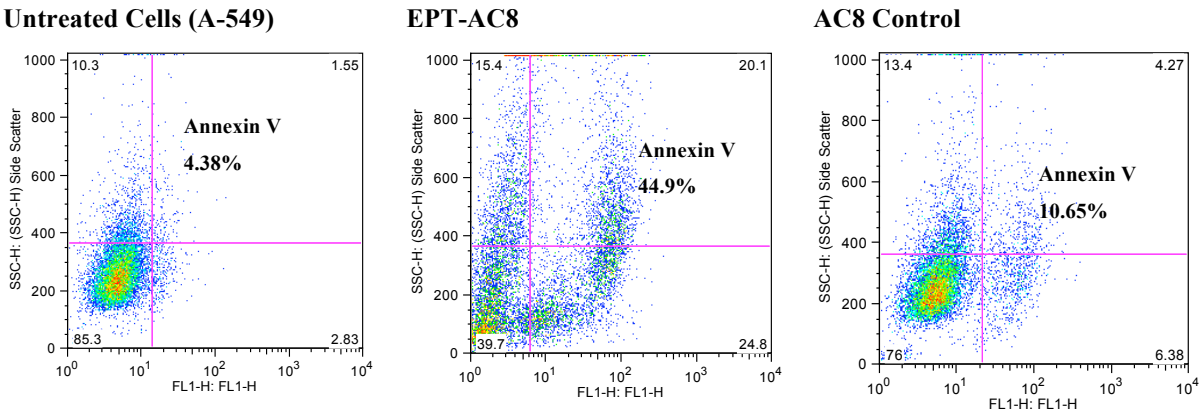

Chapter 5

Conclusions and Recommendations

5.1 Conclusions

This thesis introduced the novel all-complementary self-assembling peptide as a promising potential carrier for hydrophobic anticancer drug delivery. We explored the capability of this peptide to well self-assemble and stabilize anticancer drug ellipticine. The thesis includes the following parts: (i) Studying on concentration effect of peptide on self-assembling, (ii) Characterizing the complex formation of ellipticine with a self-assembling peptide. (iii) Investigating the therapeutic effect of the complexes *in-vitro* on two cancer cells, (iv) Detecting the apoptosis induction by the complexes *in-vitro* on cancer cells. The original contribution and conclusions for each part are presented in the following.

The all-complementary peptide AC8 was found to be able to self-assemble in aqueous solution depending on the concentration. Concentration dependent assembly of the peptide was studied by surface tension and light scattering techniques. The results of these assays indicated that a critical assembling concentration (CAC) of AC8 is around 10-15 μM (0.01-0.015 mg/ml).

The ionic complementary residue pairs (EK)s enhance the solubility of the peptide in water. The hydrogen bonding amino acid pairs (QN)s promote the peptide assembly. The hydrophobic residue pairs (FF)s also increase the peptide-peptide association and create a hydrophobic interior for encapsulation of hydrophobic compounds such as ellipticine.

Ellipticine is a potent anticancer agent, which intercalates between DNA pairs and induces G2/M phase cell cycle arrest as well as inhibition of topoisomerase II. The novel designed all-complementary peptide could encapsulate ellipticine and stabilize it aqueous solution in neutral molecular state. Concentrations of the peptide and ellipticine are an important factor to stabilize the neutral state of ellipticine. We have found in this study that AC8 can encapsulate 0.05 mg/ml ellipticine in neutral state at above its critical aggregation concentration around 0.1 mg/ml with the particle size of the complex as 100 nm, which is optimal for cell penetration.

The cellular toxicity results indicated that the complexes (≥ 2:1 ratio) with neutral ellipticine were effective at killing both MCF-7 and A-549 cell lines after 48 hr treatment, as well as their dilutions until 16 time have shown reasonable toxicity. The toxicity of the complex of peptide-to-ellipticine at 2:1 ratio showed better result than the 6:1 ratio. It could be because of the particle size of the complex and their efficacy on both cancer cell lines. The complex with ellipticine at 0.05 mg/ml and AC8 at 0.1 mg/ml has shown higher toxicity and lower particle size and more neutral form of ellipticine.

In addition, the results from apoptotic effect of ellipticine on cancer cells have shown induction of apoptosis by ellipticine-peptide complex by two methods, cell light-scatter and Annexin V labeling. This study demonstrates the capability of the all-complementary peptide AC8 as a carrier for hydrophobic anticancer drug delivery.

5.2 Recommendations and Future Work

Recommended future work to develop all-complementary peptide-based nanocarriers for hydrophobic anticancer drug delivery can be divided into four groups: (i) optimize peptide-drug formulation, (ii) enhance the efficacy of delivery system, (iii) immunogencity test for the complex, (iv)evaluate the therapeutic effect of the complex *in vivo*.

Optimize the peptide-drug formulation

This part requires three important factors; appropriate peptide, drug and formulation.

(1) A suitable peptide is required to be designed for drug encapsulation and formation of high stability, high loading capacity and controllable release. The peptide library was constructed by our group with considering all aspects of assembly and complexation as shown in table 5.1. It is the goal of our research group to screen the peptide library and identify the optimal candidates for drug delivery system.

(2) An appropriate drug is another key factor to develop the drug delivery system and increase the efficiency. Numbers of anticancer drugs are found to be applicable for cancer therapy, but most of them have the problem with delivery and their side effects. The objective here, after this study, is identifying some suitable drug candidates and formulate with selected peptide as carrier. The list of drug candidates is tabulated in table 5.2.

(3) Current study has shown the method to formulate the optimal complex with the appropriate size and efficiency. The new candidates of drug and peptide should formulate the stable complex. Hopefully, the new method and formulations will be

developed to quantify the amount of peptides as well as the drugs in the complexes, to determine the loading capacity. Ultracentrifuge and filtration are suggested for this work.

Enhance the efficiency of delivery system

(1) Targeted delivery is the advance achievement in cancer chemotherapy. Peptides can be incorporated with targeted motifs as well as encapsulate anticancer agent to construct an ideal drug delivery system. This project requires the following steps: (a) finding appropriate peptide sequence that can be incorporate with targeting motifs, (b) finding desirable targeting peptide from previous published research, (c) formulating the targeting motifs and peptide with the anticancer agent to develop nano-delivery system. (d) test the principle of the delivery system *in vitro* and *in vivo*.

(2) Detailed cell biology studies on the mechanism of the fate of delivery system are required. Cell penetration, EPR effect, controlled release, biodistribution and pharmacokinetic are the biological studies that recommended for future work to characterize the cellular uptake of mechanism of our drug delivery system.

Immunogenicity test

Drug delivery systems are circulating in bloodstream. Foreign materials activate the complement system in human blood. Thus, the peptide-drug complex must avoid significant complement activation. The complement activation properties of the complexes should be examined with current methods such as Total Hemolytic Complement (CH50).

Evaluate the therapeutic effect of the complex in vivo

As soon as promising drug-peptide complex is recognized, it should be examined *in vivo* experiments on cancer tumor animal models. For this purpose, the promising drug formulation is required, because *in vivo* studies cost incomparably with *in vitro* studies. Reliable formulation should have good stability and biocompatibility. Different cancer models are recognized to apply for our drug delivery system.

Table 5.1 Peptide library for hydrophobic anticancer drug delivery[24]

Design Category	#of Amino Acids	Sequence (n-c)	Charges at pH 7	Charges at pH 4.5
	16	n-GEGGKGKGEGEGKGK-c	4+, 4-	4+, 4-
	16	n-IEIEIKIKIEIEIKIK-c	4+, 4-	4+, 4-
	8	n-EEKKEEKK-c	4+, 4-	4+, 4-
	16	n-EEIIIIEERRIIIIRR-c	4+, 4-	4+, 4-
	16	n-AAEEAAEEAAKKAAKK-c	4+, 4-	4+, 4-
	16	n- AAAAEEEEAAAAKKKK-c	4+, 4-	4+, 4-
	8	n- LLEELLRR-c	2+,2-	2+,2-
	8	n- FFEEFFRR-c	2+,2-	2+,2-
	8	n- IIEEIIRR-c	2+,2-	2+,2-
	8	n- EEIIIIRR-c	2+,2-	2+,2-
	2	FF		
	3	n- FFR-c	1+	1+
	4	FFFF		
	2	n- YY-c		
	2	YY		
	4	YYYY		
	4	n- YYYQ-c		
	2	FF	1+	1+
	4	n- NFFR-c		
	4	n- NFFQ-c		
	8	n-FNFNFRFR-c	2+	2+
	8	n- LNLNLRLR-c	2+	2+
	8	n- VNVNVRVR-c	2+	2+
	8	n- ININIRIR-c	2+	2+
	16	n- ININIRIRININIRIR-c	4+	4+
	16	n- IINRIINRIINRIINR-c	4+	4+
	20	n- WHIHININININIRIRIRIR-c	4+	6+
	8	n- IINNIIRR-c	2+	2+

8	n- NNIIIIRR-c	2+	2+
12	n- WNNNIIIIIRRR-c	3+	3+
18	n- WHIINNIIHHIINNIIRR-c	5+	6+
20	n- WHHNNNSINISINISINRRR-c	2+	5+
11	n- WRIRIFININW-c	2+	2+
13	n- WQQQIIIIIRRRH-c	3+	3+
17	n- NNNISISIWININIRRR-c	3+	3+
13	n- NIEIINWRIIRIR-c	3+, 1-	3+, 1-
17	n- NNNNEIIIWIIIRHHHR-c	2+, 1-	5+, 1-
21	n- WHHENNININIFISISIRRRN-c	3+	5+

Note: n- and –c refer to the end protection by acetylation and amidation, respectively.

Table 5.2 Anticancer Drug Candidates proposed by our group. *

Drug Name	Solubility ug/ml	Administration route	Speciality	Dosage (mg/m^2)
Epirubicin	93	injection	breast/lung	100-120
Daunorubicin	39.2	injection	non-specific anti tumor drug/leukemia	20
Cisplatin	1000	injection	solid tumor	20
Topotecan	1000	injection	cytotoxic anti cancaer drug/small cell lung cancer	1.5
Vinorelbin	>1000	injection	non-small cell lung/breast	25-30
Docetaxel	0.025	injection	lung/cancer	75/3 weeks
Teniposide	>1000	oral injection	lymph/lung	60
Etoposide	58.7	oral injection	small cell lung cance/solid tumor/leukemia	60-100
Paclitaxel	0.7	injection	lung	135-200
Carboplatin	14	Injection	Ovarian/Lung Cancer	10-20 mg/kg

* Thanks Hui Wang for providing this table

Appendix A

Dynamic Light Scattering Theory

The objective of this section is to describe the basic **Size** and **Zeta Potential** principles behind the dynamic light scattering.

Particle Size Distribution

Dynamic Light Scattering also known as Photon Correlation Spectroscopy (PCS) measures the Brownian motion and relates it to size of particles. The instrument illuminates the laser to the particles and analyses the intensity fluctuations in the scattered light. In practice, particles suspended in a liquid solution constantly move because of the Brownian motion. Brownian motion is the movement of the particles due to the collision of the particles with the surrounding molecules. The important fact about the particles related to DLS is the smaller particles move fast and the larger ones move slowly. The relationship between size and speed of the particles is defined in Stokes-Einstein equation.

$$d_H = \frac{kT}{3\pi\eta D}$$

d_H is hydrodynamic diameter, D corresponds translational diffusion coefficient, η is viscosity and k is Boltzmann's constant. The instrument measures the fluctuation in scattering intensity and uses it to calculate the size of particle suspended in the sample based on the correlation function. A correlator basically measures the degree of similarity between the signals over a period of time. The size of the particles affects the fluctuation of speckle

pattern. Therefore, the rate of decay for the correlation function is related to particle size as the rate of decay is much faster for small particles than it is for larger.

$$G(\tau) = (t).(t + \tau)$$

τ is the time difference (the sample time) of the correlator. For the large number of monodisperse samples the correlation function is and exponential decaying:

$$G(\tau) = A[1 + B\exp(-2\Gamma\tau)]$$

where A is the baseline of the correlation function and B is the intercept of the correlation function. $\Gamma = Dq^2$, D is translational diffusion coefficient, and $q = (4\pi n/\lambda_0)\sin(\theta/2)$. n is refractive index, λ_0 is the wavelength of the laser and θ is scattering angle.

However, for the polydisperse sample the correlation function follows as:

$$G(\tau) = A[1 + Bg_1(\tau)^2]$$

$g_1(\tau)$ is the sum of all the exponential decays contained in the correlation function.

Figure A.1 Correlation function for small and large particles.

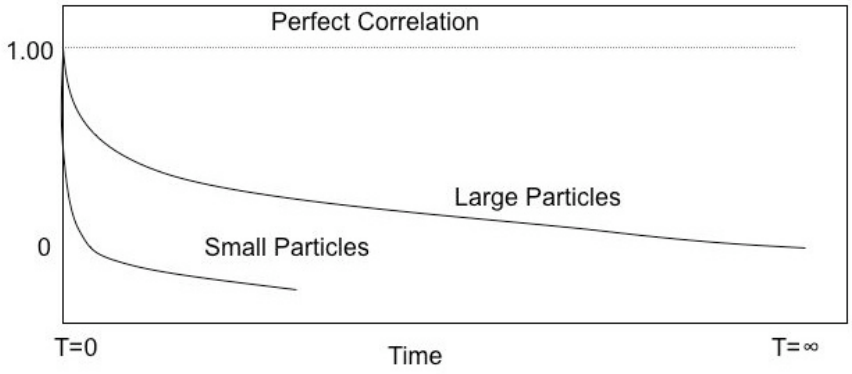

The information from correlation function are being used to calculate the size distribution. The Zetasizer software uses the standard algorithms to extract the decay rates for a number of size classes to produce a size distribution. There are three different distribution generated from the DLS: Intensity, volume and number distributions. Actually, the fundamental size distribution is obtained from intensity distribution, but it can be converted to volume distribution based on the Mei theory or number distribution. Figure A.2 shows the difference between three different distributions. Again, the basic distribution is obtained from intensity and the other ones generated from that.[54-55]

Figure A.2 Number, volume, intensity distribution of a bimodal mixture of 5 and 50 nm lattices presented in equal numbers.

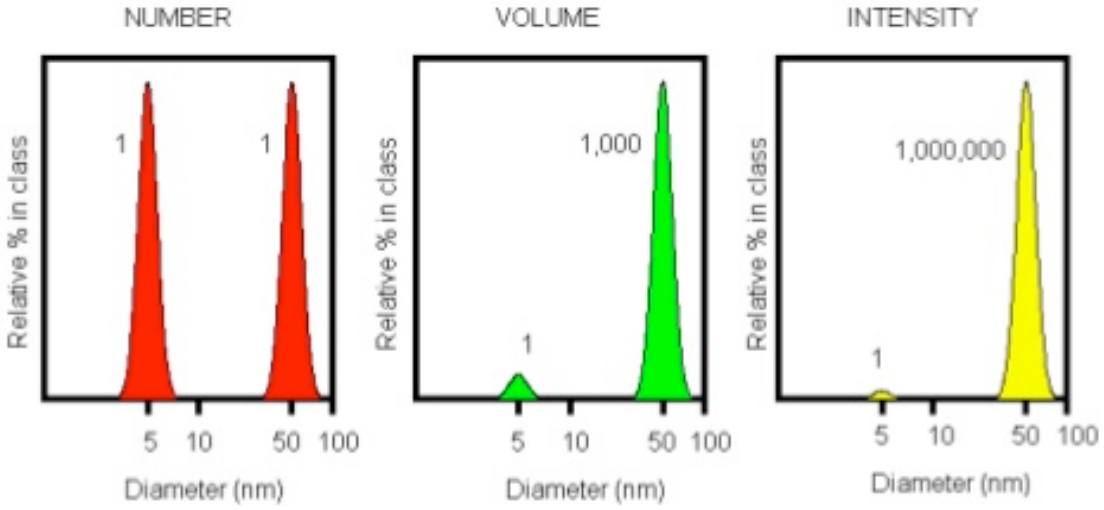

Zeta Potential

The mobility of the particles in an electric field is called electrophoretic mobility. It occurs when the charged double layers are sheared from each other. By this mobility the electric potential establishes between two layers and the medium, which is called as zeta potential. [59] Most liquids contain ions; either negatively or positively charged atoms. The net charge of

the particle at the surface affects the distribution of ions in the interfacial region, resulting in an increased concentration of opposite charge to the particle close to the surface. Therefore, the layer will form around the particle called electrical double layer. This layer surrounding the particle has two parts: an inner region called the Stern layer and outer region or diffuse region. The ions are strongly attached in Stern layer, but they are less bound in outer layer. When the particle moves, ions within the boundary moves with the particle, but the ions beyond the boundary do not travel with it. This boundary called slipping plane. The potential that exists at slipping boundary is known as Zeta potential. Figure A.3 depicts the above explanations for the charged particles.

The net surface charge of particles helps to investigate the tendency of the particle to aggregate and absorb onto surface. The magnitude of the zeta potential indicates the potential stability of the colloidal system. Theoretically, if all the particles in suspension have a large negative or positive zeta potential then they will tend to repel each other and to tendency to flocculate (i.e., no aggregation). However, if they have lower zeta potential, there is no force to prevent them from flocculating. The most important factor that affects zeta potential is pH. Basically the zeta potential value on its own without a quoted pH is a meaningless number. Zeta potential alters in solution by adding alkali or acid. Adding alkali to solution the particles will tend to be more negative charge and then by adding acid in suspension the particles change to neutral from negative and any further addition of acid can cause a build up of positive charge. Therefore, a zeta potential versus pH curve will be positive at low pH and negative at high pH. The point where the plot passes the zero zeta potential is called the isoelectric point. It shows normally where the colloidal system is less stable.[54-55]

Figure A.3 Schematic of Zeta potential

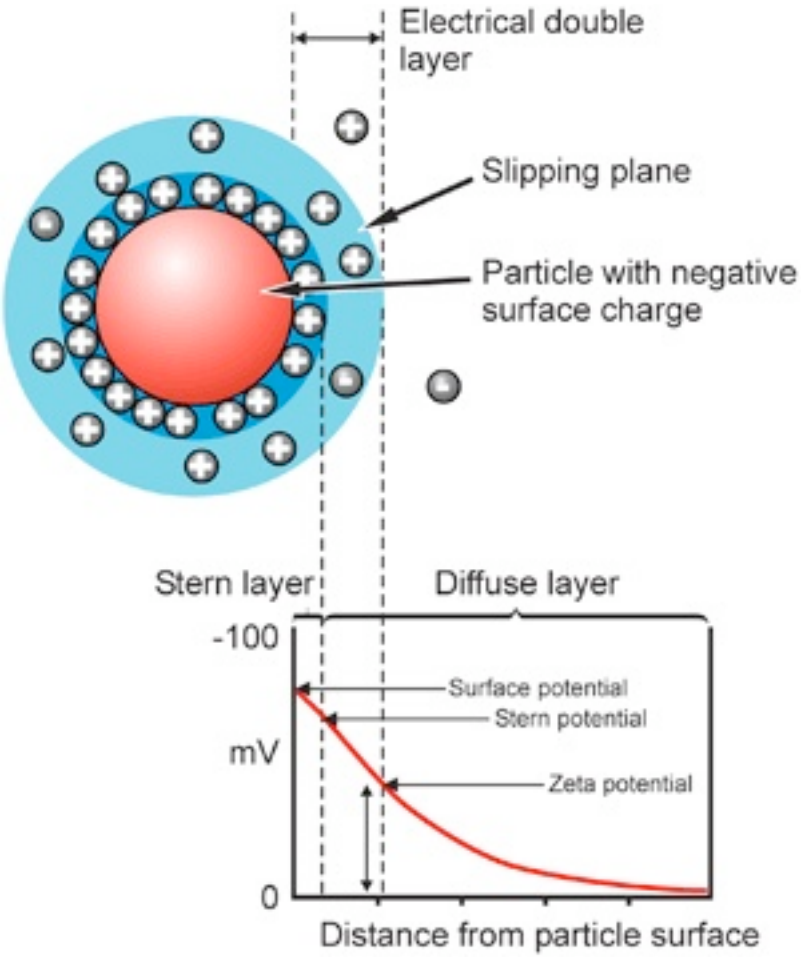

Appendix B

Cell viability test by MTT assay

The measurement of cell viability is the valuable tool in a wide range of research areas. There were several methods in the past for this purpose such as trypan blue staining and radioactive substances up taking. Trypan blue staining is no the sensitive and cannot be adapted for high throughput screening. Also, uptaking the radioactive substances is a time-consuming method and it has a issue of handling of the radioactive materials.

MTT assay is now recognized as a safe, accurate and alternative to other methods for cell viability tests. The yellow tetrazolium salt (MTT) is reduced in metabolically to form insoluble purple formazan crystals, which are solubilized by the addition of a detergent. The ELISA plate reader at wavelength of 570 nm can then quantify the color. The amount of color is directly proportional to alive cells. The reduction of the tetrazolium takes place only reductase enzyme in mitochondria is active, so the color change is often used as a measure of viable cell. Among the applications for the method are drug sensitivity, cytotoxicity, response to growth factors, and cell activation.[62-63]

Figure B.1 The molecular structure of MTT and its function in alive cell

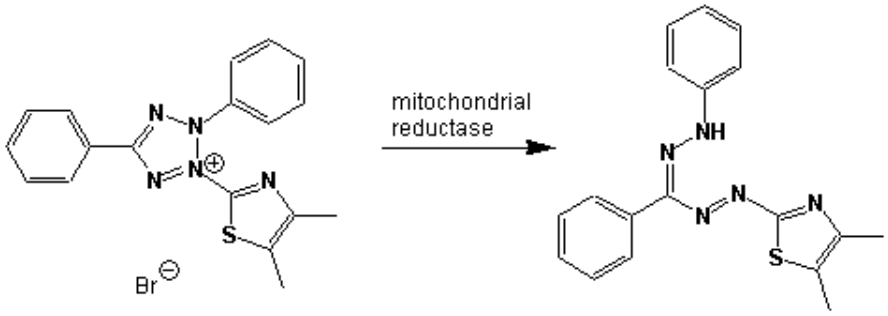

Appendix C

Flow Cytometry

Flow Cytometry is the technological process that allows for the individual measurements of cell fluorescence and light scattering. This process is performed at rates of thousands of cells per second. Flow cytometry integrates electronics, fluidics, computer, optics, software, and laser technologies in a single platform. It is a powerful technique for simultaneously measuring and analyzing multiple physical characteristics of single cell as it flow in a fluid stream through a beam of light. Flow Cytometry consists the following basic parts: [64]

(1) Fluidic system: contains the central channel for sample injection, which enclosed by outer sheath that provides faster flowing fluid. The flow characteristics of the central flow can be determined by using Reynolds Number:

$\mathrm{Re} = \frac{\rho V D}{\mu}$, ρ: Density of fluid, V: mean velocity of fluid, D: tube diameter, μ: viscosity of fluid.

As the outer fluid sheath moves it creates the massive drag effect on the narrowing central chamber. This changes the velocity over the fluid flow as maximum velocity on the central chamber and zero velocity on the walls. This effect called hydrodynamic focusing. Figure C.1 shows the schematic of this part of flow Cytometry.

Figure C.1. Hydrodynamic focusing produces a single stream of particles

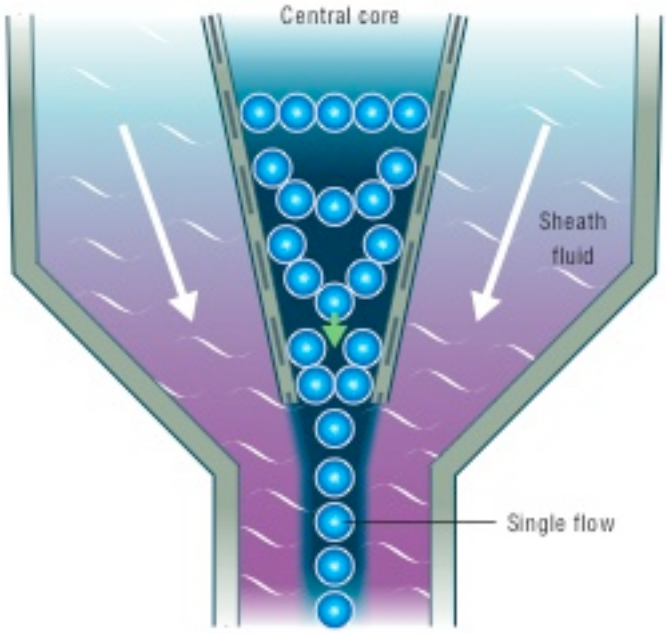

(2) Optics and Detections: after hydrodynamic focusing each cell passes through one or more light beam. Light scattering or fluorescence emission provides the information about particles' properties. There is two detection for scattered light; light that is scattered in the forward direction at 20º offset from the laser beam and it is collected by lens known as forward scatter channel (FSC). The FSC intensity roughly correlates to the particle's size and can also be used to distinguish between cellular debris and living cells. Light measured approximately at a 90 angle to the excitation line is called side scatter. The side scatter channel (SSC) provides information about the granular content within a particle. Both FSC and SSC are unique for every particle and a combination of the two may be used to differentiate different cell types in a heterogeneous sample. Figure C.2 shows the relationship between SSC and FSC in flow Cytometry for cell light scattered. The larger particles have larger forward scatter light and more granular cells scatter larger in side channel.

Figure C.2. Schematic of FSC and SSC properties in Flow Cytometry

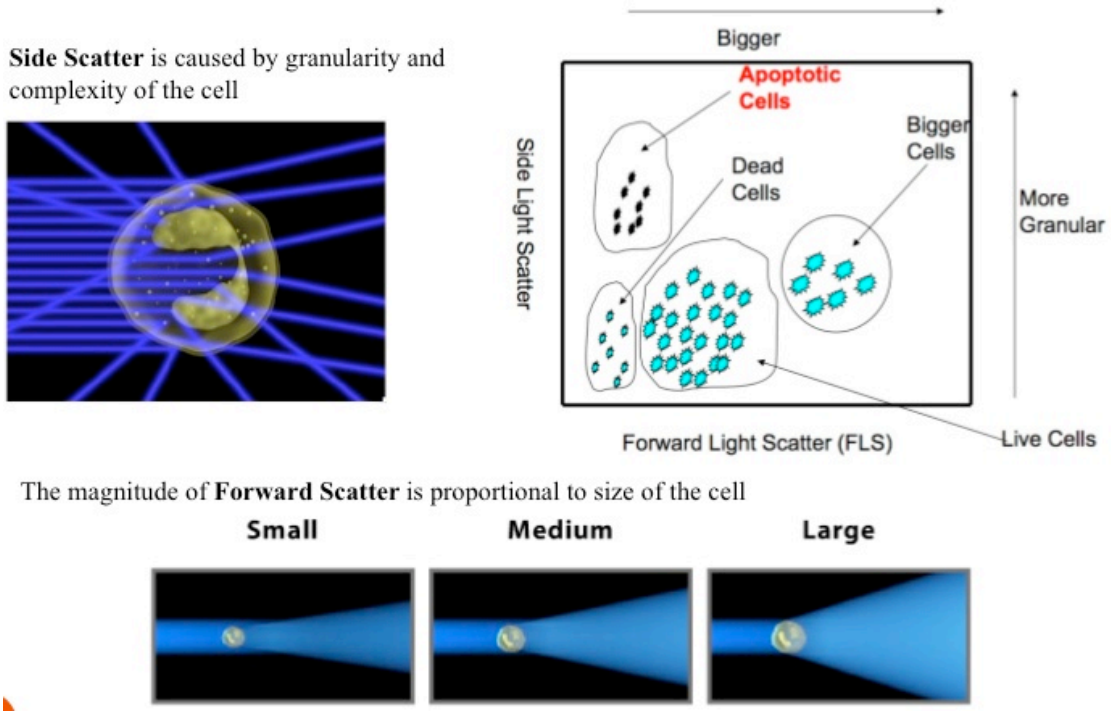

Fluorescence measurements taken at different wavelength provides quantitative and qualitative information about fluorochrome-labeled cells. Flow Cytometry has separate (FL-) channels for different fluorescence labels. Table C.1 shows the popular fluorescence probes using in flow Cytometry and their excitation and emission wavelengths. PI, PE, annexin V are the common labels used in this study as well.

Table C.1 List of common fluorescence labels.

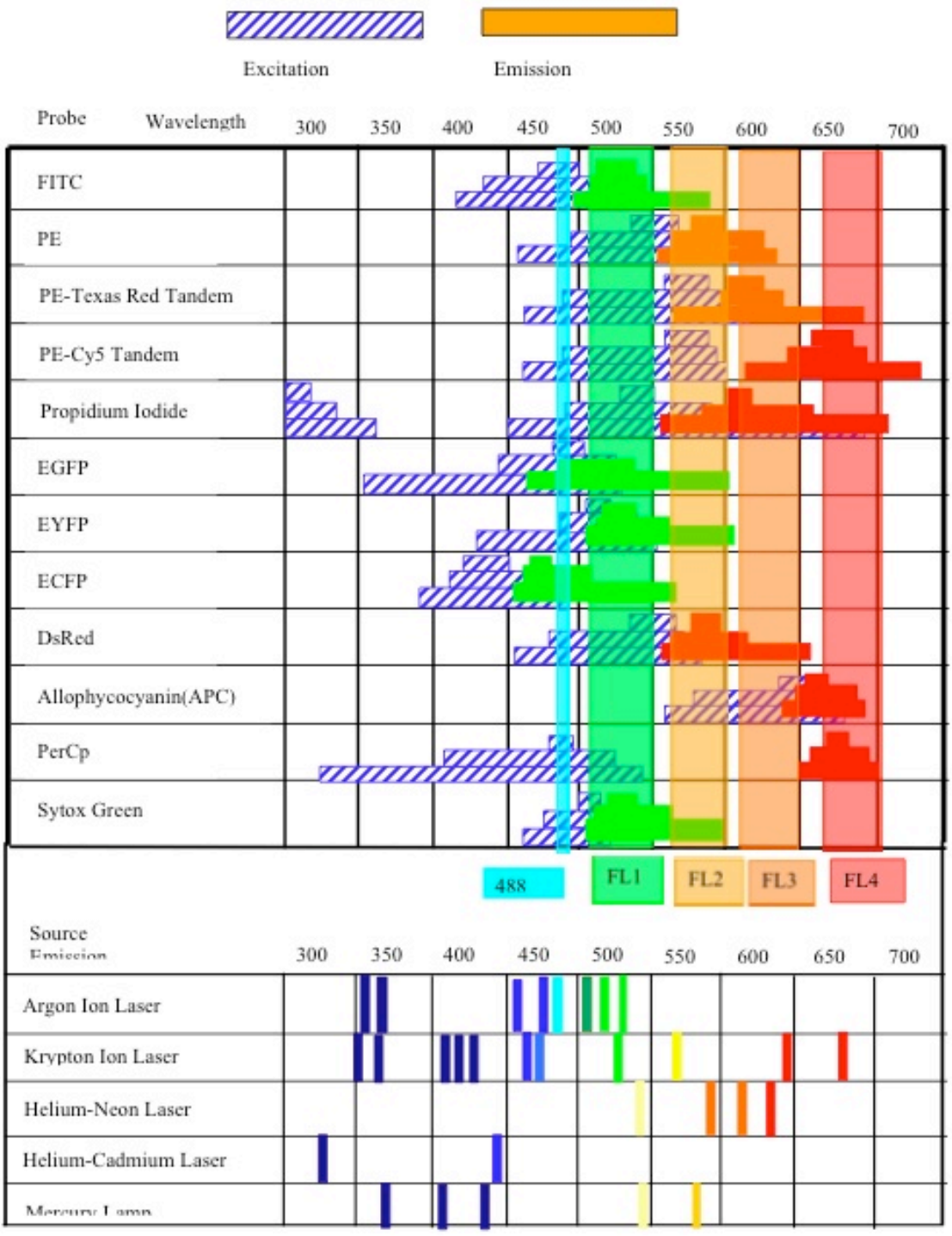

(3) Signal Processing: The electronics system, which converts the signals from the detectors into digital data that can be processed by the computer. When the light hits the photodetector a small current generated. The voltage associated with this current is proportional to the total number of photons. This voltage is converted to electrical signals by a series of linear or algorithmic amplifiers and by analog to digital converters (ADCs). Figure C.3 shows the schematic of whole setup of flow Cytometry.[64]

Figure C.3. Schematic overview of a typical flow cytometer setup

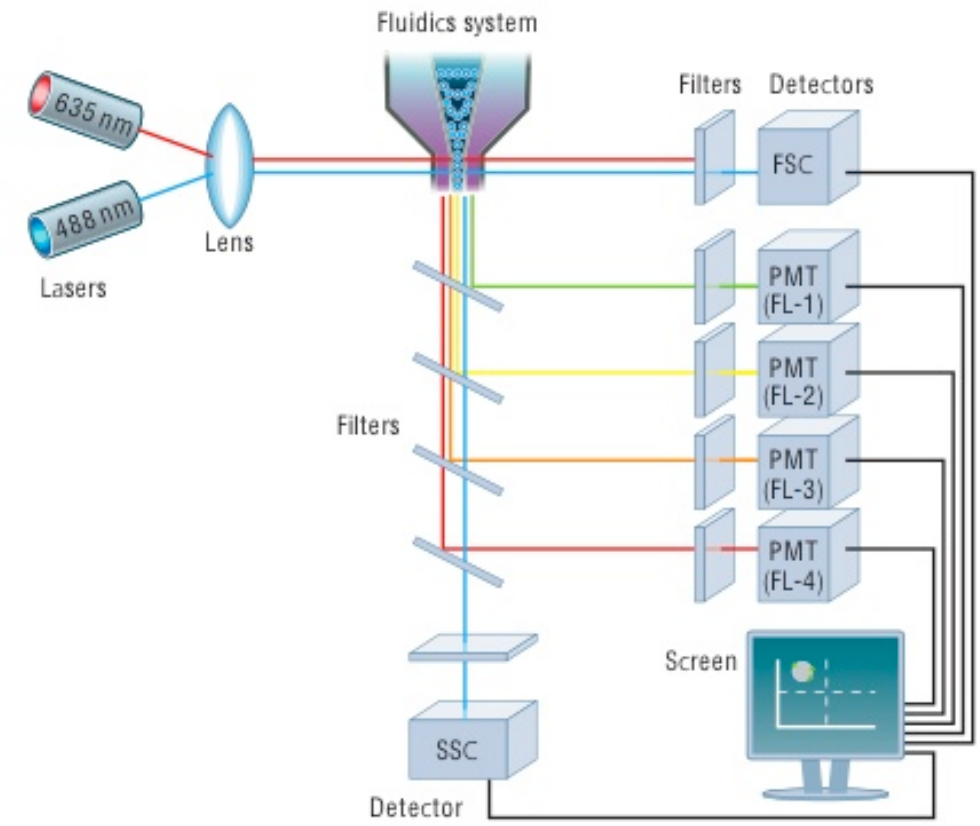

Bibliography

1. Canadian cancer statistics. ; 2008.

2. Karp G, Geer Pvd. Cell and molecular biology : Concepts and experiments. 4th ed ed. Hoboken, NJ: John Wiley; 2005. .

3. Alberts B. Molecular biology of the cell. 2nd ed. - ed. New York: Garland Pub.; 1989. .

4. Cell Biology and Cancer [Internet]; c2009 [cited 2009 02/21]. Available from: http://science.education.nih.gov/supplements/nih1/cancer/videos/act2/transcript-act2-anim.htm.

5. Lupulescu A. Cancer cell metabolism and cancer treatment. Amsterdam: Harwood Academic; 2001.

6. Pratt WB. Anticancer drugs. 2nd ed ed. New York: Oxford University Press; 1994. .

7. Brigger I, Dubernet C, Couvreur P. Nanoparticles in cancer therapy and diagnosis. Advanced Drug Delivery Reviews 2002 Sep 13;54(5):631-51.

8. Gu FX, Karnik R, Wang AZ, Alexis F, Levy-Nissenbaum E, Hong S, Langer RS, Farokhzad OC. Targeted nanoparticles for cancer therapy. 2007.

9. Wong HL, Bendayan R, Rauth AM, Li Y, Wu XY. Chemotherapy with anticancer drugs encapsulated in solid lipid nanoparticles. Adv Drug Deliv Rev 2007;59(6, pp. 491-504):July.

10. Allen TM, Cullis PR. Drug delivery systems: Entering the mainstream. Science 2004 March 19;303:1818-22.

11. Langer R. Drug delivery and targeting. Nature 1998 Apr 30;392(6679 Suppl):5-10.

12. Li C, Wallace S. Polymer-drug conjugates: Recent development in clinical oncology. 2008.

13. Burnham NL. Polymers for delivering peptides and proteins. 1994.

14. Duncan R, Dimitrijevic S, Evagorou EG. The role of polymer conjugates in the diagnosis and treatment of cancer. 1996.

15. Hoes CJT, Ankoné M, Grootoonk J, Feijen J, van der Struik E, van Doornmalen A, Pham D, de Man A, van Ettekoven A, Schlachter I, Boon PJ, Kaspersen F, Bos ES. Synthesis and biological evaluation of immunoconjugates of adriamycin and a human IgM linked by poly[N^5-(2-hydroxyethyl)-l-glutamine]. J Controlled Release 1996 February;38(2-3):245-66.

16. Nallamothu R, Wood GC, Pattillo CB, Scott RC, Kiani MF, Moore BM, Thoma LA. A tumor vasculature targeted liposome delivery system for combretastatin A4: Design, characterization, and in vitro evaluation. AAPS PharmSciTech 2006;7(2):E32.

17. Medina OP, Zhu Y, Kairemo K. Targeted liposomal drug delivery in cancer. 2004.

18. Nagayasu A., Uchiyama K., Kiwada H. The size of liposomes : A factor which affects their targeting efficiency to tumors and therapeutic activity of liposomal antitumor drugs. 1999;40:75-8.

19. Lyass O, Uziely B, Ben-Josef R, Tzemach D, Heshing NI, Lotem M, Brufman G, Gabizon A. Correlation of toxicity with pharmacokinetics of pegylated liposomal doxorubicin (doxil) in metastatic breast carcinoma. Cancer 2000;89(5):1037(11)-1048.

20. Nikanjam M, Blakely EA, Bjornstad KA, Shu X, Budinger TF, Forte TM. Synthetic nano-low density lipoprotein as targeted drug delivery vehicle for glioblastoma multiforme. 2007.

21. Agnihotri SA(, Mallikarjuna NN, Aminabhavi TM(. Recent advances on chitosan-based micro- and nanoparticles in drug delivery. J Controlled Release 2004 20041105;100(1):5-28.

22. Gupta U, Agashe HB, Asthana A, Jain NK. Dendrimers: Novel polymeric nanoarchitectures for solubility enhancement. Biomacromolecules 2006;7(3):649-58.

23. Liu Y, Miyoshi H, Nakamura M. Nanomedicine for drug delivery and imaging: A promising avenue for cancer therapy and diagnosis using targeted functional nanoparticles. International Journal of Cancer Journal International Du Cancer 2007 Jun 15;120(12):2527-37.

24. Shan-Yu Fung. Self-assembling peptides as potential carriers for the delivery of the hydrophobic anticancer agent ellipticine. University of Waterloo: University of Waterloo; 2007.

25. Hamidi M, Azadi A, Rafiei P. Hydrogel nanoparticles in drug delivery. Adv Drug Deliv Rev 2008 20081214;60(15):1638-49.

26. Arayne MS, Sultana N. Review: Nanoparticles in drug delivery for the treatment of cancer. Pakistan Journal of Pharmaceutical Sciences 2006 Jul;19(3):258-68.

27. Keyes-Baig C, Duhamel J, Fung S, Bezaire J, Chen P. Self-assembling peptide as a potential carrier of hydrophobic compounds. J Am Chem Soc 2004 June;126(24):7522-32.

28. S.Y. Fung, H. Yang, Priya T. Bhola, Parisa Sadatmousavi, Edward Muzar, Mingyao Liu, P. Chen. Self-assembling peptide as a potential carrier for hydrophobic anticancer drug ellipticine: Complexation and relaese. Adv Funct Mater 2009;19(1):74-83.

29. Zhang SG, Gelain F, Zhao XJ. Designer self-assembling peptide nanofiber scaffolds for 3D tissue cell cultures. Semin Cancer Biol 2005;15(5):413-20.

30. Zhang S. Designer self-assembling peptide nanofiber scaffolds for study of 3-D cell biology and beyond. ; 2008. NU: 76957_if3c0807.

31. Fung SY, Keyes C, Duhamel J, Chen P. Concentration effect on the aggregation of a self-assembling oligopeptide. Biophys J 2003 07;85(1):537-48.

32. Torchilin VP. Tatp-mediated intracellular delivery of pharmaceutical nanocarriers. 2007.

33. Torchilin VP. Cell penetrating peptide-modified pharmaceutical nanocarriers for intracellular drug and gene delivery. 2008.

34. Tian E, Landowski TH, Stephens OW, Yaccoby S, Barlogie B, Shaughnessy JD. Ellipticine derivative NSC 338258 represents a potential new antineoplastic agent for the treatment of multiple myeloma. 2008.

35. Chen P, Fung SY, Yang H. Formation of colloidal suspension of hydrophobic compounds with an amphiphilic self-assembling peptide. Colloids and Surfaces B (Biointerfaces) 2007 04;55(2):200-11.

36. Langer R. New methods of drug delivery. Science 1990 September 28;249:1527-33.

37. Zhang S. Emerging biological materials through molecular self-assembly. Biotechnol Adv 2002 December;20(5-6):321-39.

38. Lim YB, Lee E, Lee M. Cell-penetrating-peptide-coated nanoribbons for intracellular nanocarriers. 2007.

39. Zhang S, Marini DM, Hwang W, Santoso S. Design of nanostructured biological materials through self-assembly of peptides and proteins. Curr Opin Chem Biol 2002 December;6(6):865-71.

40. Zhang S, Holmes T, Lockshin C. Spontaneous assembly of a self-complementary oligopeptide to form a stable macroscopic membrane. Proc Natl Acad Sci U S A 1993 April 15;90:3334-8.

41. Shuguang Z, Holmes TC, DiPersio CM, Hynes RO, Xing S, Rich A. Self-complementary oligopeptide matrices support mammalian cell attachment. Biomaterials 1995 December;16(18):1385-93.

42. Hong Y, Lau L, Legge R, Chen P. Critical self-assembly concentration of an ionic-complementary peptide Eak16-i. The Journal of Adhesion 2004 October;80(10-11):913.

43. Jun S, Hong Y, Imamura H, Ha BY, Bechhoefer J, Chen P. Self-assembly of the ionic peptide EAK16: The effect of charge distributions on self-assembly. 2004.

44. Wang X, Horii A, Zhang S. Designer functionalized self-assembling peptide nanofiber scaffolds for growth, migration, and tubulogenesis of human umbilical vein endothelial cells. Soft Matter 2008;4(12):2388-95.

45. Zhang S, Lockshin C, Cook R, Rich A. Unusually stable β‐sheet formation in an ionic self‐complementary oligopeptide. Biopolymers 1994;34(5, pp. 663-672):May.

46. Chen P. Molecular interfacial phenomena of polymers and biopolymers. Cambridge : Boca Raton, FL: Woodhead ; CRC Press; 2005.

47. Hong Y, Legge RL, Zhang S, Chen P. Effect of amino acid sequence and pH on nanofiber formation of self-assembling peptides EAK16-II and EAK16-IV. Biomacromolecules 2003 September;4(5):1433-42.

48. Liu JB, Xiao YH, Allen C. Polymer-drug compatibility: A guide to the development of delivery systems for the anticancer agent, ellipticine. 2004.

49. Multon E, Riou J, LeFevre D, Ahomadegbe J, Riou G. Topoisomerase II-mediated DNA cleavage activity induced by ellipticines on the human tumor cell line N417. Biochem Pharmacol 1989 July;38(13):2077-86.

50. Fung SY, Yang H, Chen P. Sequence effect of self-assembling peptides on the complexation and in vitro delivery of the hydrophobic anticancer drug ellipticine. PLoS ONE 2008;3(4):e1956.

51. Firooz A, Chen P. Effect of surface expansion and compression on the surface tension of 1-octanol solutions. 2008.

52. P. C(, Lahooti S(, Policova Z, Cabrerizo-Vílchez MA, Neymann AW. Concentration dependence of the film pressure of human serum albumin at the water/decane interface. Colloids and Surfaces B: Biointerfaces 1996 May;6(4-5):279-89.

53. Cabrerizo-Vilchez MA, Policova Z, Kwok DY, Chen P, Neumann AW. The temperature dependence of the interfacial tension of aqueous human albumin solution/decane. Colloids and Surfaces B (Biointerfaces) 1995 09;5(1-2):1-9.

54. Malvern Instruments Ltd. Zetasizer nano series, user manual. England: Malvern; 2007.

55. Kaszuba M, Connah MT. Protein and nanoparticle characterisation using light scattering techniques. Part. Part. Syst. Char.2006;23(2):193-6.

56. Hong Yang. Assembly of an ionic-complementary peptide on surfaces and its potential applications University of Waterloo: University of Waterloo; 2007.

57. Patrickios CS, Yamasaki EN. Polypeptide amino acid composition and isoelectric point II. comparison between experiment and theory. Anal Biochem 1995;231(1, pp. 82-91):January.

58. Darzynkiewicz Z, Juan G, Li X, Gorczyca W, Murakami T, Traganos F. Cytometry in cell necrobiology: Analysis of apoptosis and accidental cell death (necrosis). Cytometry 1997 1;27(1):1-20.

59. Vermes I, Haanen C, Reutelingsperger C. Flow cytometry of apoptotic cell death. Journal of Immunological Methods 2000 Sep 21;243(1-2):167-90.

60. Ormerod MG, Paul F, Cheetma M, Sun XM. Discrimination of apoptotic thymocytes by forward light scatter. 1995.

61. Ormerod MG, Sun XM, Snowden RT, Davies R, Fearhead H, Cohen GM. Increased membrane-permeability of apoptotic thymocytes - a flow cytometric study. 1993.

62. MTT Cell Proliferation Assay

[Internet]USA: ATCC; c2008 [cited 2009 May/20]. Available from: http://www.atcc.org/MTTCellProliferationAssay/tabid/569/Default.aspx.

63. van de Loosdrecht AA, Beelen RHJ, Ossenkoppele GJ, Broekhoven MG, Langenhuijsen MMAC. A tetrazolium-based colorimetric MTT assay to quantitate human monocyte mediated cytotoxicity against leukemic cells from cell lines and patients with acute myeloid leukemia. J Immunol Methods 1994;174(1-2, pp. 311-320):September.

64. Introduction to Flow Cytometry [Internet]USA: AbD Serotec; c2009June/15].